RI 9290

REPORT OF INVESTIGATIONS/1990



# Shield Mechanics and Critical Load Studies for Unsymmetric Contact Configurations

By Thomas M. Barczak

1910 ★ 80 YEARS ★ 1990

BUREAU OF MINES

UNITED STATES DEPARTMENT OF THE INTERIOR

**Mission:** As the Nation's principal conservation agency, the Department of the Interior has responsibility for most of our nationally-owned public lands and natural and cultural resources. This includes fostering wise use of our land and water resources, protecting our fish and wildlife, preserving the environmental and cultural values of our national parks and historical places, and providing for the enjoyment of life through outdoor recreation. The Department assesses our energy and mineral resources and works to assure that their development is in the best interests of all our people. The Department also promotes the goals of the Take Pride in America campaign by encouraging stewardship and citizen responsibility for the public lands and promoting citizen participation in their care. The Department also has a major responsibility for American Indian reservation communities and for people who live in Island Territories under U.S. Administration.

Report of Investigations 9290

# Shield Mechanics and Critical Load Studies for Unsymmetric Contact Configurations

By Thomas M. Barczak

UNITED STATES DEPARTMENT OF THE INTERIOR
Manuel Lujan, Jr., Secretary

BUREAU OF MINES
T S Ary, Director

**Library of Congress Cataloging in Publication Data:**

**Barczak, Thomas M.**
Shield mechanics and critical load studies for unsymmetric contact configurations / by Thomas M. Barczak.

p. cm. – (Report of investigations; 9290)

Includes bibliographical references.

Supt. of Docs. no.: I 28.23:9290.

1. Mine roof control–Testing. 2. Longwall mining. I. Title. II. Series: Report of investigations (United States. Bureau of Mines); 9290.

TN23.U43 [TN288] 622 s–dc20 [622'.28] 89-600237
CIP

# CONTENTS



## ILLUSTRATIONS

## ILLUSTRATIONS--Continued

## ILLUSTRATIONS--Continued

## ILLUSTRATIONS--Continued

*Page*



## UNIT OF MEASURE ABBREVIATIONS USED IN THIS REPORT

| | | | |
|---|---|---|---|
| in | inch | pct | percent |
| in/min | inch per minute | psi | pound per square inch |
| lbf | pound (force) | | |

# SHIELD MECHANICS AND CRITICAL LOAD STUDIES FOR UNSYMMETRIC CONTACT CONFIGURATIONS

By Thomas M. Barczak[1]

## ABSTRACT

This U.S. Bureau of Mines report investigates shield mechanics and component stress development in a two-legged longwall shield for unsymmetric canopy and base contact configurations. Previous studies analyzed shield behavior for symmetric contact configurations. The goals of these efforts are to improve longwall support selection and design. This study provides vital information that will help develop improved procedures for performance testing of longwall supports and will benefit future research to improve support design through stress optimization and evaluation of failure mechanisms. Combinations of six canopy (three symmetric and three unsymmetric) and six base (four symmetric and two unsymmetric) contacts provided a total of 36 configurations for evaluation. Of these 36 configurations, 10 were eliminated because of fixture limitations or shield instability. Controlled vertical and horizontal displacements were applied by the Bureau's mine roof simulator to the remaining 26 configurations. Component responses were determined from pressure transducer and strain gage instrumentation in order to identify contact configurations and boundary displacements that produced maximum loading in each of the support components. This report describes these test results and provides conclusions relevant to critical contact configurations for performance testing of longwall supports.

[1]Research physicist, Pittsburgh Research Center, U.S. Bureau of Mines, Pittsburgh, PA.

## INTRODUCTION

Two primary goals of the Bureau's research in underground coal mining are to reduce the cost of mining coal and to ensure the health and safety of the miner. This study is one of a series of projects that strive to achieve these goals by improving the selection and design of longwall roof supports. An overview of the Bureau's technical approach for the longwall roof support research program is shown in figure 1. Two principal objectives of the program are (1) to develop an understanding of shield mechanics for various boundary conditions (contact configurations and displacements) that will enable definition of critical load conditions, and (2) to evaluate failure mechanisms and assess their impact on support safety.

This particular study investigates shield mechanics and critical loading for unsymmetric contact configurations by full-scale testing of a two-legged shield in the Bureau's mine roof simulator.[2] The simulator, shown in figure 2, is designed to simulate underground loading by applying controlled vertical and horizontal forces or displacements to mine roof support structures. Previous studies have evaluated critical shield loading and shield mechanics for symmetric contact configurations.[3]

These studies have identified load conditions for symmetric canopy and base contact configurations that produce maximum loading in shield components. Because unsymmetric loading may induce additional (out-of-plane) stress development, unsymmetric load conditions may be more severe than symmetric load conditions, and thus are essential to a study of critical shield loading.

Improvements in support selection and design require a better understanding of the geomechanics of strata control and the interaction of the support with the strata. The capacity and structural integrity of a longwall support must be compatible with the maximum loading it is expected to sustain underground. Stress optimization can be considered only after the load conditions have been defined that subject each of the support components to maximum loading. Likewise, evaluation of support failures requires an understanding of load transfer mechanics and stress development within the support structure.

Longwall supports are subjected to numerous load conditions (contact configurations) during their service life; those inducing critical stresses compromise the structural integrity of the support and potentially endanger the safety of the miner. Although longwall supports are routinely tested by manufacturers prior to field service, roof support failures still commonly occur.[4] Obviously, these

[4]Barczak, T. M. Safety Evaluations of Longwall Roof Supports. BuMines IC 9221, 1989, 17 pp.

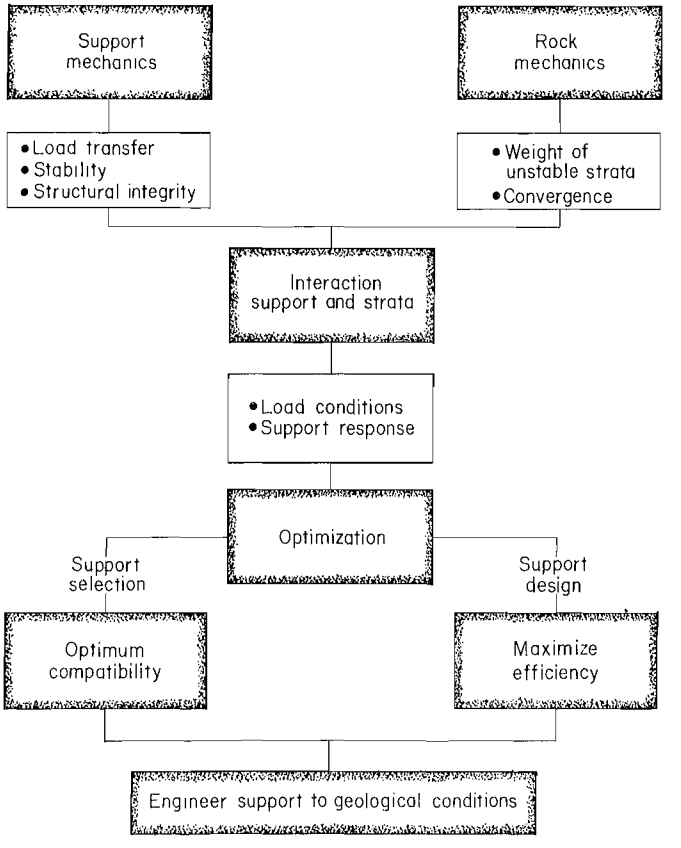


**Figure 1.–Bureau's technical approach for longwall roof support research.**

[2]Testing was conducted by Boeing Services International (BSI), Pittsburgh, PA, under the direction of Carol L. Tassilo, operations engineer, BSI. David E. Schwemmer, lead structural engineer, BSI, assisted in experimental design and data analysis.

[3]Barczak, T. M., and D. E. Schwemmer. Critical-Load Studies of a Shield Support. BuMines RI 9141, 1987, 15 pp.

_____. Two-leg Longwall Shield Mechanics. BuMines RI 9220, 1989, 34 pp.

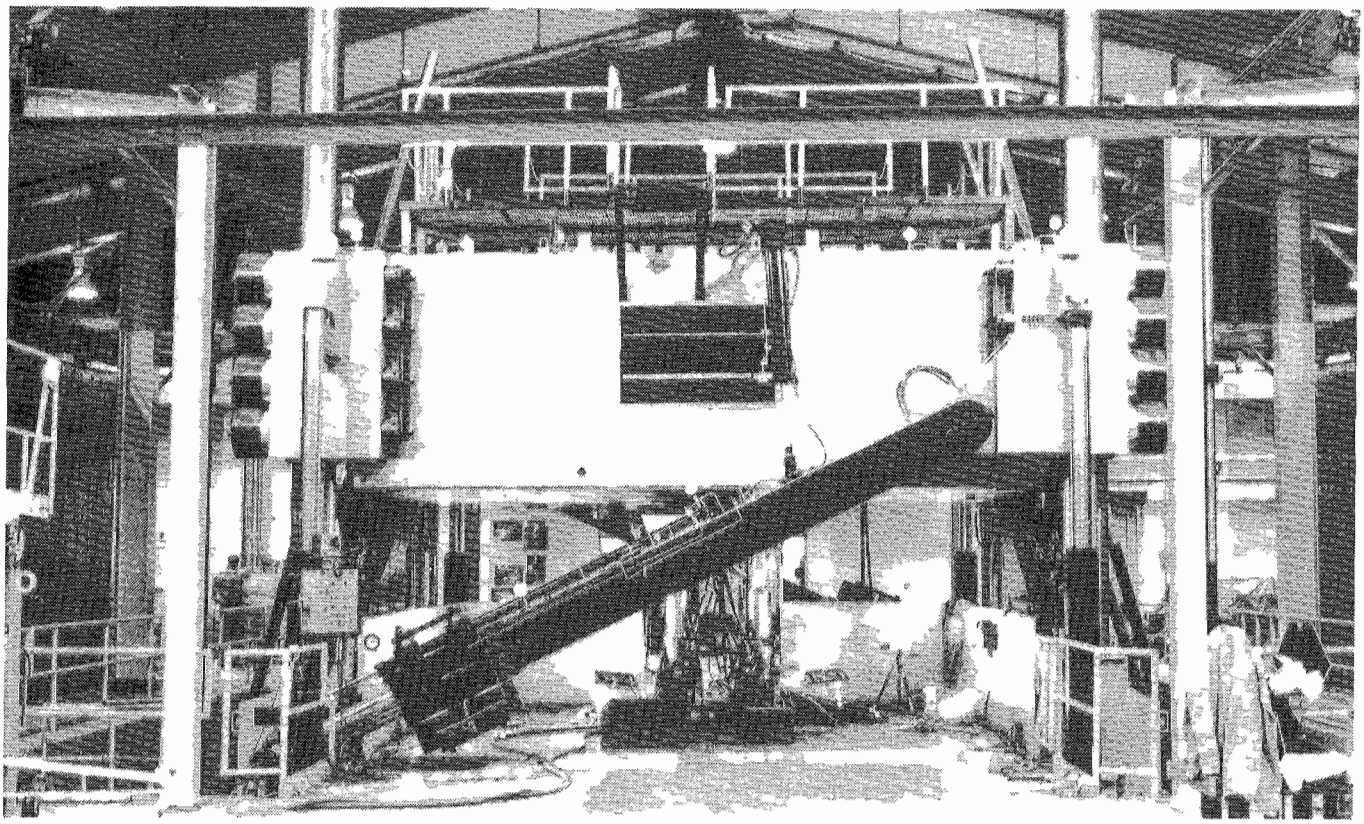

Figure 2.–Bureau's mine roof simulator.

manufacturer tests do not properly simulate underground load conditions and improvements in performance testing methodologies are required. In addition to jeopardizing the safety of the miner, roof support failures reduce productivity and significantly add to the cost of mining coal. In the opinion of the author, longwall mining including support selection and design must be optimized if the United States is to remain competitive in the world coal market.

The recent trend in support selection, as illustrated in figure 3, has been toward higher capacity support systems to provide insurance against the risk of failure. However, there is no conclusive evidence to indicate that support failures have been substantially reduced as a result of this increase in support capacity. Structural failures have been reported on supports with capacities in the upper 25 percentile. Hence, it is apparent that increasing support capacity is not an acceptable substitute for inadequate designs or ineffective performance testing.

In summary, the motivation for longwall support optimization is to reduce the risk of failure and improve the efficiency of the support by providing a more uniformly stressed design. This particular study is intended to provide additional insight into critical loading of longwall supports in preparation for developing improved guidelines for performance testing and future studies to evaluate failure mechanisms and design improvements.

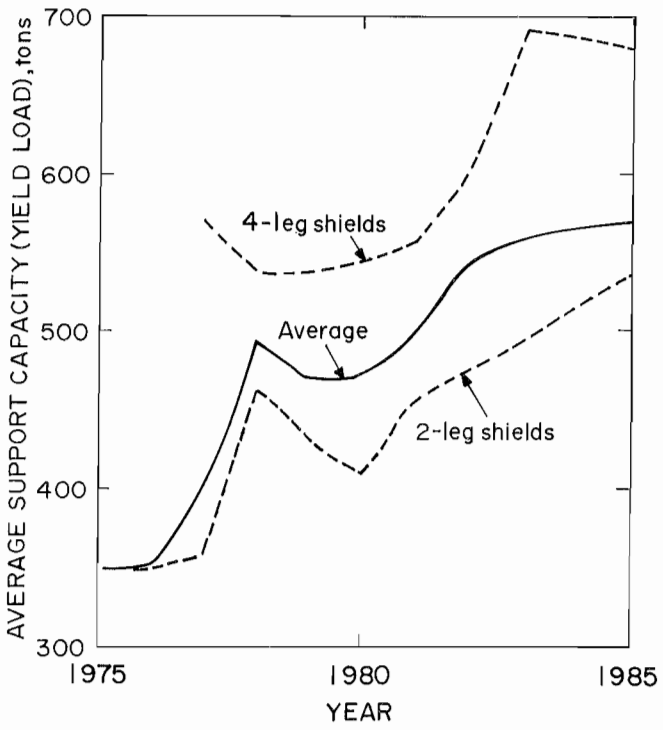


Figure 3.–Recent trend in support selections.

## DESCRIPTION OF CONTACT CONFIGURATIONS AND TEST PROCEDURES

A 350-ton-capacity[5] two-leg longwall shield that is considered to be representative of two-leg shields used in the industry was selected as the test specimen. The support was obtained on loan from a mining company and was about 1 year old at the time of the test. A two-dimensional illustration of the shield's components is shown in figure 4.

The support was instrumented with pressure transducers in the hydraulic leg cylinder circuit and 28 strain gages strategically located on the structure to evaluate the shield's response and component loading. Figure 5 depicts instrumentation locations on the shield. The motivation in the strain gage placement was to identify basic component responses by quantification of nominal strain development in each of the shield components. No attempt was made to identify localized areas of maximum stress, which are likely to occur at geometric discontinuities. This does not forbid determination of critical load conditions because stress development at stress concentrators is proportional to nominal (general) stress development in the component. Localized high stresses at stress concentrators are shield specific and may or may not destroy the structural integrity of the component, as the structure may be able to transfer this load elsewhere. However, if the nominal stresses exceed the material's yield stress, the structure will lose its elastic response any may develop sufficient fracturing or yielding to cause loss of structural integrity. Therefore, critical load analysis for performance testing should be derived from nominal component responses, but failure evaluations must consider localized stress concentrations as well.

Six canopy (three symmetric and three unsymmetric) and six base (four symmetric and two unsymmetric) contacts were selected for evaluation. A nomenclature for referencing specific canopy and base contacts is depicted in figures 6 and 7. Combinations of these canopy and base contacts provides a possible 36 contact configurations for investigation. Of these 36 configurations, 10 were eliminated because of test fixture limitations or shield instability, leaving 26 configurations that were evaluated in this study. Of these 26, six had symmetric canopy and symmetric base contacts; while either the canopy, base, or both had unsymmetric contact on the remaining 20 configurations. The contact combinations evaluated in this study are illustrated in figure 8. Reference to specific contact configurations will be made by row and column number in the matrix shown in figure 8. For example, configuration 2,4 refers to test configuration depicted in row 2 and column 4 of figure 8.

[5]In this report, "ton" indicates 2,000 lbf.

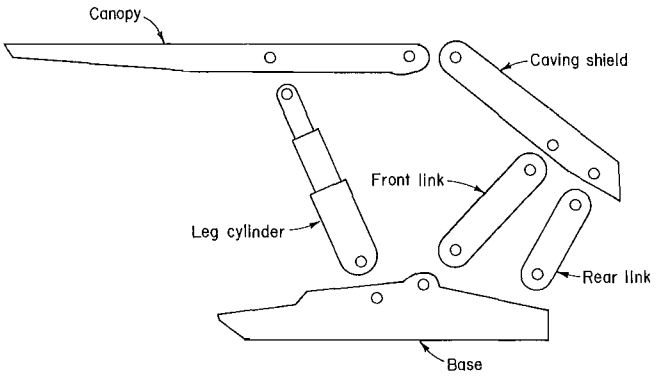


Figure 4.–Two-dimensional diagram of shield support.

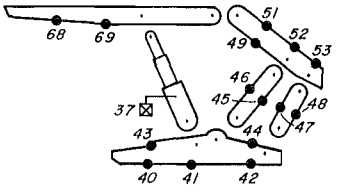


Left side

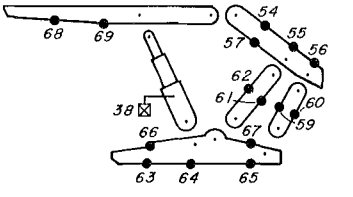


Right side

KEY
• Strain gage
⊠ Pressure transducer

Figure 5.–Instrumentation locations on shield support.

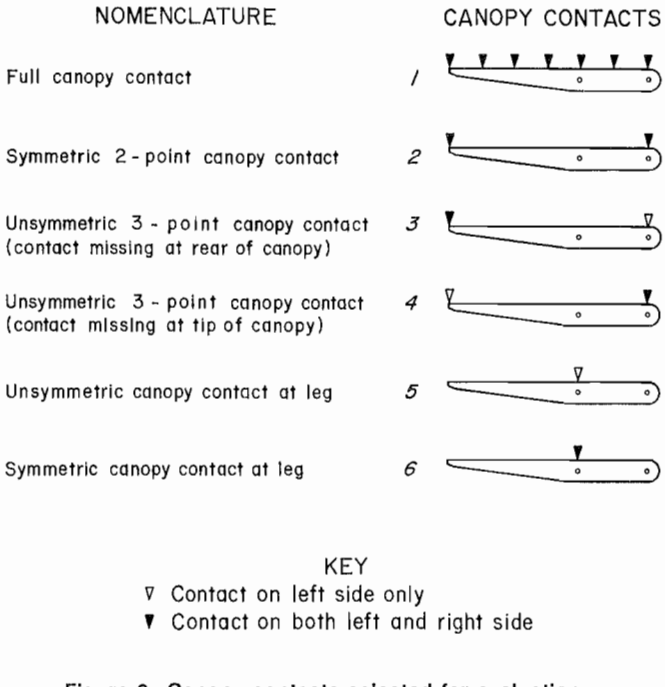


Figure 6.–Canopy contacts selected for evaluation.

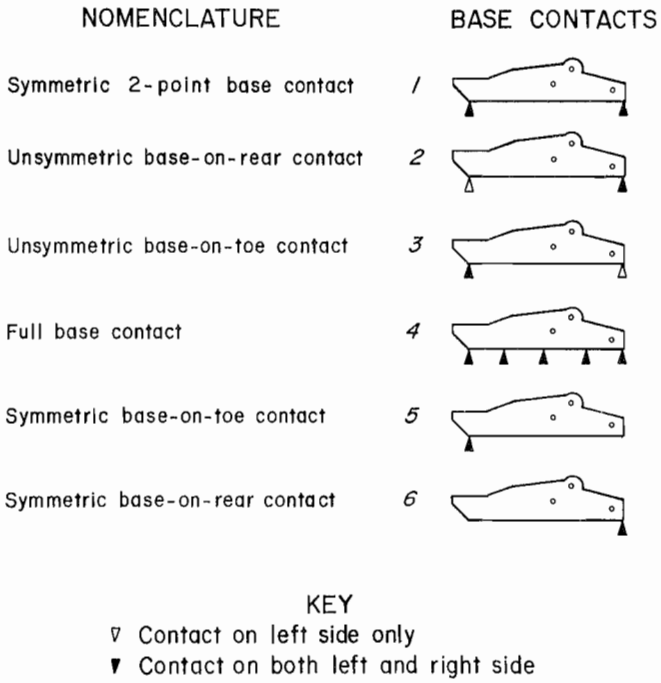


Figure 7.–Base contacts selected for evaluation.

The shield was placed in the mine roof simulator with appropriate fixture restraints. Prior to pressurization of the leg cylinders to setting pressure, the shield was horizontally constrained by displacement of the canopy relative to the base in a face-to-waste horizontal direction to remove (or at least reduce) pin-clevis tolerance in the numerous pin joints of the structure. This technique was established on previous tests[6] and is intended to allow full participation of the caving shield-lemniscate assembly in the load transfer mechanics within the shield. Previous tests have shown that unconstrained two-leg shield supports permit up to 3/4 in of horizontal displacement without any significant resistance by the caving shield-lemniscate assembly.

Following horizontal constrainment, the support was set against the simulator platens with the leg pressure at 4,000 psi. Controlled vertical displacement of the canopy relative to the base was then applied by the simulator at a rate of 0.1 in/min for 0.2 to 0.4 in. During this vertical displacement, no horizontal displacement of the canopy relative to the base was permitted in order to isolate the effects of the vertical displacement and to allow external horizontal force reactions to develop on the canopy and base. Then the canopy was displaced 0.2 to 0.4 in horizontally in a face-to-waste direction at a rate of 0.1 in/min while maintaining the vertical displacement in order to evaluate the effects of horizontal displacement independent of simultaneous vertical displacement. Figure 9 illustrates these test procedures.

To ensure elastic recovery of the shield components (at least at the measured deformations), the tests were terminated whenever 85-pct yield for that component was reached. If all measured deformations were below this limit, the test was terminated at hydraulic leg yield or as a result of instability that altered the original contact configuration.

[6]Barczak, T. M., and D. E. Schwemmer. Horizontal Vertical Load Transferring Mechanisms in Longwall Roof Supports. BuMines RI 9188, 1988, 24 pp.

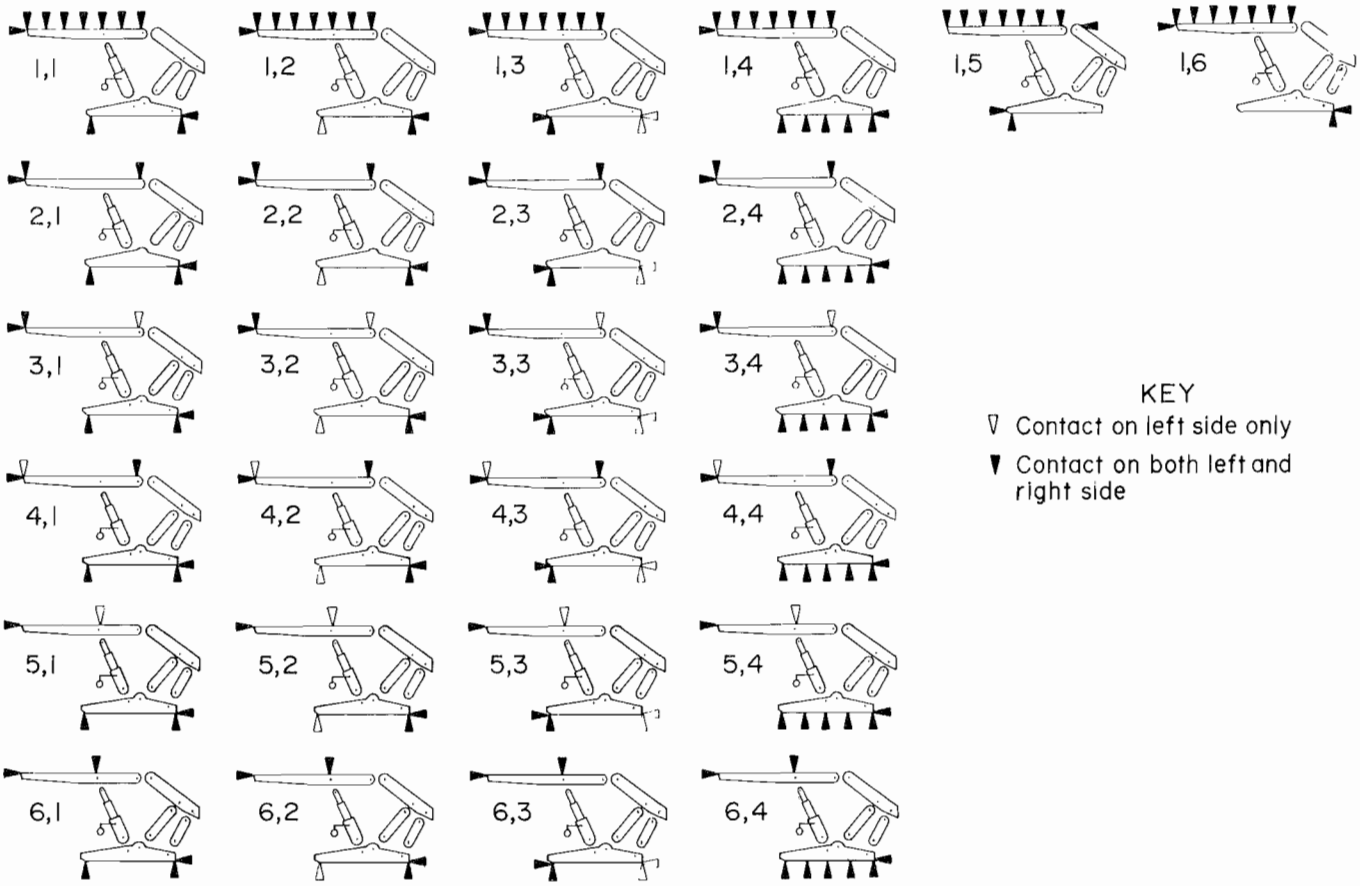


**Figure 8.–Contact configurations illustrating combinations of canopy and base contacts selected for evaluation.**

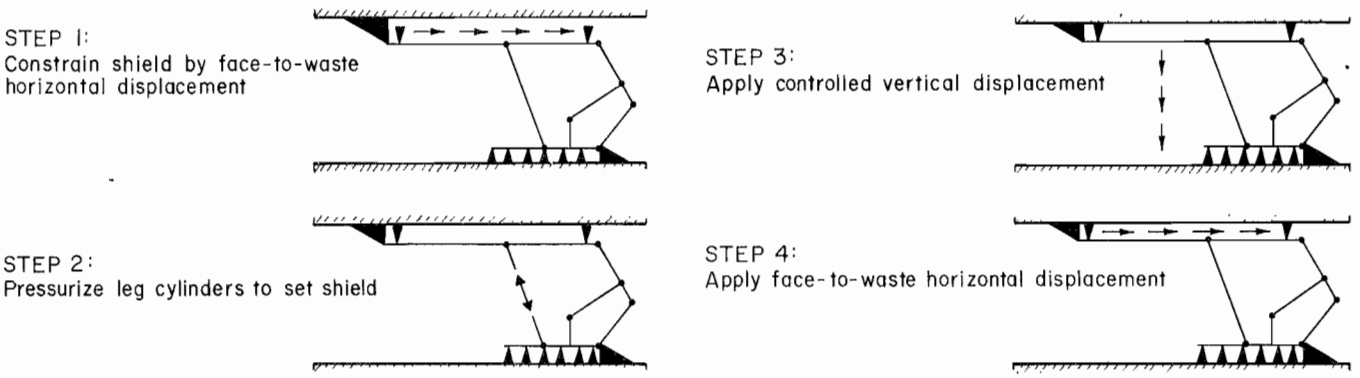


**Figure 9.–Illustration of critical load test procedures.**

## SUMMARY ASSESSMENT OF SYMMETRIC CONTACT CONFIGURATION RESPONSES

The unsymmetric contact configurations were derived by combining previously tested symmetric configurations, one established on the left side of the shield and the other on the right side of the shield as viewed in the two-dimensional plane shown in figure 4. For example, the unsymmetric base-on-toe configuration depicted in figure 8 (configuration 2,3) is derived by combining a symmetric base-on-toe configuration with a two-point base contact. Hence, an understanding of shield response for these symmetric contact configurations is useful in evaluating the impact on shield behavior of unsymmetric contacts.

Conclusions drawn from previous studies[7] of symmetric contact configurations are summarized below and component responses for specific symmetric canopy and base contact configurations are depicted in appendix A.

1. The canopy and base interface with roof and floor strata and induced loading must be transferred between these components either through the leg cylinders or the caving shield-lemniscate assembly.

2. The primary loading mechanism for the canopy, base, and caving shield is bending. Leg cylinders and link components are generally axially loaded members.

3. For full canopy and base contact, there is likely to be very little loading in the caving shield-lemniscate assembly for vertical displacements because this assembly has very little vertical stiffness. Horizontal displacement of the canopy relative to the base can produce significant loading in the caving shield-lemniscate assembly provided the shield is sufficiently constrained to permit full participation of this assembly in the shield's load transfer mechanics.

4. Loading of all components but the canopy are controlled by the behavior of the base as determined by the base contact. Bending of the base can significantly influence the loading and behavior of the caving shield-lemniscate assembly.

5. The most severe (symmetric) load conditions for two-leg shield supports are single-point base contacts, which require participation of the caving shield-lemniscate assembly to maintain base stability. Two such base contacts evaluated in previous studies were (1) standing the support on the toe of the base and (2) standing the support on the rear of the base. These contact conditions produce maximum stresses in the base, caving shield, and lemniscate links.

6. Initial conditions from setting the shield are influenced by leg mechanics (effective leg force) and horizontal constrainment. Full extension of the bottom stage of the leg cylinders against the pressure chamber stops can reduce effective leg force by as much as 50 pct. Constrained shield configurations, which remove rigid-body translational freedom in the pin joints, can increase strain energy in the caving shield-lemniscate assembly by several hundred percent.

7. Shield response is also dependent upon shield height and contact stiffness.[8] Shields are generally stiffer at lower heights and therefore produce less strain than identical canopy-base contacts at higher shield heights with comparable forces acting on the shield.

## ANALYSIS OF SHIELD RESPONSES FOR UNSYMMETRIC CONTACT CONFIGURATIONS

An analysis of shield component responses for each contact configuration depicted in figure 8 is made to evaluate the following: (1) component strain energy as a function of vertical and horizontal displacement, (2) load distribution between the left and right side of the shield, and (3) shield mechanics that describe observed component responses. Using this analysis, shield responses for contact configurations that have the same canopy contact are compared as are shield responses for contact configurations that have the same base contact. In addition, shield responses for symmetric contact configurations are compared to responses for unsymmetric contact configurations. From these evaluations, controlling factors are determined and worst case contact configurations are identified.

Measured pressure transducer and strain gage data for each test configuration are documented in appendix B. The tabulations show strain or pressure for each of the 28 strain gages and 2 pressure transducers after the support is set (initial conditions), after vertical displacement, and after horizontal displacement.

[7]Works cited in footnotes 2 and 4.

[8]First work cited in footnote 2.

## LOAD TRANSFER

Appendix C documents load transfer between the left and right side of the shield support for each contact configuration. Results and conclusions drawn from analysis of these data are as follows:

1. For symmetric contact configurations, load distribution between the left and right side of the shield is usually controlled by the side with the most leg pressure, with larger strains developed on that side. For balanced leg pressures with evenly distributed base loading, there is fairly uniform load transfer down both sides of the shield provided initial conditions produce a balanced distribution of forces between the left- and right-side canopy-caving shield hinge pins. Sometimes, the horizontal loading in the pins can be different from differential horizontal movement of the base units or horizontal constraint on one side of the canopy and not the other. In these cases, the response of the left side and right side of the caving shield-lemniscate assembly will be dominated by the side with maximum forces at the canopy-caving shield joint but the difference is likely to be small.

2. For the two unsymmetric base contacts evaluated in this study, combination of two-point and one-point contacts as illustrated in columns 2 and 3 of figure 8, maximum loading will be down the side of the shield with the single-point base contact. This occurs regardless of whether the canopy contact is symmetric or unsymmetric. The reason for this behavior is that these are the more dominant base contacts and they dominate over all canopy contacts.

3. For configurations with unsymmetric canopy contacts and symmetric base contacts, load distribution through the caving shield-lemniscate assembly is less defined than for unsymmetric base contacts, but will generally be down the side with the one-point canopy contact. Again, the dominating factor will be canopy deformations at the rear of the canopy, which produce associated reactions in the canopy-caving shield hinge pins. Maximum canopy deformations are also likely to occur on the side with the fewer contacts since it less restrained. Strain development in the base units are dependent upon leg pressures and relative base stiffness. Hence, maximum base strains will likely be developed on the side of the canopy with the contact or resultant force closest to the leg.

## SHIELD MECHANICS

Appendix C also describes shield mechanics that produced the observed component responses for each of the contact configurations evaluated. Shown in appendix C are the observed tension or compression responses of the left- and right-side front and rear lemniscate links and observed (increasing or decreasing) changes in leg pressure. Comparing these diagrams to the free-body diagrams for symmetric contact configurations depicted in appendix A, the following observations are made:

1. Because this shield was a split base design, the left- and right-side base members behave as individual units. The contact configuration on the respective base unit generally dominates the behavior of the links (and caving shield) on that side. Examination of the symmetric configurations in appendix A shows that opposite link behavior is produced for two-point base contact compared to base-on-toe contact. Examination of contact configurations in column 3 of figure 8, where the left side is a two-point base contact and the right side is a base-on-toe contact, reveals that all configurations show opposite link behavior on the left and right side for vertical displacement.

2. The horizontal restraint (contact) is the same (across the front of the canopy and across the rear of the base) for all configurations except the unsymmetric base-on-toe contact cases. Hence, for those cases with the same horizontal restraint, shield component responses for face-to-waste horizontal displacement is the same regardless of the vertical restraint (contact configuration). As shown in the diagrams in appendix C, face-to-waste horizontal displacement produces tension in the front link and compression in the rear link. These results are consistent with those reported in appendix A for symmetric load cases from previous studies.

For unsymmetric base contacts shown in column 3 of figure 8 (two-point base contact and base-on-toe contact), the right front link behavior for horizontal displacements was opposite the left front link behavior when it was thought they would be the same. The side with the base-on-toe configuration indicated compression in the front link when the expected result was tension. It is also noted that the leg pressure decreased on the base-on-toe side during the face-to-waste horizontal displacement. Therefore, a probable explanation for the link behavior is that the base-on-toe unit underwent rigid-body displacement as the rear of the support was displaced downward and rearward (towards the gob). Hence, it appears the left and right base units were displacing horizontally in opposite directions. This would explain the observed difference in link behavior.

3. The most inconsistent behavior in shield mechanics was observed for contact configurations in column 1 of figure 8, which are symmetric two-point base configurations. Expected behavior from vertical displacement for such a two-point base contact is to produce bending of the base units, which causes tension in the front links and compression in the rear links. Observation of component responses indicated that some unsymmetric canopy contacts (configurations 3,1 and 5,1 in particular) exhibited a different link response. These configurations produced compression in the front links and tension in the rear links, which is opposite that of symmetric canopy contacts (configurations 1,1, 2,1, and 6,1) and one unsymmetric canopy contact (configuration 4,1).

Hence it appears that these unsymmetric canopy contacts (configurations 3,1 and 5,1) have control over the symmetric two-point base contact. However, it should be noted that the link strains were small (less than 50 microstrain) and the base members for this particular shield are fairly stiff. Hence, minimal base bending occurred and apparently the canopy deformations produced by these unsymmetric canopy contacts were sufficient to overcome base bending responses in the lemniscate links. For shields with more flexible bases, it is likely that the base units would control for all canopy contact configurations. Therefore, these conclusions are qualified as such until other shields are examined.

## COMPARISON OF LIKE BASE CONFIGURATIONS

A comparison of component loading in shield components for like base configurations with different canopy contacts is shown in figures 10 and 11. Figure 10 shows component responses for the left side of the shield and figure 11 shows component responses for the right side of the shield. Illustrated in these figures are the components with the maximum strain as determined from initial conditions at setting and subsequent strain development in response to vertical displacement. For example, examination of column 1 in figures 10 and 11 (various canopy contacts with symmetric two-point base contact) reveals the following behavior.

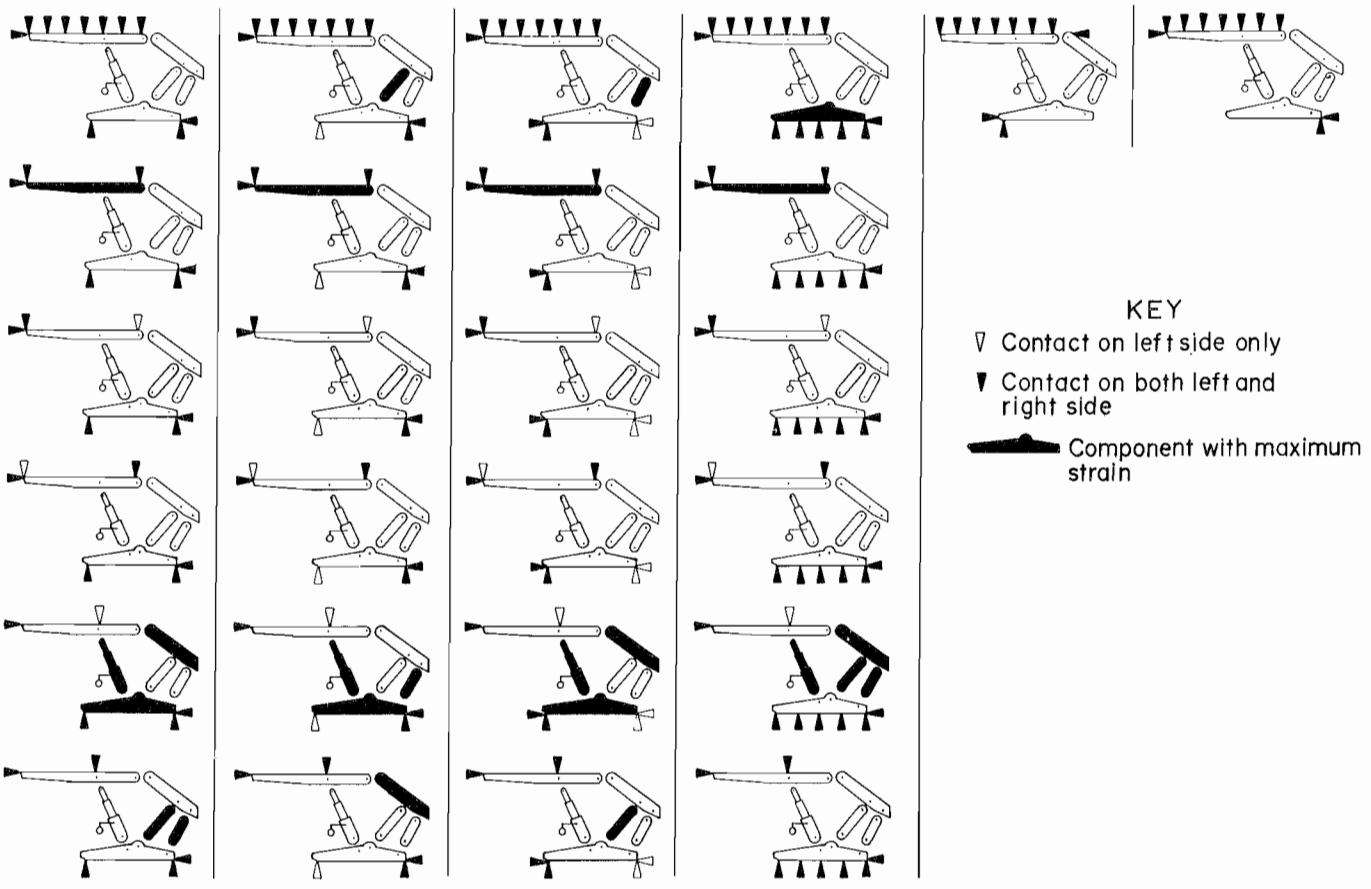


Figure 10.–Maximum left side component strains for like base configurations.

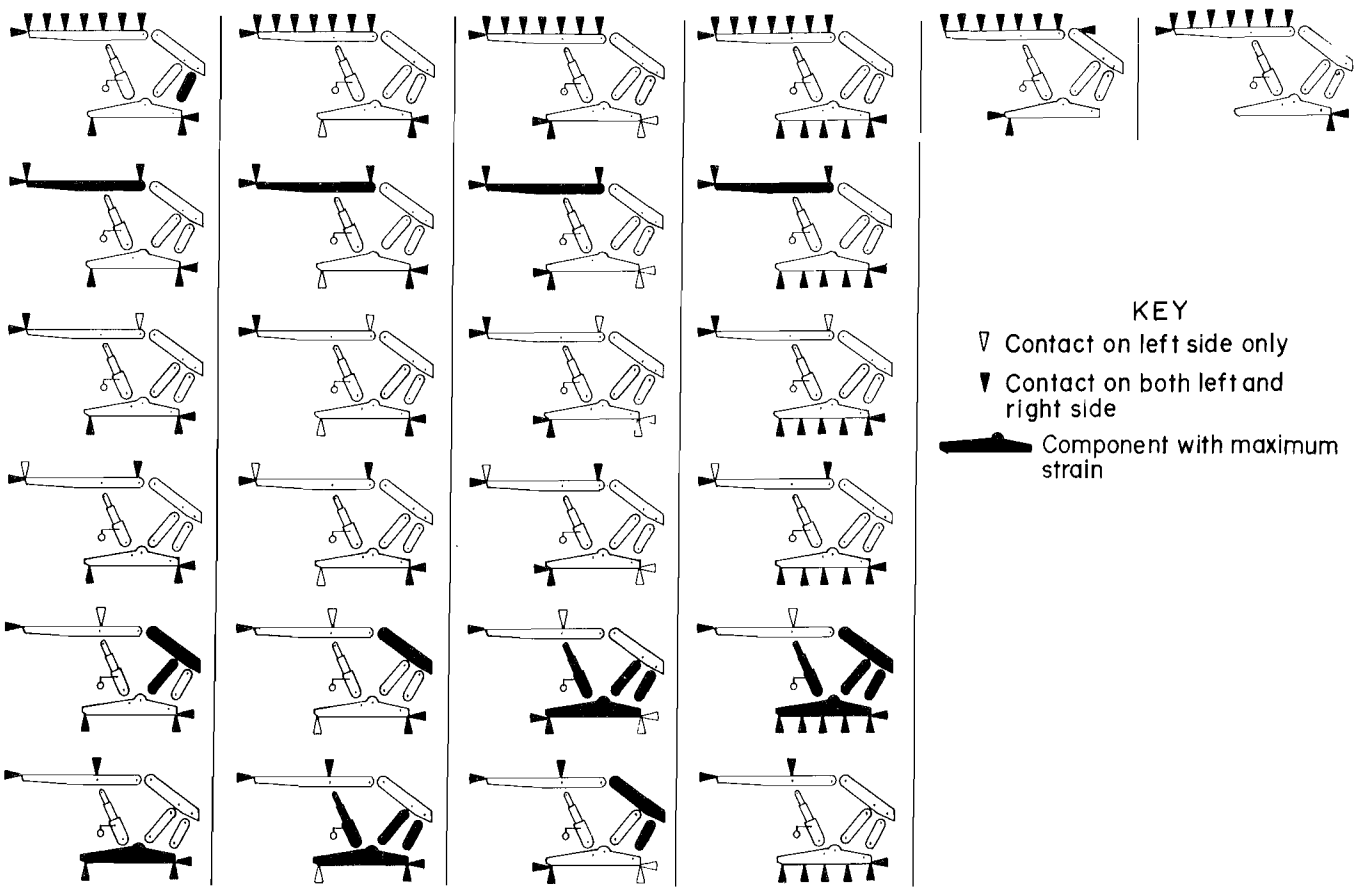


**Figure 11.–Maximum right side component strains for like base configurations.**

- The canopy was subjected to maximum strain for the symmetric two-point canopy contact (configuration 2,1).
- Unsymmetric canopy contact at one leg location (configuration 5,1) produced maximum strain in the leg, base, and caving shield.
- The lemniscate links were most severely strained for the symmetric canopy contact at the leg locations (configuration 6,1).

Analysis of figures 10 and 11 shows that for all components except the canopy, the worst case canopy contacts for configurations with the same base contact are symmetric and unsymmetric canopy contact at the leg locations and full canopy contact. Of these, the symmetric and unsymmetric canopy contact at the leg locations are the more dominant with the unsymmetric canopy contact (at one leg location) somewhat more dominant than the symmetric canopy leg contact. Concentration of load at the leg location minimizes canopy deformation and maximizes load transfer through the leg cylinders. The load transfer through the leg cylinders maximizes base bending and, since the response of the caving shield and lemniscate links are dependent upon base bending, this behavior also maximizes strain development in the caving shield-link assembly. Canopy contacts away from the leg location (contacts in rows 2, 3, and 4 of figure 8) produce less base bending; hence they are not as critical as the canopy contacts at the leg locations. Maximum canopy deformation for like base contacts occurred with symmetric two-point canopy contact as shown in row 2 of figures 10 and 11. As expected, this configuration produced maximum bending of the canopy (at least at the measured locations).

A complete comparison of strain development for each component for like base contacts is provided in appendix D. Figures in the appendix depict strain development as a function of vertical displacement. The elastic response of the shield is indicated by the linear development of strain as a function of the applied displacement. Comparing the slopes of the curves provides a means to compare strain development for any combination of the tested configurations. Some examples follow.

Comparison of three-point unsymmetric canopy contacts reveals that the unsymmetric contact with a missing contact at the rear of the canopy (configurations in row 3 of figure 8) produces more strain in the caving shield-lemniscate assembly than the unsymmetric contact with the missing contact at the front of the canopy (configurations in row 4 of figure 8). For example, figure 12 compares strain development in the caving shield and right front link for full base contact and unsymmetric three-point canopy contact (configurations 3,4 and 4,4 in figure 8). As seen in the figure, caving shield and front link strain development as a function of vertical displacement is significantly greater for the canopy configuration with the missing rear contact than for the canopy configuration with the missing front contact.

However, comparing the unsymmetric canopy configuration with the missing rear contact to the unsymmetric canopy contact at the leg location reveals that the unsymmetric canopy leg contact is the more critical configuration. Strain development for the caving shield and front link for these canopy configurations are shown in figure 13 for full base contact. Full base contact was chosen for these comparisons of unsymmetric canopy contact because base bending, which is a controlling factor in shield response, is minimized for the full base contact. This allows evaluation of the unsymmetric canopy contact behavior without the influence of the base behavior.

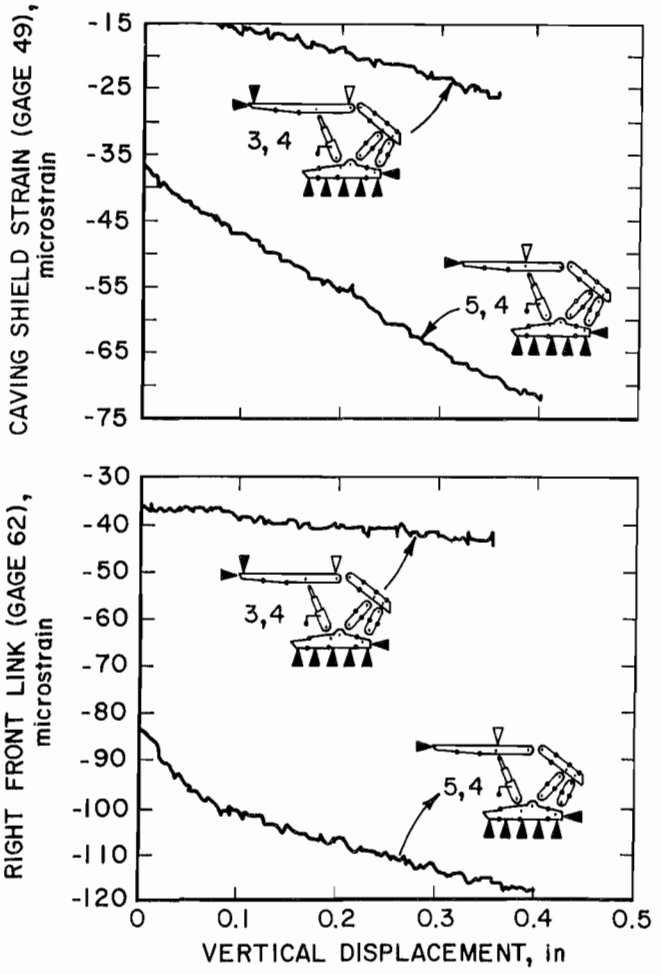


Figure 12.–Comparison of strain development in caving shield and front link for two different unsymmetric canopy contact configurations.

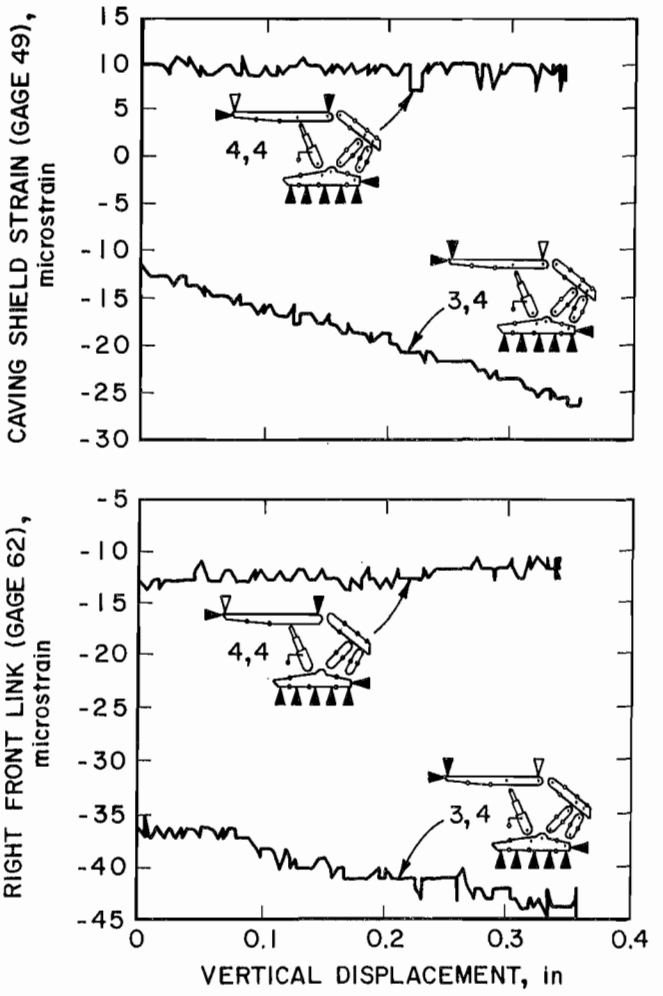


Figure 13.–Comparison of strain development in caving shield and right front link for full base contact with unsymmetric canopy contact.

## COMPARISON OF LIKE CANOPY CONTACT CONFIGURATIONS

A comparison of like canopy contact configurations is accomplished in the same manner as the comparison of like base contact configurations. Figures 14 and 15 depict maximum strain in each component (figure 14 shows left-side shield response while figure 15 shows right-side shield response) for each of the six different canopy contacts.

Analysis of figures 14 and 15 reveal the most dominant base configurations for like canopy contacts for each of the five canopy contacts depicted in rows 2 through 6 in figure 8 are unsymmetric base-on-toe and unsymmetric base-on-rear contacts. It is also seen that for full canopy contact where symmetric base-on-toe and base-on-rear configurations were achieved, these base configurations produced maximum strain development. Hence, it is concluded that regardless of the canopy contact, shield response primarily will be dominated by these base configurations.

It is recalled from the analysis of shield mechanics that the responses of the lemniscate links and caving shield are opposite for the base-on-toe configuration compared to the base-on-rear configuration. This difference in behavior makes it difficult to establish loading trends and to determine which of these two base contacts will provide maximum loading for like canopy contacts. Some observations are as follows.

- The caving shield is likely to be loaded more for the unsymmetric base-on-rear configuration than the unsymmetric base-on-toe configuration.
- For unsymmetric canopy contact configurations, maximum link loading was opposite for the left- and right-side members. This suggests out-of-plane loading from the unsymmetric canopy contact is twisting the caving shield and this behavior is reflected in the link loading.
- For like canopy contacts, maximum base strain for the left base unit consistently occurred for the unsymmetric base-on-rear configuration and maximum strain in the right base unit occurred for the base-on-toe configuration. This demonstrates the independence of the base behavior as the more dominant base-on-toe contact on the right side did not significantly influence base loading on the left side.

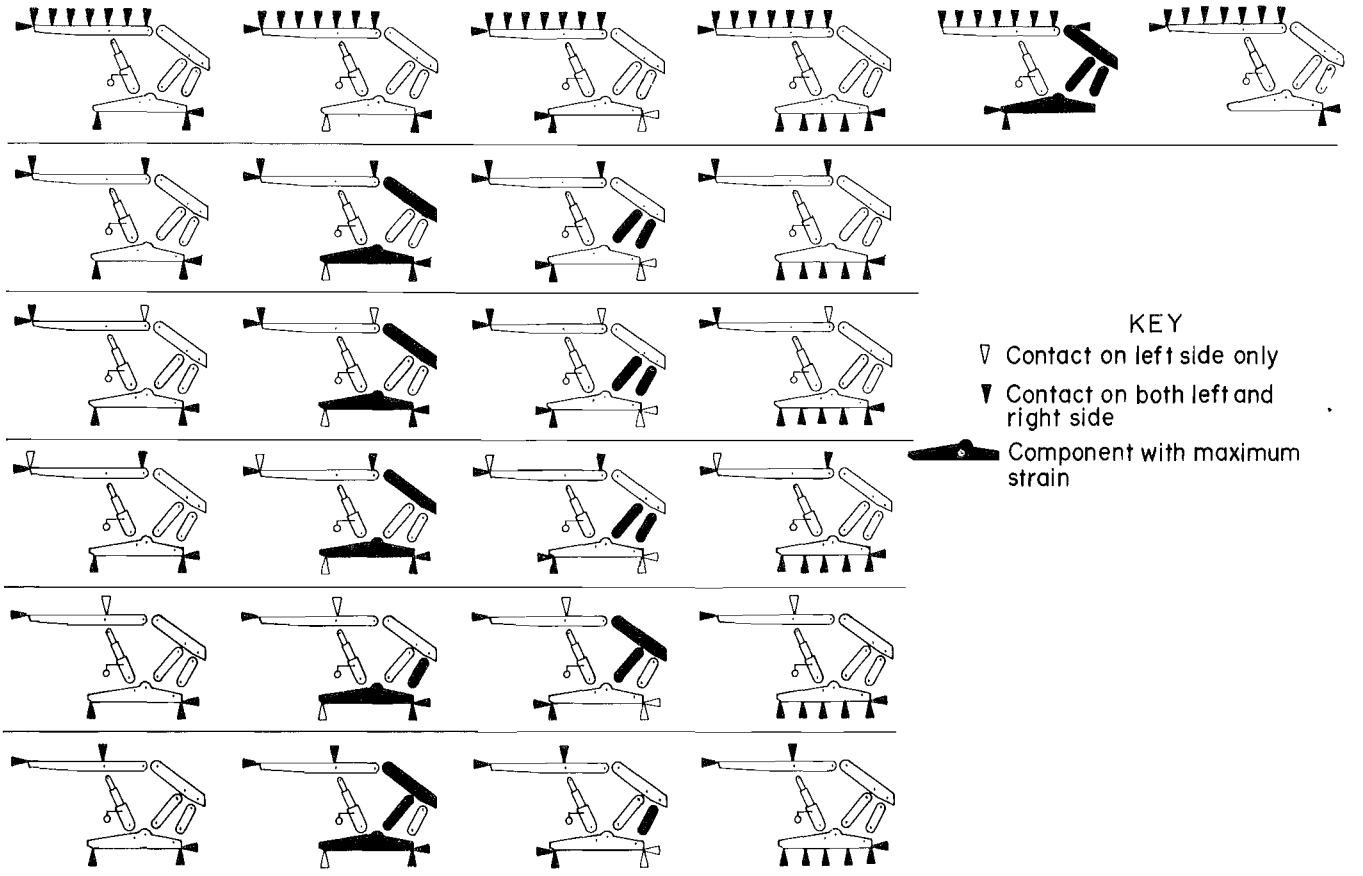


Figure 14.–Maximum left side component strains for like canopy configurations.

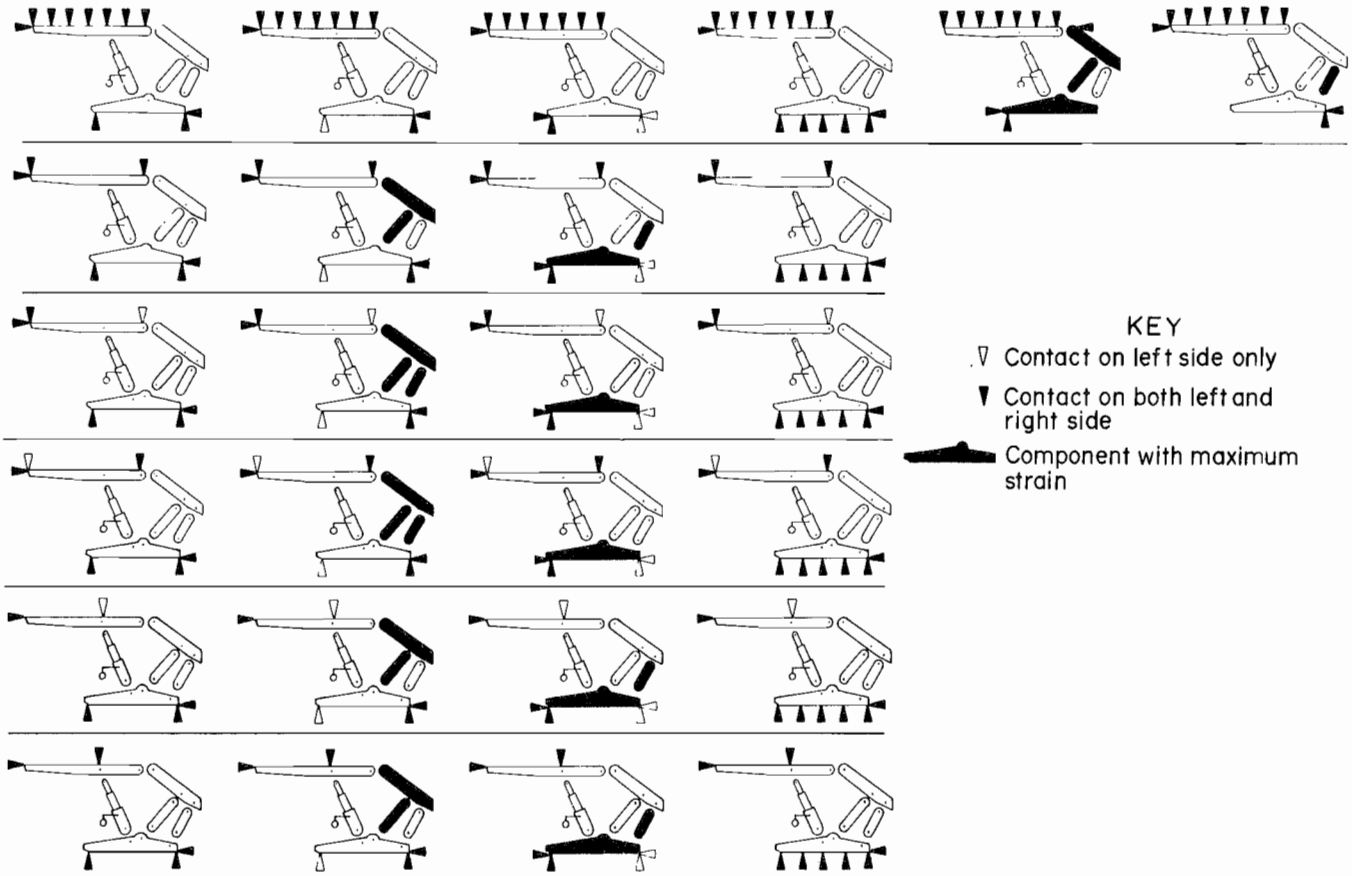


**Figure 15.–Maximum right side component strains for like canopy configurations.**

A complete comparison of component strain development for like canopy contacts is provided in appendix E. As with the like base contacts previously discussed, comparison of the slopes of the curves in the appendix permits comparison of strain development as a function of vertical displacement for any of the tested contact configurations. Some observations of shield response for like canopy contact configurations are made as follows:

- The symmetric base-on-toe contact (configuration 1,5) produces larger strains in the base and caving shield-lemniscate assembly than the unsymmetric base-on-toe contact (configuration 1,3). Figure 16 compares strain development as a function of vertical displacement for the caving shield (right side) and right front link for the symmetric and unsymmetric base-on-toe configuration.
- Comparison of unsymmetric base-on-rear contact (configuration 1,2) with symmetric base-on-rear contact (configuration 1,6) shows slightly higher strain development as a function of vertical displacement and significantly higher strain magnitudes for the rear link (on the right side) for the symmetric load case as shown in figure 17. Similar rates of strain development as a function of vertical displacement were observed for the other components on the right side, but the final strain magnitudes were significantly higher for the unsymmetric base contact as a result of initial conditions at shield setting. On the left side, both strain magnitude and rate of development per unit vertical displacement were significantly larger for the symmetric base configuration for the caving shield, front links, and rear links (fig. 18). This is expected since the base-on-rear configuration that appears on the left side for configuration 1,6 is a more severe loading conditions than the two-point base contact on the left side for configuration 1,2.

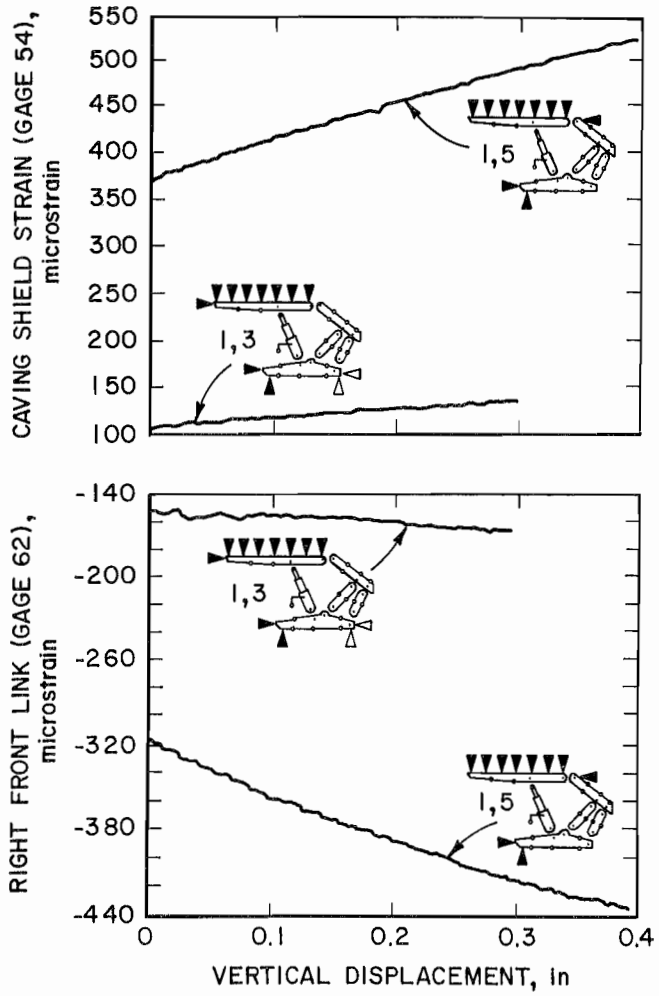


Figure 16.–Comparison of strain development in caving shield and right front link for symmetric and unsymmetric base-on-toe configurations.

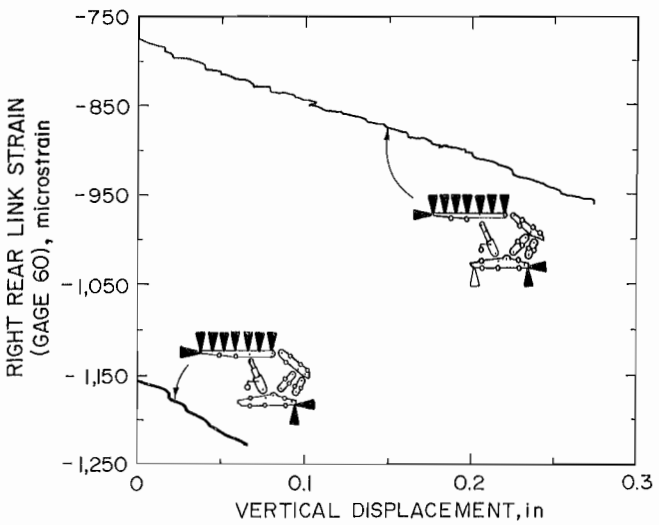


Figure 17.–Comparison of strain development for caving shield and right front link for symmetric and unsymmetric base-on-rear configurations.

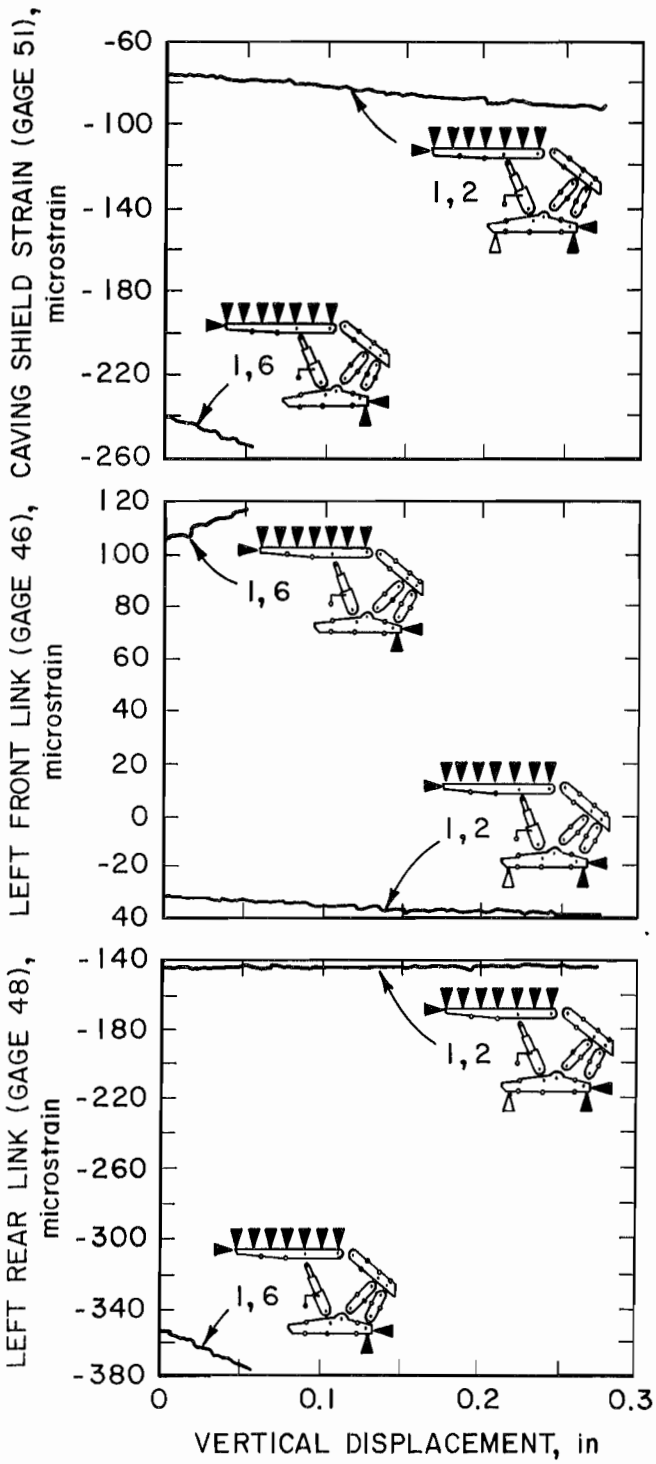


Figure 18.–Comparison of left side caving shield and link strains for symmetric and unsymmetric base-on-rear configurations.

## IDENTIFICATION OF CRITICAL LOAD CONTACT CONFIGURATIONS

Identification of critical load contact configurations was made by combining the results of like base shield responses and like canopy shield responses in the following manner. Component responses for like base contacts (figs. 10-11) were compared with component responses for like canopy contacts (figs. 14-15). Contact configurations were identified that had maximum component strains for one or more components for both like canopy and like base contacts. These critical contact configurations are shown in figure 19. As seen in the figure, the critical contact configurations are dominated by the base-on-toe and base-on-rear configurations. These continuation product maximum loading in all components except the canopy. Maximum canopy loading occurred for the symmetric two-point canopy and base contact.

Comparing strain development for the six configurations that produce maximum loading in the majority of shield components (see figures 20 through 23) indicates that the symmetric base-on-toe and base-on-rear configurations produce larger strain developments than the unsymmetric configurations employing these base contacts. Overall, the symmetric base-on-toe configuration is the most critical for a two-leg shield support.

In addition to the contact configurations identified in figure 19, it is suggested that a full canopy and base contact configuration be used as a test standard because full canopy and base contact is the desired contact. Other configurations (fig. 8) that are considered optional for critical load testing are configurations 3,2; 3,3, 6,1, 5,1, 3,4, 5,4 and 2,4. These configurations evaluate unsymmetric canopy contacts that maximize out-of-plane stress development in the canopy and concentrated load applications that produce leg imbalances. Figure 24 depicts all canopy and base contact configurations (required and optional) that are recommended for performance testing of two-leg longwall shields.

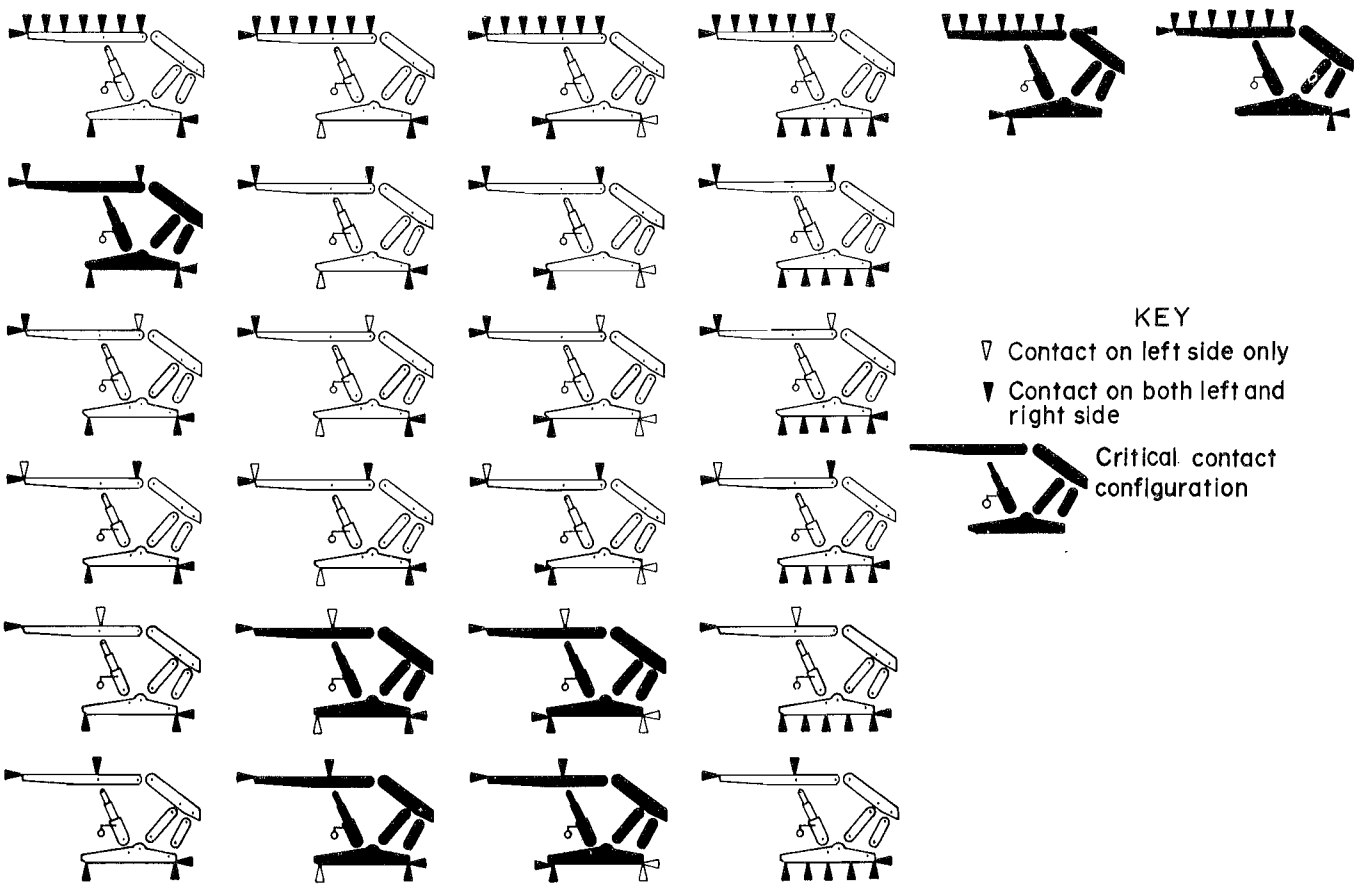


**Figure 19.–Critical load contact configurations for two-leg shield supports.**

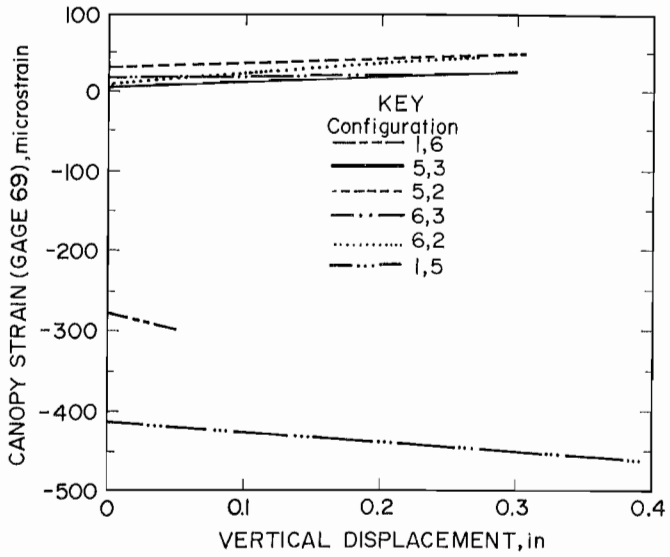


**Figure 20.–Comparison of strain development in canopy for critical load contact configurations.**

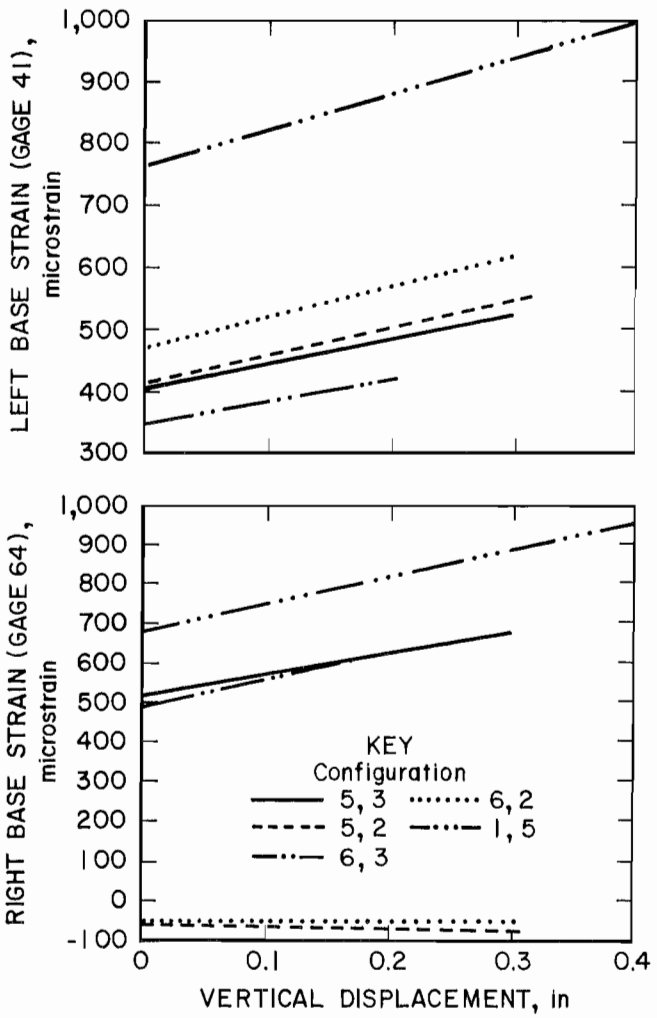


**Figure 21.–Comparison of strain development in base members for critical load contact configurations.**

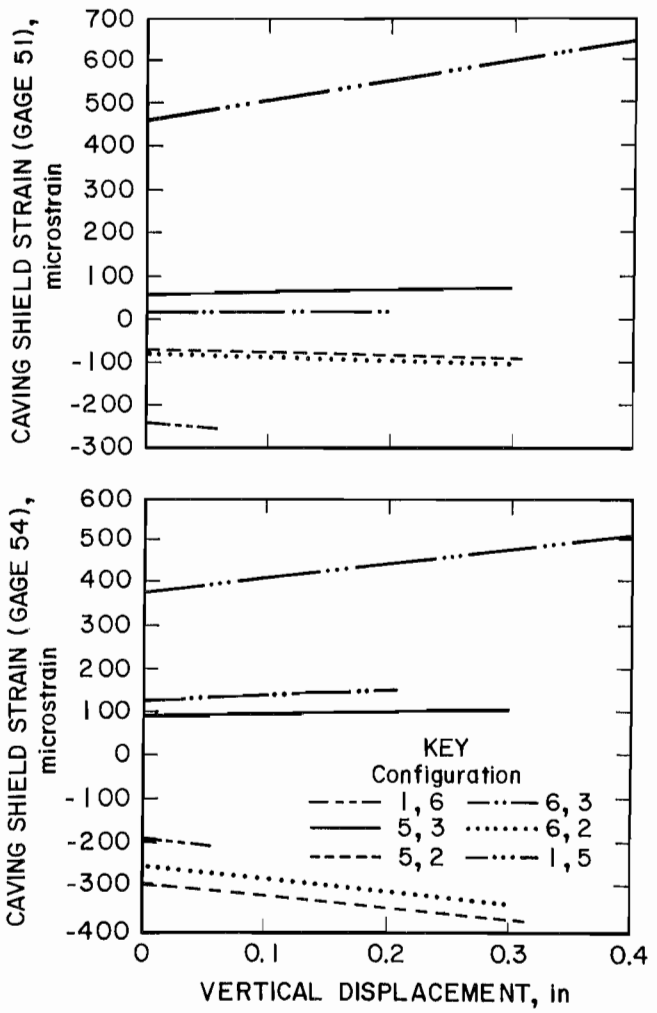


**Figure 22.–Comparison of strain development in caving shield for critical load contact configurations.**

The response of this particular shield to the contact configurations evaluated in this study are shown in figures 25 through 28. Figures 25 and 26 depict components which had strains below 10 pct yield. As seen in these figures, 23 of the 26 configurations tested have one or more components that were not stressed beyond 10 pct of the yield stress.

Figures 27 and 28 depict components that had strains above 50 pct yield. The canopy and rear link were the only components that were stressed beyond 50 pct of the yield stress for more than one contact configuration. Overall, the rear link developed the most strain, with maximum strain near yield for the symmetric base-on-rear configuration. Large rear link strains were developed for most of the symmetric or unsymmetric base-on-toe and base-on-rear configurations. However, it should be noted that this particular shield had a somewhat uncommon link design. The rear link was angled, presumably to provide

clearance in the collapsed shield position, such that the line of action of the link pins was not coincident with the centroid of the member. This link configuration produced considerable bending in the link and this bending was largely responsible for the large rear link strains observed in this particular shield. Overall, the canopy appears to be the weakest member of this shield, assuming a better rear link design could be incorporated.

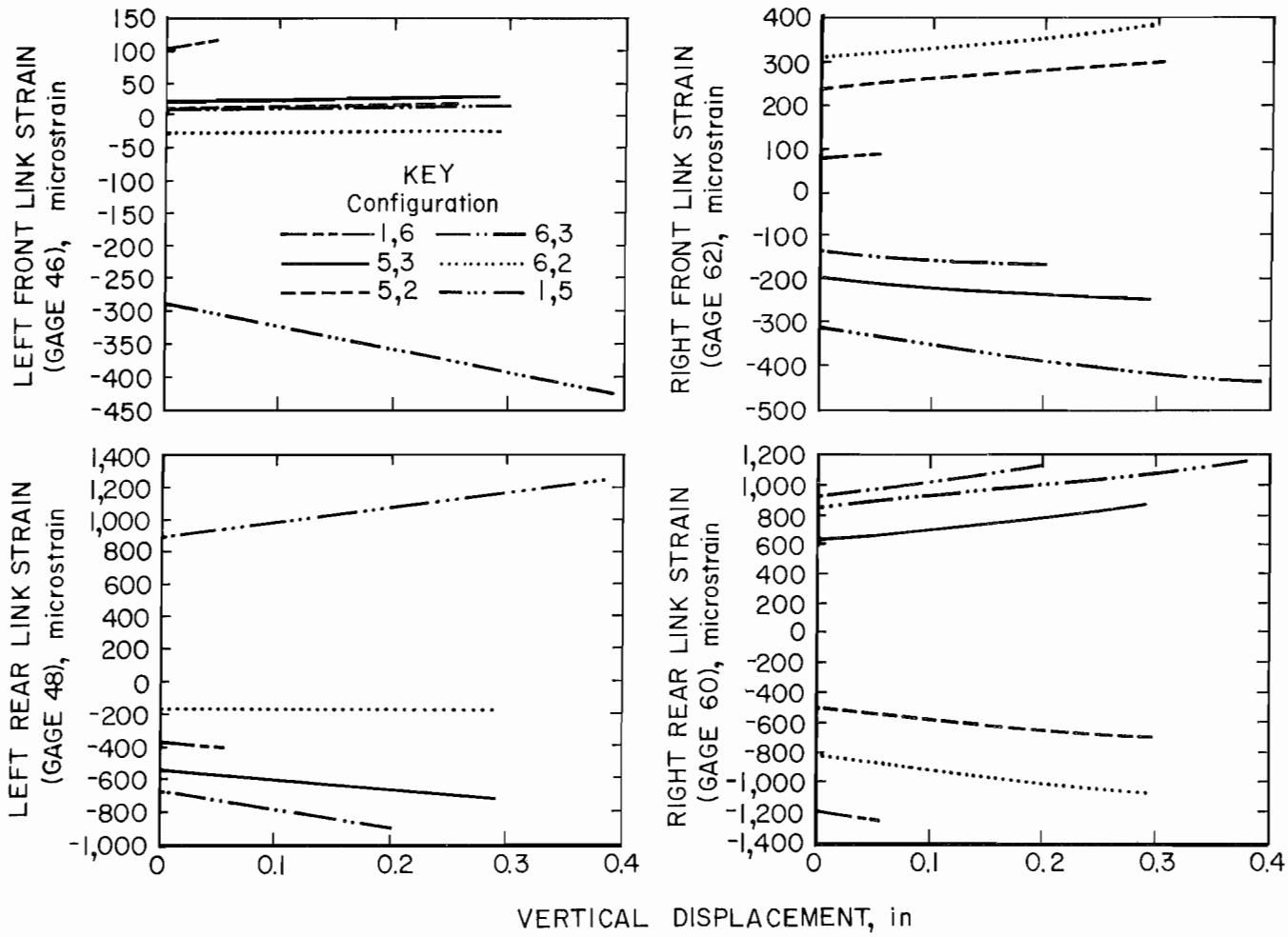


**Figure 23.–Comparison of strain development in lemniscate links for critical load contact configurations.**

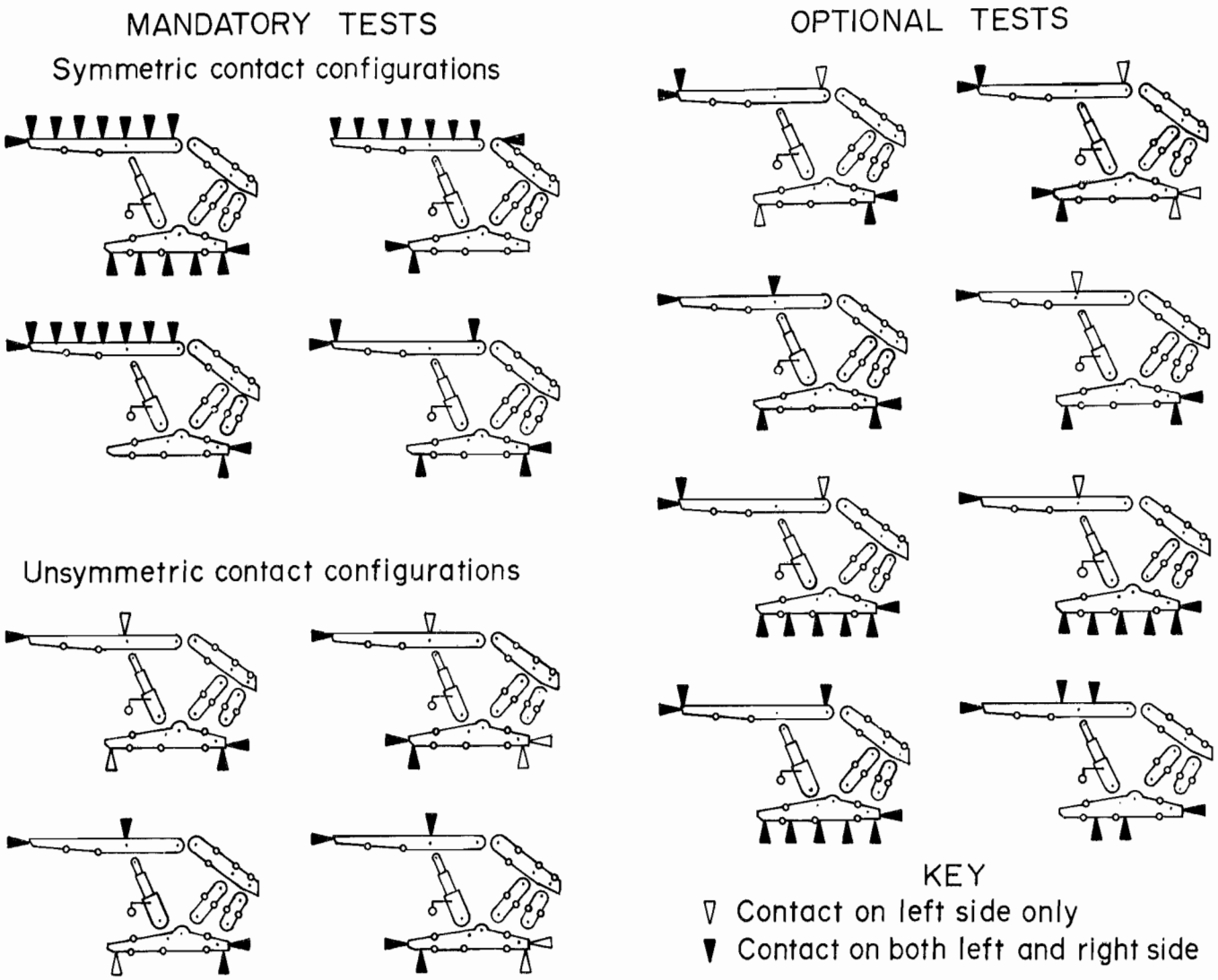


**Figure 24.–Recommended contact configurations for two-leg shield performance testing.**

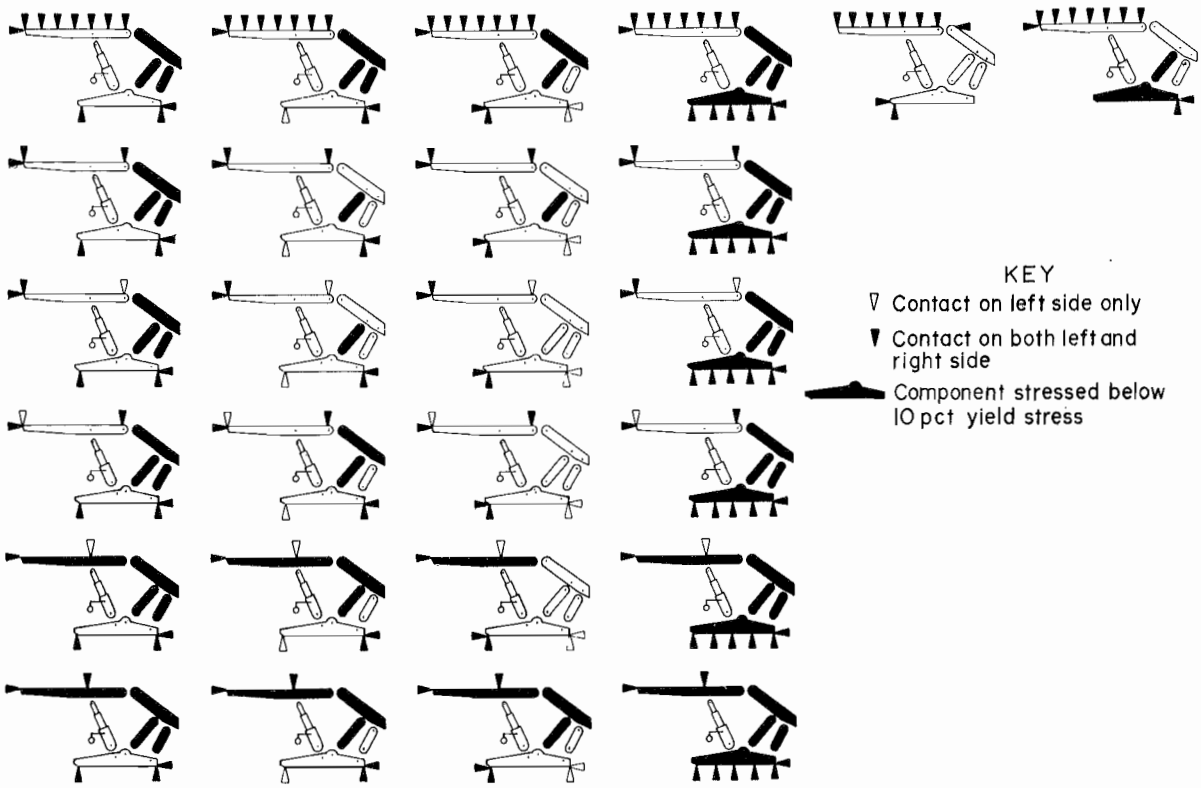


Figure 25.–Component left side strain magnitudes below 10 pct yield.

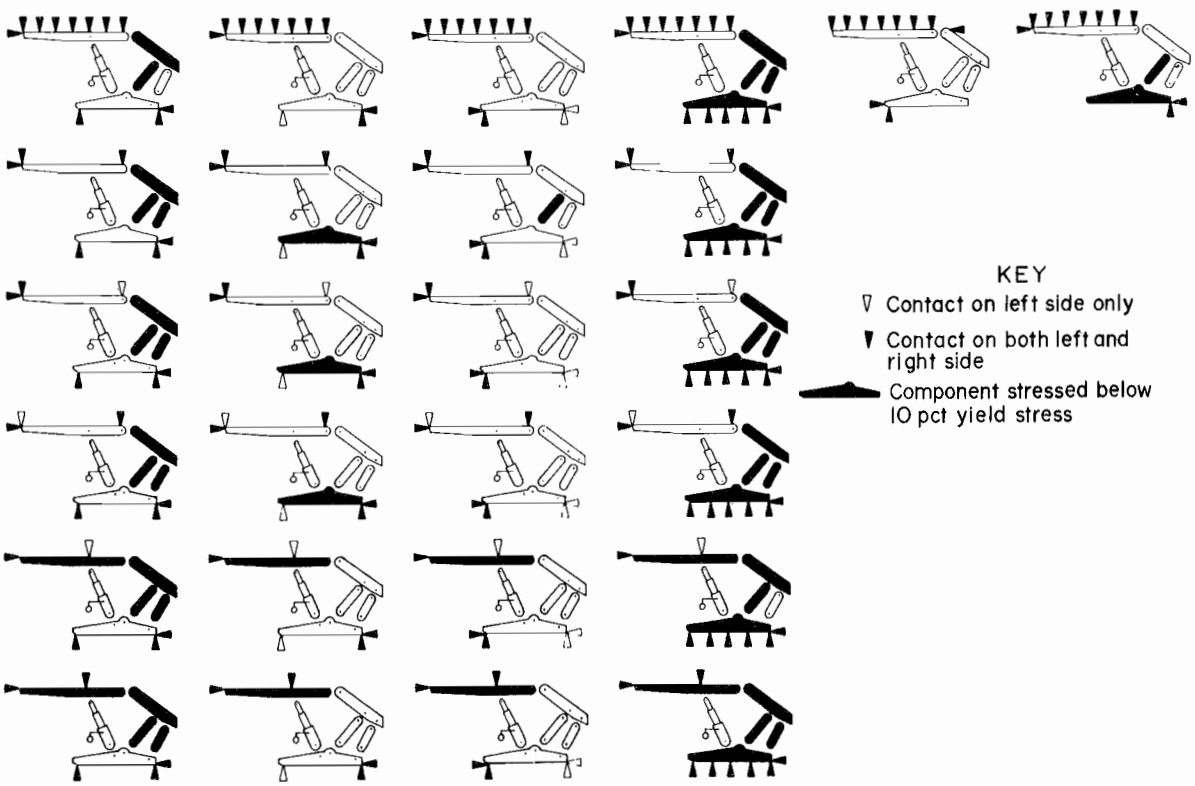


Figure 26.–Component right side strain magnitudes below 10 pct yield.

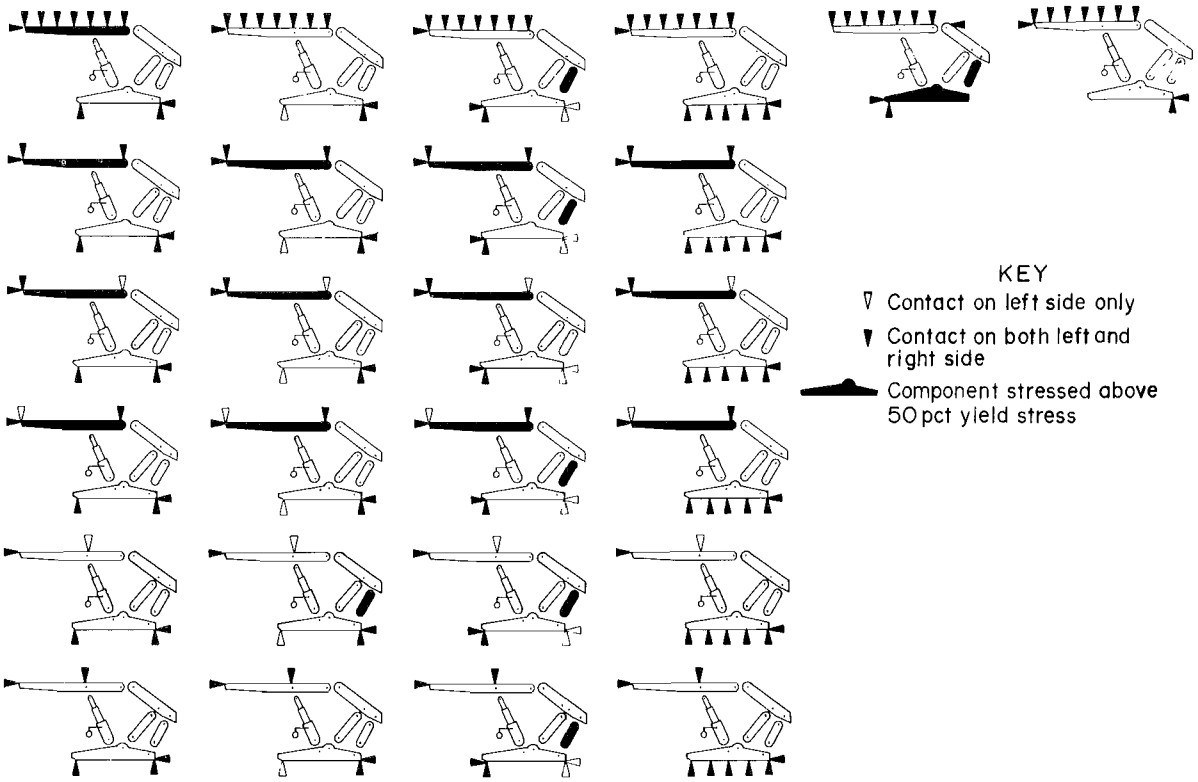


Figure 27.–Component left side strain magnitudes above 50 pct yield.

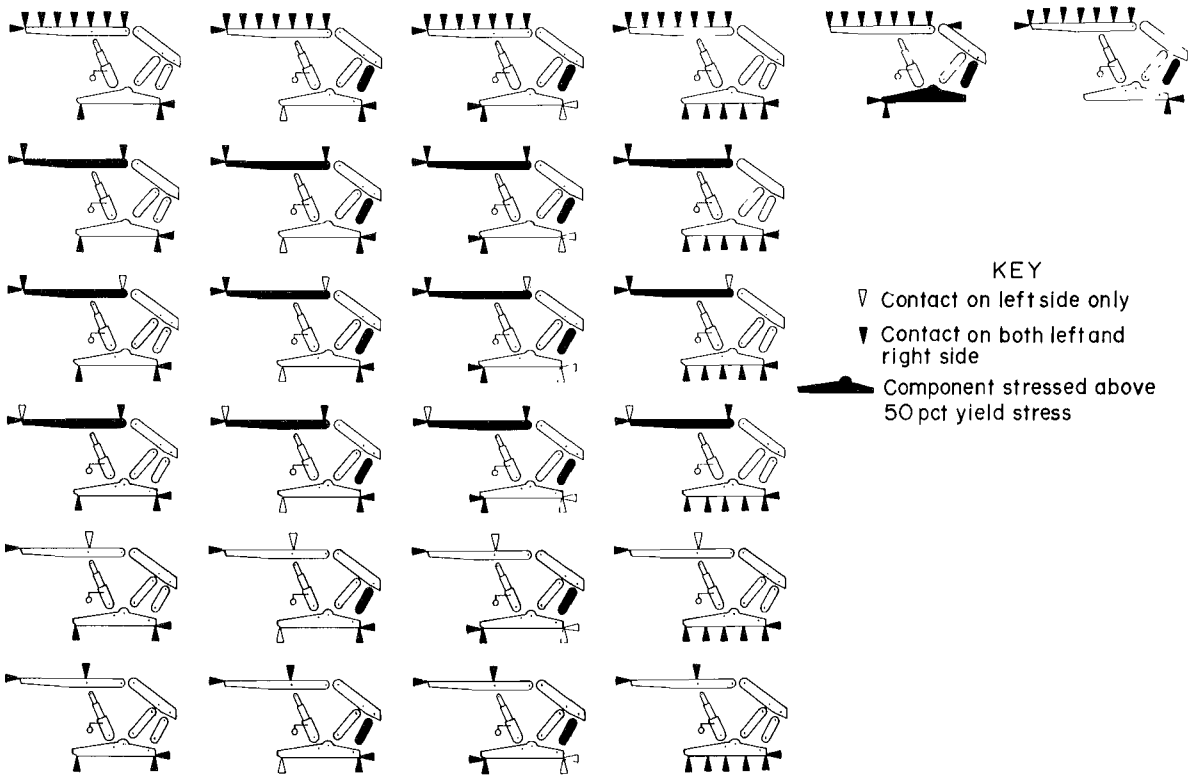


Figure 28.–Component right side strain magnitudes above 50 pct yield.

## EFFECT OF HORIZONTAL DISPLACEMENT

Appendix B documents component strains for each contact configuration at shield setting, after vertical displacement, and after (face-to-waste) horizontal displacement. Figures 29 and 30 illustrate the effect of horizontal displacement by identification of components that saw a reduction in strain as a result of the horizontal displacement. It is recalled from the test procedures that the horizontal displacement was preceded by a vertical displacement. Analysis of these figures indicates that with the exception of the base-on-toe configurations, the general trend is for the base strains to decrease and the caving shield and lemniscate links to increase in strain as a result of the horizontal displacement. For these configurations, more of the horizontal force acting on the shield is being transferred through the caving shield-lemniscate assembly instead of the leg cylinders. This causes a modest reduction in maximum base strains and a similar increase in caving shield and link strains.

Analysis of the shield mechanics provided in appendix A for the base-on-toe configuration reveals opposite behavior of the lemniscate links for horizontal displacement compared to vertical displacement. This accounts for the decrease in loading (strain) in the caving shield-lemniscate assembly for the base-on-toe configurations. It is also noted that this behavior holds true even for unsymmetric base-on-toe configurations as indicated in column 3 of figure 8. Notice also that the left-side behavior for these configurations was consistent with other base configurations because the left side employs a two-point base contact.

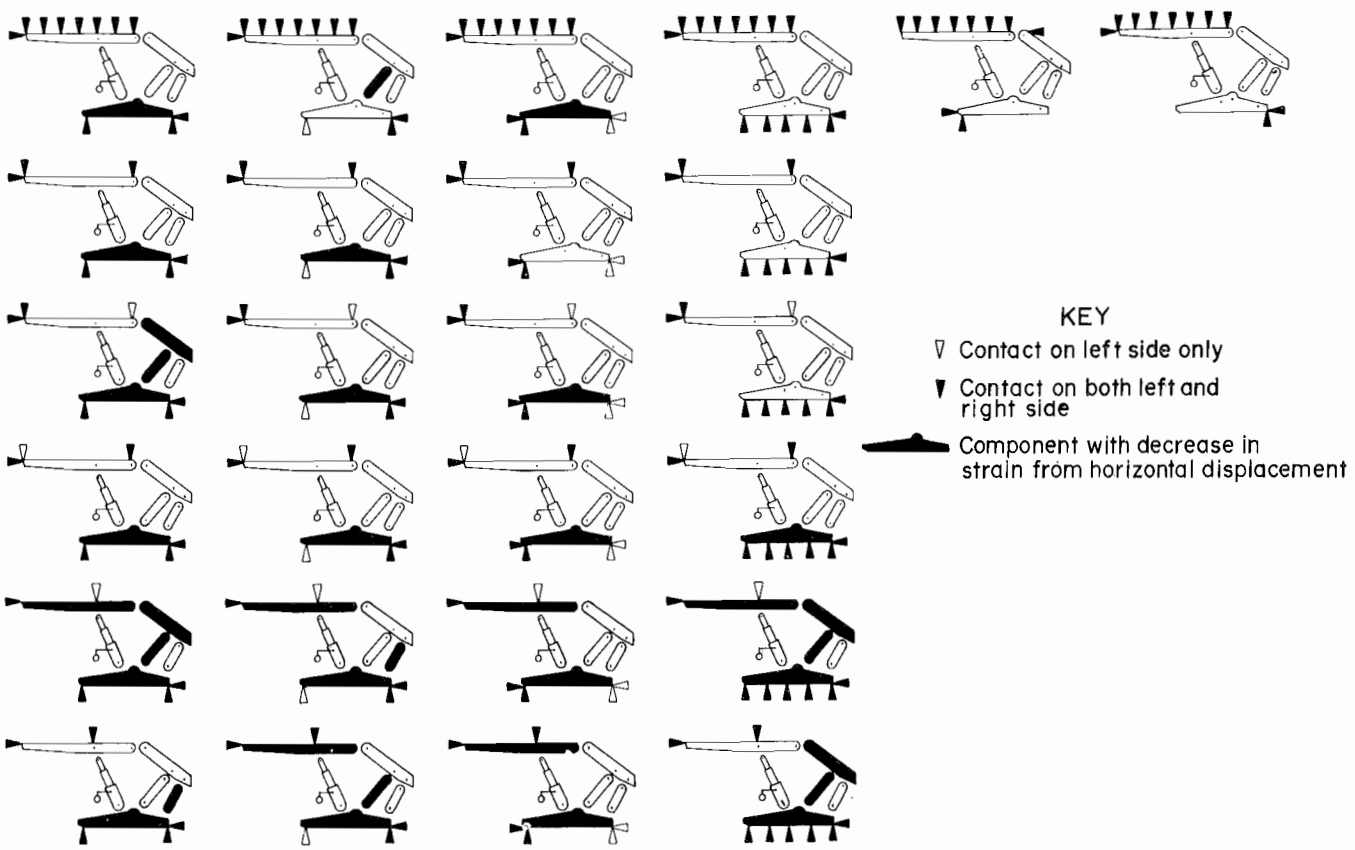


**Figure 29.–Effect of horizontal displacement on left side component strain development.**

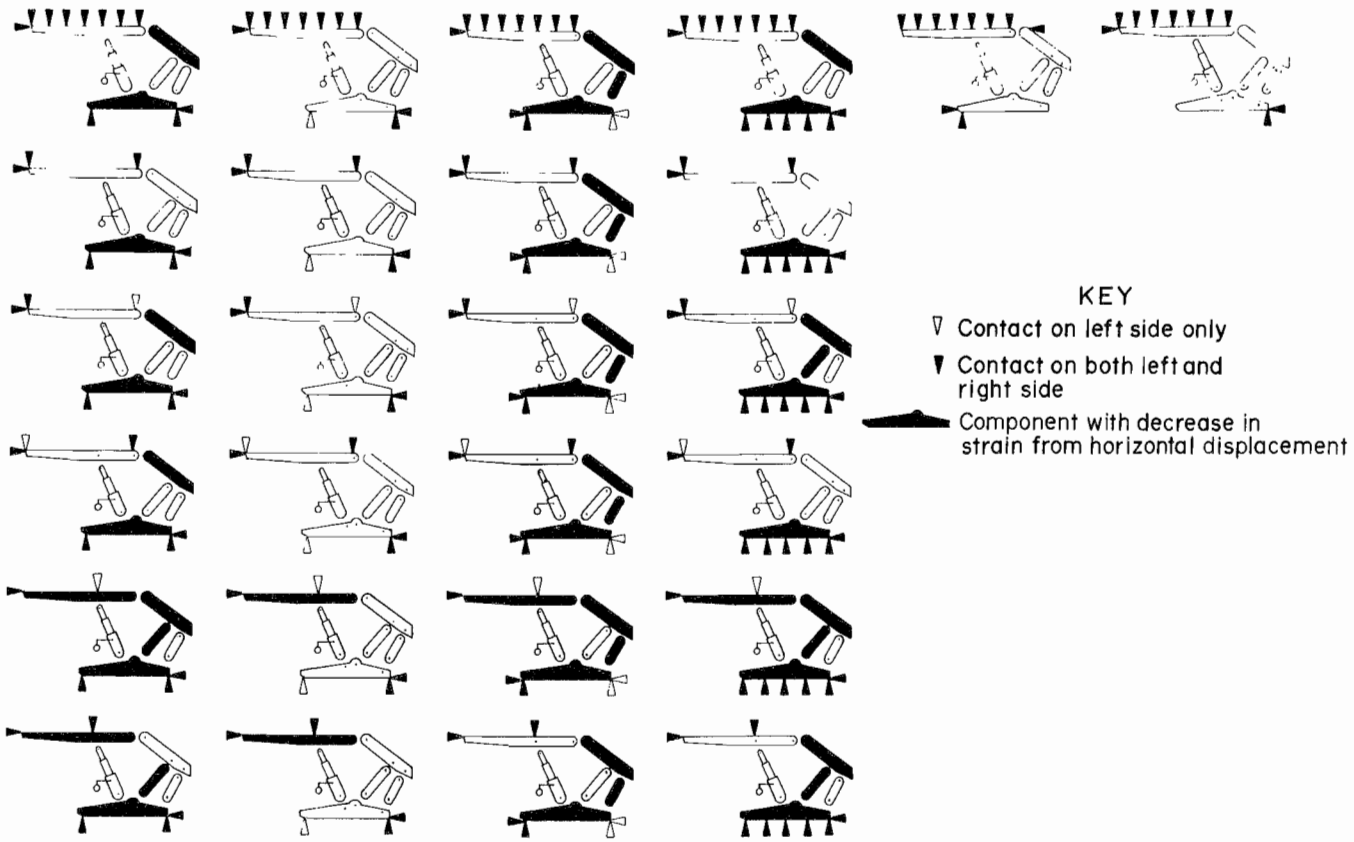


**Figure 30.–Effect of horizontal displacement on right side component strain development.**

A few other observations concerning the effect of (face-to-waste) horizontal displacement on strain development are as follows. It is important to be aware that initial conditions can significantly affect the impact of horizontal displacement. It is recalled from the test procedures that the shield was initially horizontally constrained prior to the setting operation to remove pin-clevis tolerance and allow full participation of the caving shield-lemniscate assembly in the shield's load transfer mechanics. If the shield is not horizontally constrained in this fashion, the effect of horizontal displacement might be negligible. Furthermore, if the canopy and base are not horizontally restrained during shield setting, the natural tendency for the leg cylinders is to cause the canopy to move forward (toward the face). This action is resisted by the caving shield-lemniscate assembly causing associated strain development in these components. Then, if a face-to-waste horizontal displacement is applied, the previously developed loading in the caving shield lemniscate assembly from the setting operation will be relieved. Hence, for unrestrained initial conditions, face-to-waste horizontal displacement will initially decrease not increase component stress development.

## CONCLUSIONS

The Bureau recognizes the importance of longwall mining to the economy and safety of underground coal mining and is conducting research to optimize support selection and design. It is concluded that this study of two-leg shield response to unsymmetric load conditions provides vital information necessary to develop more effective methodologies for performance testing these support systems. The major accomplishment of this study is the identification of critical load configurations for both symmetric and unsymmetric canopy and base contacts.

Observations and conclusions formed from this study are summarized as follows.

- In general, the behavior of a two-leg shield support is determined by the base contact configuration. Base contacts dominate over most canopy contacts and largely determine stress development in the base members and caving shield-lemniscate assembly. The only exception is unsymmetric canopy contact, with one contact missing at the rear of the canopy. It appears that this canopy

configuration may dominate shield mechanics for symmetric two-point base contacts with stiff base designs.

- For split-base shield designs, left- and right-side base members behave as independent units as contact on one base unit does not significantly affect the response of the other base unit. Unsymmetric base contacts are derived by different contact on the left base unit compared to the right base unit.
- Shield mechanics for the unsymmetric base contacts are consistent with symmetric base contact responses in that link behavior on either side of the shield is controlled by the respective base contact. For example, base configurations that produce opposite link behavior in symmetric base configurations will produce this opposite link behavior on the left side compared to the right side when these base configurations are combined in an unsymmetric base configuration.
- Load distribution in the left and right side of the shield is dominated by respective base contacts. The side with the more dominant base contact will develop the most load.
- The most critical contact configurations for two-leg shield supports are symmetric base-on-toe and base-on-rear configurations. These symmetric configurations produce larger strain development than unsymmetric configurations employing these base configurations. Excluding symmetric base-on-toe and symmetric base-on-rear configurations, comparison of like base contacts shows worst case canopy contacts are symmetric and unsymmetric canopy contact at the leg location. These canopy contacts maximize base activity (bending) by maximizing load transfer through the leg cylinders.
- The effect of horizontal displacement is usually to increase strain development in all but the base units provided pin-clevis tolerance is eliminated to allow full participation of the caving shield-lemniscate assembly in the shield load transfer mechanics.

# APPENDIX A.–SYMMETRIC CONTACT COMPONENT RESPONSES

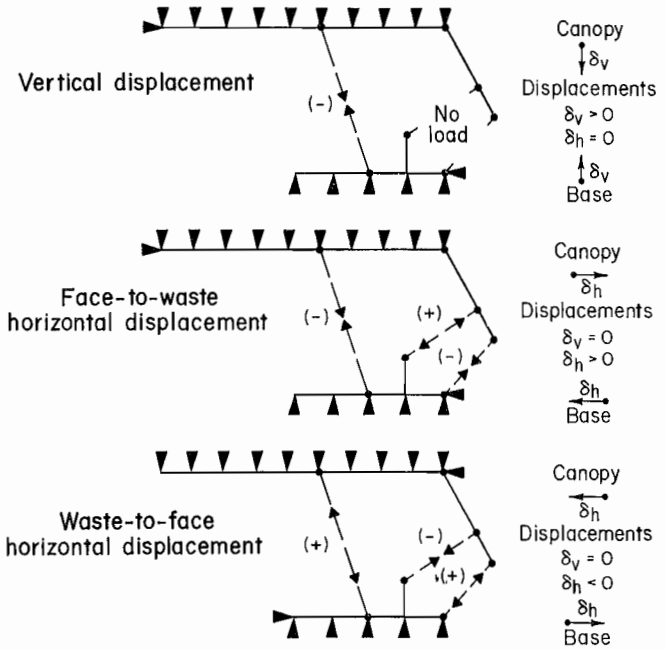


**Figure A-1.–Component responses for full canopy and base contact.**

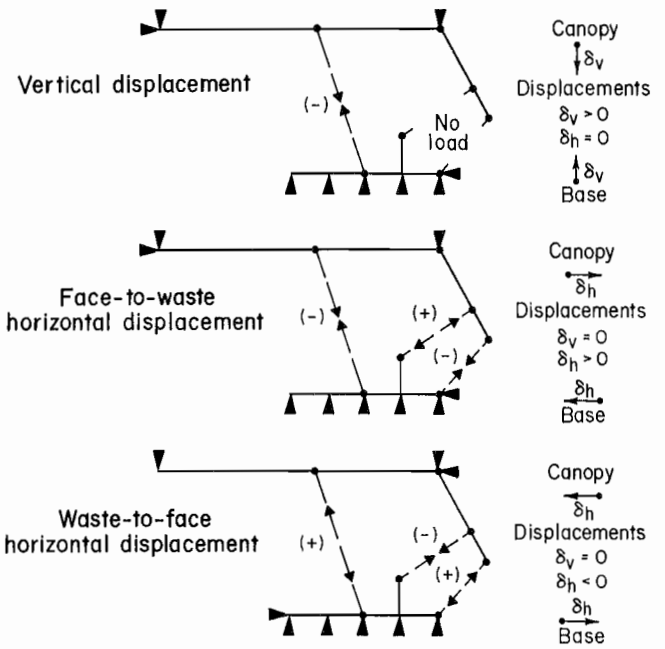


**Figure A-2.–Component responses for two-point canopy contact with full base contact.**

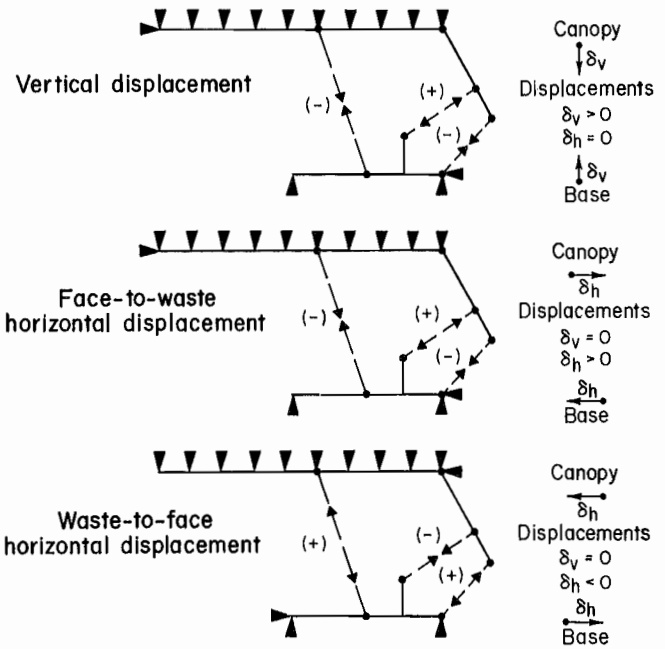


**Figure A-3.–Component responses for two-point base contact with full canopy contact.**

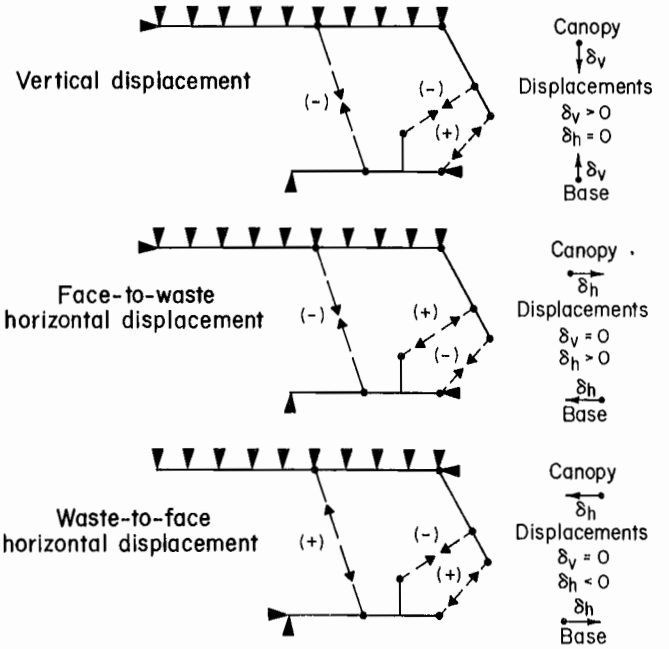


**Figure A-4.–Component responses for base-on-toe contact with full canopy contact.**

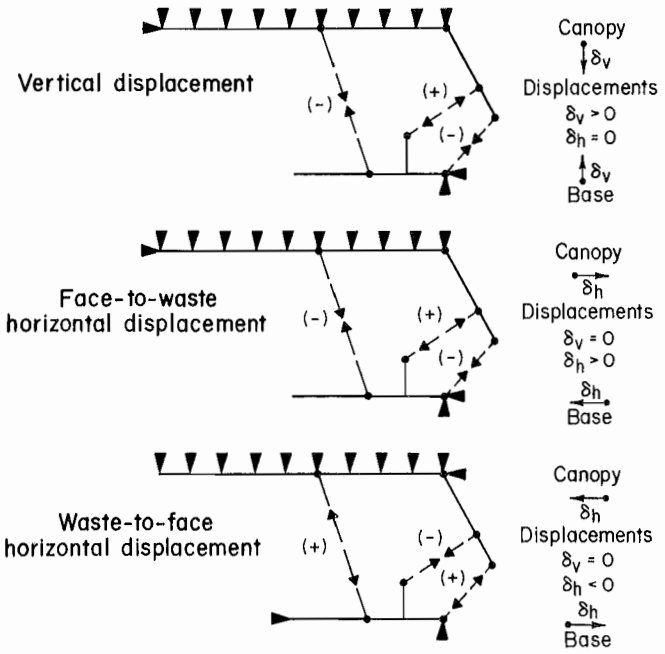


**Figure A-5.–Component responses for base-on-rear contact with full canopy contact.**

# APPENDIX B.–MEASURED COMPONENT STRAINS FOR SYMMETRIC-UNSYMMETRIC CONTACT CONFIGURATION

The tabulations in this appendix show strain (microstrain) or pressure (pounds per square inch) for each of the 28 strain gages and 2 pressure transducers after the support is set (initial condition), after vertical displacement, and after horizontal displacement. Figure 5 of the main text shows the instrumentation locations and figure 8 shows the test configurations.

| Component and gage | Test configuration 1,1 | | | Test configuration 1,2 | | |
|---|---|---|---|---|---|---|
| | Initial condition | After displacement | | Initial condition | After displacement | |
| | | Vertical | Horizontal | | Vertical | Horizontal |
| STRAIN | | | | | | |
| Canopy: | | | | | | |
| 68 | -567.38 | -708.98 | -785.16 | -608.40 | -700.20 | -768.55 |
| 69 | -425.78 | -525.39 | -582.03 | -449.22 | -516.60 | -568.36 |
| Left base: | | | | | | |
| 40 | 206.05 | 282.23 | 314.45 | 65.43 | 104.49 | 143.55 |
| 41 | 407.23 | 570.31 | 533.20 | 461.91 | 583.01 | 584.96 |
| 42 | 144.53 | 182.62 | 193.36 | 197.27 | 250.00 | 259.77 |
| 43 | -60.55 | -91.80 | -96.68 | -57.62 | -78.13 | -83.01 |
| 44 | -28.32 | -42.97 | -55.66 | -35.16 | -47.85 | -49.80 |
| Right base: | | | | | | |
| 63 | 253.91 | 345.70 | 367.19 | -6.84 | -8.79 | -8.79 |
| 64 | 347.66 | 508.79 | 458.01 | -42.97 | -54.69 | -65.43 |
| 65 | 254.88 | 324.22 | 338.87 | -76.17 | -119.14 | -169.92 |
| 66 | -95.70 | -138.67 | -141.60 | 14.65 | 15.63 | 20.51 |
| 67 | -59.57 | -81.06 | -86.91 | -26.37 | -35.16 | -49.80 |
| Caving shield: | | | | | | |
| 49 | 37.11 | 24.41 | 41.99 | 64.45 | 69.34 | 89.84 |
| 51 | -7.81 | -9.77 | -51.76 | -75.20 | -91.80 | -122.07 |
| 52 | -5.86 | -7.81 | -46.88 | -44.92 | -53.71 | -75.20 |
| 53 | -7.81 | -6.84 | -25.39 | -7.81 | -9.77 | -14.65 |
| 57 | -14.65 | -15.63 | -5.86 | 119.14 | 117.19 | 141.60 |
| 54 | 21.48 | 15.63 | 3.91 | -249.02 | -320.31 | -387.70 |
| 55 | 28.32 | 25.39 | 2.93 | -273.44 | -345.70 | -421.88 |
| 56 | 29.30 | 27.34 | 33.20 | 228.52 | 289.06 | 330.08 |
| Left front link: | | | | | | |
| 45 | 7.81 | 5.86 | 26.37 | -29.30 | -39.06 | -22.46 |
| 46 | 13.67 | 12.70 | 41.99 | -31.25 | -39.06 | -14.65 |
| Right front link: | | | | | | |
| 61 | -7.81 | -11.72 | 17.58 | 236.33 | 276.37 | 318.36 |
| 62 | -30.27 | -15.63 | 11.72 | 254.88 | 342.77 | 410.16 |
| Left rear link: | | | | | | |
| 47 | 8.79 | 10.74 | 24.41 | 26.37 | 25.39 | 25.39 |
| 48 | -73.24 | -83.98 | -139.65 | -143.55 | -143.55 | -143.55 |
| Right rear link: | | | | | | |
| 59 | 23.44 | 24.41 | 50.78 | 205.08 | 257.81 | 322.27 |
| 60 | -151.37 | -152.34 | -283.20 | -768.55 | -960.94 | -1,221.70 |
| PRESSURE | | | | | | |
| Left leg: 37 | 4,033.20 | 5,849.60 | 6,342.80 | 4,013.70 | 5,317.40 | 5,576.20 |
| Right leg: 38 | 4,028.30 | 5,878.90 | 6,430.70 | 3,989.30 | 4,838.90 | 5,678.70 |

| Component and gage | Test configuration 1,3 | | | Test configuration 1,4 | | |
|---|---|---|---|---|---|---|
| | Initial condition | After displacement | | Initial condition | After displacement | |
| | | Vertical | Horizontal | | Vertical | Horizontal |
| STRAIN | | | | | | |
| Canopy: | | | | | | |
| 68 | -560.55 | -648.44 | -663.09 | -572.27 | -698.24 | -770.51 |
| 69 | -418.95 | -481.45 | -491.21 | -425.78 | -514.65 | -566.41 |
| Left base: | | | | | | |
| 40 | 189.45 | 242.19 | 278.32 | NR | NR | NR |
| 41 | 375.00 | 485.35 | 422.85 | NR | NR | NR |
| 42 | 161.13 | 187.50 | 160.16 | NR | NR | NR |
| 43 | -55.66 | -75.20 | -57.62 | 5.86 | 8.79 | 7.81 |
| 44 | -38.09 | -46.88 | -56.64 | 3.91 | 5.86 | 7.81 |
| Right base: | | | | | | |
| 63 | 235.35 | 322.27 | 305.66 | NR | NR | NR |
| 64 | 559.57 | 749.02 | 711.91 | NR | NR | NR |
| 65 | 317.38 | 399.41 | 389.65 | NR | NR | NR |
| 66 | -126.95 | -167.97 | -162.11 | 28.32 | 41.02 | 38.09 |
| 67 | -58.59 | -69.34 | -68.36 | -12.70 | -15.63 | -20.51 |
| Caving shield: | | | | | | |
| 49 | -5.86 | -25.39 | 9.77 | 14.65 | 11.72 | 17.58 |
| 51 | 17.58 | 29.30 | -78.13 | 1.95 | 2.93 | -15.63 |
| 52 | -43.95 | -57.62 | -164.06 | 5.86 | 5.86 | -14.65 |
| 53 | 1.95 | 5.86 | 10.74 | 4.88 | 3.91 | .98 |
| 57 | 13.67 | -2.93 | 15.63 | 1.95 | .98 | 7.81 |
| 54 | 107.42 | 134.77 | 96.68 | 8.79 | 10.74 | .00 |
| 55 | 171.88 | 224.61 | 192.38 | 19.53 | 19.53 | 9.77 |
| 56 | 23.44 | 24.41 | 25.39 | 25.39 | 22.46 | 22.46 |
| Left front link: | | | | | | |
| 45 | 13.67 | 7.81 | 82.03 | -4.88 | -6.84 | 4.88 |
| 46 | 14.65 | 22.46 | 112.30 | .98 | .98 | 17.58 |
| Right front link: | | | | | | |
| 61 | -40.04 | -56.64 | -76.17 | 7.81 | 3.911 | 3.67 |
| 62 | -152.34 | -164.06 | -169.92 | -12.70 | -9.77 | 1.95 |
| Left rear link: | | | | | | |
| 47 | 153.32 | 205.08 | 271.48 | 8.79 | 4.88 | 23.44 |
| 48 | -724.61 | -972.66 | 1,260.70 | -33.20 | -32.23 | -96.68 |
| Right rear link: | | | | | | |
| 59 | -201.17 | -265.63 | -260.74 | 24.41 | 22.46 | 25.39 |
| 60 | 817.38 | 1,110.40 | 1,068.40 | -156.25 | -157.23 | -161.13 |
| PRESSURE | | | | | | |
| Left leg: 37 | 4,077.10 | 5,429.70 | 5,639.60 | 4,140.60 | 5,888.70 | 6,337.90 |
| Right leg: 38 | 4,072.30 | 5,131.80 | 5,112.30 | 4,150.40 | 5,874.00 | 6,342.80 |

NR No reading.

| Component and gage | Test configuration 1,5 | | | Test configuration 1,6 | | |
|---|---|---|---|---|---|---|
| | Initial condition | After displacement | | Initial condition | After displacement | |
| | | Vertical | Horizontal | | Vertical | Horizontal |
| STRAIN | | | | | | |
| Canopy: | | | | | | |
| 68 . . . . . | -548.83 | -611.33 | NR | -368.16 | -394.53 | -410.16 |
| 69 . . . . . | -415.04 | -459.96 | NR | -275.39 | -294.92 | -306.64 |
| Left base: | | | | | | |
| 40 . . . . . | 589.84 | 773.44 | NR | NR | NR | NR |
| 41 . . . . . | 758.79 | 995.12 | NR | NR | NR | NR |
| 42 . . . . . | 361.33 | 486.33 | NR | NR | NR | NR |
| 43 . . . . . | -180.66 | -246.09 | NR | 18.56 | 19.53 | 20.51 |
| 44 . . . . . | -35.16 | -44.92 | NR | 2.93 | 4.88 | .98 |
| Right base: | | | | | | |
| 63 . . . . . | 563.48 | 746.09 | NR | NR | NR | NR |
| 64 . . . . . | 675.78 | 944.34 | NR | NR | NR | NR |
| 65 . . . . . | 403.32 | 532.23 | NR | NR | NR | NR |
| 66 . . . . . | -228.52 | -310.55 | NR | 12.70 | 13.67 | 15.63 |
| 67 . . . . . | -59.57 | -73.24 | NR | -8.79 | -10.74 | -12.70 |
| Caving shield: | | | | | | |
| 49 . . . . . | -61.52 | -130.86 | NR | 118.16 | 124.02 | 131.84 |
| 51 . . . . . | 458.01 | 645.51 | NR | -240.23 | -254.88 | -276.37 |
| 52 . . . . . | 438.48 | 619.14 | NR | -243.16 | -257.81 | -280.27 |
| 53 . . . . . | 181.64 | 258.79 | NR | -22.46 | -18.56 | -16.60 |
| 57 . . . . . | -59.57 | -126.95 | NR | 79.10 | 80.08 | 83.98 |
| 54 . . . . . | 372.07 | 523.44 | NR | -191.41 | -206.05 | -221.68 |
| 55 . . . . . | 387.70 | 541.02 | NR | -201.17 | -214.84 | -228.52 |
| 56 . . . . . | 25.39 | 32.23 | NR | 107.42 | 119.14 | 126.95 |
| Left front link: | | | | | | |
| 45 . . . . . | -224.61 | -298.83 | NR | 68.36 | 70.31 | 76.17 |
| 46 . . . . . | -283.20 | -425.78 | NR | 104.49 | 117.19 | 128.91 |
| Right front link: | | | | | | |
| 61 . . . . . | -178.71 | -247.07 | NR | 74.22 | 77.15 | 78.13 |
| 62 . . . . . | -318.36 | -432.62 | NR | 68.36 | 77.15 | 82.03 |
| Left rear link: | | | | | | |
| 47 . . . . . | -229.49 | -303.71 | NR | 103.52 | 111.33 | 123.05 |
| 48 . . . . . | 919.92 | 1,254.90 | NR | -351.56 | -373.05 | -411.13 |
| Right rear link: | | | | | | |
| 59 . . . . . | -237.30 | -306.64 | NR | 243.16 | 261.72 | 271.48 |
| 60 . . . . . | 840.82 | 1,140.60 | NR | -1,150.40 | -1,215.80 | -1,263.70 |
| PRESSURE | | | | | | |
| Left leg: 37 . . . . . | 4,023.40 | 5,058.60 | NR | 1,992.20 | 2,021.50 | 2,109.40 |
| Right leg: 38 . . . . | 4,013.70 | 5,039.10 | NR | 1,997.10 | 2,041.00 | 2,143.60 |

NR No reading.

| Component and gage | Test configuration 2,1 | | | Test configuration 2,2 | | |
|---|---|---|---|---|---|---|
| | Initial condition | After displacement | | Initial condition | After displacement | |
| | | Vertical | Horizontal | | Vertical | Horizontal |
| STRAIN | | | | | | |
| Canopy: | | | | | | |
| 68 | -707.03 | -975.59 | -1,070.30 | -675.78 | -861.33 | -965.82 |
| 69 | -517.58 | -708.01 | -778.32 | -484.38 | -611.33 | -684.57 |
| Left base: | | | | | | |
| 40 | 138.67 | 168.95 | 180.66 | 203.13 | 258.79 | 287.11 |
| 41 | 352.54 | 480.47 | 439.45 | 387.70 | 497.07 | 412.11 |
| 42 | 110.35 | 135.74 | 148.44 | 171.88 | 206.05 | 200.20 |
| 43 | -62.50 | -84.96 | -92.77 | -58.59 | -79.10 | -71.29 |
| 44 | -30.27 | -40.04 | -43.95 | -37.11 | -45.90 | -53.71 |
| Right base: | | | | | | |
| 63 | 134.77 | 166.99 | 179.69 | -4.88 | -4.88 | -5.86 |
| 64 | 292.97 | 425.78 | 335.94 | -57.62 | -69.34 | -83.98 |
| 65 | 151.37 | 196.29 | 217.77 | -49.80 | -85.94 | -136.72 |
| 66 | -85.94 | -117.19 | -124.02 | 8.79 | 12.70 | 14.65 |
| 67 | -55.66 | -73.24 | -81.06 | -27.34 | -38.09 | -43.95 |
| Caving shield: | | | | | | |
| 49 | 7.81 | 4.88 | 6.84 | 61.52 | 67.38 | 96.68 |
| 51 | -4.88 | -6.84 | -6.84 | -100.59 | -114.26 | -194.34 |
| 52 | -.98 | -2.93 | -3.91 | -76.17 | -85.94 | -186.52 |
| 53 | -.98 | -.98 | -.98 | -17.58 | -18.56 | -33.20 |
| 57 | 6.84 | 5.86 | 6.84 | 80.08 | 73.24 | 117.19 |
| 54 | 3.91 | 1.95 | 1.95 | -260.74 | -328.13 | -412.11 |
| 55 | .98 | .98 | .00 | -263.67 | -335.94 | -412.11 |
| 56 | 4.88 | 4.88 | 4.88 | 219.73 | 278.32 | 272.46 |
| Left front link: | | | | | | |
| 45 | .98 | 1.95 | .98 | 4.88 | 3.91 | 14.65 |
| 46 | 3.91 | 5.86 | 7.81 | 7.81 | 10.74 | 37.11 |
| Right front link: | | | | | | |
| 61 | 6.84 | 4.88 | 6.84 | 209.96 | 247.07 | 252.93 |
| 62 | 5.86 | 7.81 | 6.84 | 253.91 | 325.20 | 344.73 |
| Left rear link: | | | | | | |
| 47 | 6.84 | 6.84 | 7.81 | 55.66 | 59.57 | 136.72 |
| 48 | -10.74 | -15.63 | -15.63 | -295.90 | -317.38 | -666.02 |
| Right rear link: | | | | | | |
| 59 | 11.72 | 11.72 | 12.70 | 206.05 | 261.72 | 297.85 |
| 60 | -74.22 | -74.22 | -76.17 | -777.34 | -1,010.70 | -1,207.00 |
| PRESSURE | | | | | | |
| Left leg: 37 | 4,033.20 | 5,522.50 | 5,869.10 | 4,008.80 | 5,014.60 | 5,200.20 |
| Right leg: 38 | 4,018.60 | 5,512.70 | 5,839.80 | 3,994.10 | 4,560.50 | 5,117.20 |

| Component and gage | Test configuration 2,3 | | | Test configuration 2,4 | | |
|---|---|---|---|---|---|---|
| | Initial condition | After displacement | | Initial condition | After displacement | |
| | | Vertical | Horizontal | | Vertical | Horizontal |
| STRAIN | | | | | | |
| Canopy: | | | | | | |
| 68 | -719.73 | -832.03 | -873.05 | -692.38 | -969.73 | -1,069.30 |
| 69 | -524.41 | -605.47 | -632.81 | -500.00 | -697.27 | -767.58 |
| Left base: | | | | | | |
| 40 | 114.26 | 125.00 | 181.64 | NR | NR | NR |
| 41 | 350.59 | 406.25 | 323.24 | NR | NR | NR |
| 42 | 143.55 | 157.23 | 120.12 | NR | NR | NR |
| 43 | -48.83 | -58.59 | -38.09 | 8.79 | 11.72 | 6.84 |
| 44 | -37.11 | -42.97 | -53.71 | -1.95 | 1.95 | 4.88 |
| Right base: | | | | | | |
| 63 | 157.23 | 193.36 | 184.57 | NR | NR | NR |
| 64 | 447.27 | 535.16 | 510.74 | NR | NR | NR |
| 65 | 284.18 | 332.03 | 322.27 | NR | NR | NR |
| 66 | -121.09 | -141.60 | -137.70 | 26.37 | 35.16 | 35.16 |
| 67 | -52.73 | -59.57 | -59.57 | -12.70 | -14.65 | -18.56 |
| Caving shield: | | | | | | |
| 49 | 1.95 | -17.58 | 18.56 | 7.81 | 6.84 | 13.67 |
| 51 | 16.60 | 20.51 | -100.59 | -1.95 | .00 | -18.56 |
| 52 | -46.88 | -53.71 | -180.66 | 4.88 | 8.79 | -14.65 |
| 53 | -2.93 | .98 | 13.67 | 3.91 | 4.88 | 1.95 |
| 57 | 30.27 | 11.72 | 41.99 | 5.86 | 2.93 | 10.74 |
| 54 | 119.14 | 136.72 | 90.82 | 13.67 | 15.63 | .00 |
| 55 | 185.55 | 219.73 | 183.59 | 18.56 | 22.46 | 7.81 |
| 56 | -1.95 | -0.98 | -3.91 | 23.44 | 23.44 | 23.44 |
| Left front link: | | | | | | |
| 45 | 15.63 | 8.79 | 94.73 | -14.65 | -18.5 | 63.91 |
| 46 | 14.65 | 20.51 | 122.07 | -7.81 | -9.77 | 16.60 |
| Right front link: | | | | | | |
| 61 | -46.88 | -47.85 | -69.34 | 6.84 | 3.91 | 15.63 |
| 62 | -137.70 | -158.20 | -164.06 | -15.63 | -13.67 | .00 |
| Left rear link: | | | | | | |
| 47 | 148.44 | 183.59 | 265.63 | 8.79 | 8.79 | 24.41 |
| 48 | -709.96 | -868.16 | -1,227.50 | -39.06 | -37.11 | -95.70 |
| Right rear link: | | | | | | |
| 59 | -213.87 | -241.21 | -237.30 | 21.48 | 21.48 | 25.39 |
| 60 | 865.23 | 1,017.60 | 979.49 | -154.30 | -153.32 | -161.13 |
| PRESSURE | | | | | | |
| Left leg: 37 | 3,999.00 | 4,638.70 | 4,838.90 | 4,023.40 | 5,483.40 | 5,830.10 |
| Right leg: 38 | 3,974.60 | 4,565.40 | 4,521.50 | 4,018.60 | 5,498.00 | 5,849.60 |

NR No reading.

| Component and gage | Test configuration 3,1 | | | Test configuration 3,2 | | |
|---|---|---|---|---|---|---|
| | Initial condition | After displacement | | Initial condition | After displacement | |
| | | Vertical | Horizontal | | Vertical | Horizontal |
| STRAIN | | | | | | |
| Canopy: | | | | | | |
| 68 | -655.27 | -916.99 | -1,003.90 | -643.55 | -810.55 | -916.02 |
| 69 | -485.35 | -668.95 | -732.42 | -468.75 | -583.01 | -658.20 |
| Left base: | | | | | | |
| 40 | 202.15 | 236.33 | 256.84 | 196.29 | 243.16 | 277.34 |
| 41 | 375.00 | 516.60 | 466.80 | 412.11 | 518.55 | 438.48 |
| 42 | 163.09 | 195.31 | 208.01 | 176.76 | 208.01 | 201.17 |
| 43 | -64.45 | -88.87 | -98.63 | -61.52 | -81.06 | -73.24 |
| 44 | -36.13 | -46.88 | -50.78 | -36.13 | -45.90 | -56.64 |
| Right base: | | | | | | |
| 63 | 163.09 | 180.66 | 187.50 | -3.91 | -4.88 | -4.88 |
| 64 | 326.17 | 462.89 | 373.05 | -59.57 | -67.38 | -76.17 |
| 65 | 136.72 | 173.83 | 183.59 | -47.85 | -100.59 | -140.63 |
| 66 | -88.87 | -118.16 | -119.14 | 8.79 | 13.67 | 12.70 |
| 67 | -51.76 | -67.38 | -73.24 | -29.30 | -36.13 | -42.97 |
| Caving shield: | | | | | | |
| 49 | -2.93 | -14.65 | -1.95 | 38.09 | 27.34 | 56.64 |
| 51 | 3.91 | 11.72 | -1.95 | -90.82 | -108.40 | -201.17 |
| 52 | 2.93 | 9.77 | -.98 | -75.20 | -91.80 | -194.34 |
| 53 | 2.93 | 5.86 | 3.91 | -4.88 | -.98 | 7.81 |
| 57 | 18.56 | 26.37 | 17.58 | 112.30 | 125.98 | 167.97 |
| 54 | 4.88 | 5.86 | .00 | -272.46 | -339.84 | -409.18 |
| 55 | 4.88 | 7.81 | -2.93 | -279.30 | -349.61 | -413.09 |
| 56 | .98 | -1.95 | 1.95 | 184.57 | 217.77 | 235.35 |
| Left front link: | | | | | | |
| 45 | .00 | -4.88 | 1.95 | 5.86 | 5.86 | 20.51 |
| 46 | -3.91 | -9.77 | 5.86 | 11.72 | 9.77 | 31.25 |
| Right front link: | | | | | | |
| 61 | 4.88 | .98 | 8.79 | 213.87 | 237.30 | 250.98 |
| 62 | 1.95 | -3.91 | 7.81 | 234.38 | 310.55 | 338.87 |
| Left rear link: | | | | | | |
| 47 | 5.86 | 4.88 | 5.86 | 64.45 | 80.08 | 141.60 |
| 48 | -13.67 | -13.67 | -18.56 | -329.10 | -402.34 | -669.92 |
| Right rear link: | | | | | | |
| 59 | 5.86 | .00 | 7.81 | 221.68 | 263.67 | 297.85 |
| 60 | -62.50 | -45.90 | -69.34 | -903.32 | -1,080.10 | -1,226.60 |
| PRESSURE | | | | | | |
| Left leg: 37 | 4,018.60 | 5,512.70 | 5,913.10 | 3,999.00 | 5,131.80 | 5,380.90 |
| Right leg: 38 | 4,003.90 | 5,307.60 | 5,522.50 | 3,979.50 | 4,570.30 | 5,170.90 |

| Component and gage | Test configuration 3,3 | | | Test configuration 3,4 | | |
|---|---|---|---|---|---|---|
| | Initial condition | After displacement | | Initial condition | After displacement | |
| | | Vertical | Horizontal | | Vertical | Horizontal |
| STRAIN | | | | | | |
| Canopy: | | | | | | |
| 68 | -703.13 | -865.23 | -921.88 | -692.38 | -919.92 | -1,010.70 |
| 69 | -513.67 | -625.98 | -665.04 | -506.84 | -669.92 | -735.35 |
| Left base: | | | | | | |
| 40 | 121.09 | 144.53 | 191.41 | NR | NR | NR |
| 41 | 361.33 | 462.89 | 327.15 | NR | NR | NR |
| 42 | 154.30 | 182.62 | 98.63 | NR | NR | NR |
| 43 | -51.76 | -69.34 | -37.11 | 10.74 | 12.70 | 8.79 |
| 44 | -41.02 | -49.80 | -62.50 | -2.93 | -1.95 | 3.91 |
| Right base: | | | | | | |
| 63 | 149.41 | 196.29 | 184.57 | NR | NR | NR |
| 64 | 456.05 | 592.77 | 546.88 | NR | NR | NR |
| 65 | 283.20 | 351.56 | 333.98 | NR | NR | NR |
| 66 | -121.09 | -151.37 | -142.58 | 30.27 | 39.06 | 33.20 |
| 67 | -50.78 | -60.55 | -57.62 | -12.70 | -14.65 | -20.51 |
| Caving shield: | | | | | | |
| 49 | -28.32 | -63.48 | 11.72 | -11.72 | -25.39 | -3.91 |
| 51 | 27.34 | 50.78 | -135.74 | 15.63 | 25.39 | -4.88 |
| 52 | -36.13 | -33.20 | -230.47 | 16.60 | 24.41 | -9.77 |
| 53 | 45.90 | 53.71 | 82.03 | 11.72 | 16.60 | 4.88 |
| 57 | 76.17 | 62.50 | 99.61 | 23.44 | 33.20 | 31.25 |
| 54 | 113.28 | 138.67 | 67.38 | 19.53 | 21.48 | -13.67 |
| 55 | 181.64 | 227.54 | 175.78 | 30.27 | 37.11 | .00 |
| 56 | -11.72 | -10.74 | -12.70 | 17.58 | 13.67 | 17.58 |
| Left front link: | | | | | | |
| 45 | 31.25 | 23.44 | 162.11 | -17.58 | -23.44 | .00 |
| 46 | 30.27 | 32.23 | 203.13 | -22.46 | -22.46 | 9.77 |
| Right front link: | | | | | | |
| 61 | -89.84 | -121.09 | -141.60 | .00 | -10.74 | -6.84 |
| 62 | -169.92 | -211.91 | -212.89 | -36.13 | -42.97 | -24.41 |
| Left rear link: | | | | | | |
| 47 | 124.02 | 158.20 | 264.65 | 5.86 | 1.95 | 21.48 |
| 48 | -576.17 | -732.42 | -1,160.20 | -20.51 | -9.77 | -96.68 |
| Right rear link: | | | | | | |
| 59 | -200.20 | -250.00 | -241.21 | 9.77 | 5.86 | 21.48 |
| 60 | 774.41 | 991.21 | 940.43 | -142.58 | -137.70 | -161.13 |
| PRESSURE | | | | | | |
| Left leg: 37 | 4,047.90 | 5,185.50 | 5,483.40 | 4,155.30 | 5,644.50 | 6,088.90 |
| Right leg: 38 | 4,023.40 | 4,877.90 | 4,741.20 | 4,106.40 | 5,410.20 | 5,585.90 |

NR No reading.

| Component and gage | Test configuration 4,1 | | | Test configuration 4,2 | | |
|---|---|---|---|---|---|---|
| | Initial condition | After displacement | | Initial condition | After displacement | |
| | | Vertical | Horizontal | | Vertical | Horizontal |
| STRAIN | | | | | | |
| Canopy: | | | | | | |
| 68 | -689.45 | -970.70 | -1,062.50 | -681.64 | -863.28 | -924.80 |
| 69 | -497.07 | -698.24 | -764.65 | -485.35 | -612.30 | -655.27 |
| Left base: | | | | | | |
| 40 | 148.44 | 179.69 | 190.43 | 198.24 | 247.07 | 265.63 |
| 41 | 333.01 | 464.84 | 416.99 | 408.20 | 514.65 | 473.63 |
| 42 | 120.12 | 143.55 | 158.20 | 166.99 | 199.22 | 204.10 |
| 43 | -61.52 | -84.96 | -94.73 | -60.55 | -78.13 | -75.20 |
| 44 | -31.25 | -41.02 | -46.88 | -37.11 | -43.95 | -46.88 |
| Right base: | | | | | | |
| 63 | 116.21 | 151.37 | 162.11 | -6.84 | -6.84 | -6.84 |
| 64 | 330.08 | 471.68 | 425.78 | -52.73 | -61.52 | -69.34 |
| 65 | 111.33 | 157.23 | 172.85 | -39.06 | -92.77 | -121.09 |
| 66 | -86.91 | -119.14 | -125.00 | 9.77 | 12.70 | 12.70 |
| 67 | -51.76 | -68.36 | -75.20 | -33.20 | -41.02 | -45.90 |
| Caving shield: | | | | | | |
| 49 | 4.88 | 3.91 | 5.86 | 58.59 | 67.38 | 81.06 |
| 51 | -4.88 | -5.86 | -8.79 | -98.63 | -114.26 | -153.32 |
| 52 | -2.93 | -2.93 | -4.88 | -69.34 | -81.06 | -129.88 |
| 53 | -.98 | -1.95 | -1.95 | -13.67 | -15.63 | -26.37 |
| 57 | 7.81 | 8.79 | 7.81 | 60.55 | 53.71 | 79.10 |
| 54 | 2.93 | 1.95 | .98 | -269.53 | -339.84 | -387.70 |
| 55 | 1.95 | 1.95 | .98 | -278.32 | -346.68 | -389.65 |
| 56 | 4.88 | 2.93 | 3.91 | 225.59 | 284.18 | 290.04 |
| Left front link: | | | | | | |
| 45 | .98 | .98 | .98 | 7.81 | 5.86 | 5.86 |
| 46 | 4.88 | 5.86 | 6.84 | 9.77 | 11.72 | 20.51 |
| Right front link: | | | | | | |
| 61 | 5.86 | 5.86 | 8.79 | 211.91 | 250.00 | 261.72 |
| 62 | 5.86 | 6.84 | 6.84 | 254.88 | 334.96 | 355.47 |
| Left rear link: | | | | | | |
| 47 | 5.86 | 5.86 | 5.86 | 37.11 | 41.99 | 84.96 |
| 48 | -14.65 | -15.63 | -17.58 | -204.10 | -233.40 | -427.73 |
| Right rear link: | | | | | | |
| 59 | 8.79 | 9.77 | 11.72 | 238.28 | 292.97 | 309.57 |
| 60 | -73.24 | -72.27 | -80.08 | -975.59 | 1,180.70 | -1,258.80 |
| PRESSURE | | | | | | |
| Left leg: 37 | 4,023.40 | 5,473.60 | 5,791.00 | 4,028.30 | 5,058.60 | 5,170.90 |
| Right leg: 38 | 4,023.40 | 5,459.00 | 5,815.40 | 4,008.80 | 4,716.80 | 5,112.30 |

| Component and gage | Test configuration 4,3 | | | Test configuration 4,4 | | |
|---|---|---|---|---|---|---|
| | Initial condition | After displacement | | Initial condition | After displacement | |
| | | Vertical | Horizontal | | Vertical | Horizontal |
| STRAIN | | | | | | |
| Canopy: | | | | | | |
| 68 | -678.71 | -923.83 | -974.61 | -702.15 | -921.88 | -1,016.60 |
| 69 | -491.21 | -665.04 | -699.22 | -498.05 | -654.30 | -721.68 |
| Left base: | | | | | | |
| 40 | 131.84 | 171.88 | 216.80 | NR | NR | NR |
| 41 | 345.70 | 464.84 | 328.13 | NR | NR | NR |
| 42 | 164.06 | 188.48 | 110.35 | NR | NR | NR |
| 43 | -52.73 | -74.22 | -43.95 | 7.81 | 10.74 | 6.84 |
| 44 | -41.02 | -53.71 | -67.38 | .98 | 1.95 | 5.86 |
| Right base: | | | | | | |
| 63 | 159.18 | 223.63 | 210.94 | NR | NR | NR |
| 64 | 454.10 | 642.58 | 591.80 | NR | NR | NR |
| 65 | 290.04 | 380.86 | 362.30 | NR | NR | NR |
| 66 | -122.07 | -162.11 | -154.30 | 28.32 | 34.18 | 32.23 |
| 67 | -50.78 | -62.50 | -60.55 | -11.72 | -13.67 | -18.56 |
| Caving shield: | | | | | | |
| 49 | -53.71 | -75.20 | -12.70 | 9.77 | 9.77 | 14.65 |
| 51 | 33.20 | 49.80 | -139.65 | 2.93 | 2.93 | -16.60 |
| 52 | -31.25 | -40.04 | -243.16 | 7.81 | 8.79 | -14.65 |
| 53 | 44.92 | 50.78 | 78.13 | 4.88 | 3.91 | .98 |
| 57 | 47.85 | 42.97 | 71.29 | 3.91 | 2.93 | 10.74 |
| 54 | 110.35 | 151.37 | 69.34 | 10.74 | 10.74 | .00 |
| 55 | 182.62 | 249.02 | 192.38 | 16.60 | 18.56 | 8.79 |
| 56 | -10.74 | -8.79 | -13.67 | 22.46 | 23.44 | 23.44 |
| Left front link: | | | | | | |
| 45 | 22.46 | 19.53 | 160.16 | -13.67 | -18.56 | 3.91 |
| 46 | 24.41 | 33.20 | 203.13 | -9.77 | -9.77 | 14.65 |
| Right front link: | | | | | | |
| 61 | -98.63 | -147.46 | -165.04 | 8.79 | 1.95 | 15.63 |
| 62 | -177.73 | -217.77 | -218.75 | -12.70 | -11.72 | .00 |
| Left rear link: | | | | | | |
| 47 | 134.77 | 175.78 | 289.06 | 9.77 | 6.84 | 21.48 |
| 48 | -615.23 | -821.29 | -1,281.30 | -42.97 | -39.06 | -97.66 |
| Right rear link: | | | | | | |
| 59 | -204.10 | -283.20 | -275.39 | 20.51 | 22.46 | 24.41 |
| 60 | 797.85 | 1,120.10 | 1,060.50 | -156.25 | -156.25 | -162.11 |
| PRESSURE | | | | | | |
| Left leg: 37 | 4,052.70 | 5,507.80 | 5,849.60 | 4,194.30 | 5,502.90 | 5,839.80 |
| Right leg: 38 | 4,023.40 | 5,210.00 | 5,073.20 | 4,194.30 | 5,595.70 | 5,976.60 |

NR No reading.

| Component and gage | Test configuration 5,1 | | | Test configuration 5,2 | | |
|---|---|---|---|---|---|---|
| | Initial condition | After displacement | | Initial condition | After displacement | |
| | | Vertical | Horizontal | | Vertical | Horizontal |
| STRAIN | | | | | | |
| Canopy: | | | | | | |
| 68 | 2.93 | 33.20 | -27.34 | 39.06 | 58.59 | 21.48 |
| 69 | -7.81 | 14.65 | -29.30 | 33.20 | 49.80 | 19.53 |
| Left base: | | | | | | |
| 40 | 212.89 | 284.18 | 321.29 | 222.66 | 296.88 | 324.22 |
| 41 | 405.27 | 576.17 | 549.80 | 415.04 | 548.83 | 520.51 |
| 42 | 221.68 | 290.04 | 302.73 | 210.94 | 238.28 | 246.09 |
| 43 | -69.34 | -101.56 | -108.40 | -64.45 | -91.80 | -98.63 |
| 44 | -44.92 | -60.55 | -64.45 | -41.99 | -52.73 | -58.59 |
| Right base: | | | | | | |
| 63 | 154.30 | 174.80 | 195.31 | -5.86 | -6.84 | -4.88 |
| 64 | 304.69 | 428.71 | 333.98 | -53.71 | -63.48 | -73.24 |
| 65 | 98.63 | 138.67 | 145.51 | -116.21 | -150.39 | -177.73 |
| 66 | -91.80 | -122.07 | -117.19 | 9.77 | 13.67 | 17.58 |
| 67 | -40.04 | -57.62 | -63.48 | -22.46 | -32.23 | -40.04 |
| Caving shield: | | | | | | |
| 49 | -55.66 | -87.89 | -65.43 | 10.74 | 1.951 | 3.67 |
| 51 | 51.76 | 64.45 | 16.60 | -68.36 | -89.84 | -120.12 |
| 52 | 35.16 | 49.80 | 8.79 | -91.80 | -107.42 | -135.74 |
| 53 | 24.41 | 35.16 | 67.38 | 29.30 | 34.18 | 42.97 |
| 57 | 92.77 | 107.42 | 124.02 | 174.80 | 196.29 | 224.61 |
| 54 | 17.58 | 18.56 | -1.95 | -298.83 | -369.14 | -412.11 |
| 55 | 24.41 | 32.23 | -1.95 | -280.27 | -352.54 | -401.37 |
| 56 | -19.53 | -19.53 | -19.53 | 145.51 | 182.62 | 201.17 |
| Left front link: | | | | | | |
| 45 | -4.88 | -15.63 | .98 | 3.91 | 3.91 | 7.81 |
| 46 | -18.56 | -20.51 | .00 | 12.70 | 10.74 | 12.70 |
| Right front link: | | | | | | |
| 61 | -15.63 | -16.60 | 4.88 | 242.19 | 262.70 | 267.58 |
| 62 | -35.16 | -45.90 | -7.81 | 228.52 | 293.95 | 325.20 |
| Left rear link: | | | | | | |
| 47 | 5.86 | 4.88 | 17.58 | 174.80 | 183.59 | 177.73 |
| 48 | -11.72 | -10.74 | -24.41 | -822.27 | -860.35 | -835.94 |
| Right rear link: | | | | | | |
| 59 | -21.48 | -28.32 | -11.72 | 128.91 | 178.71 | 215.82 |
| 60 | -24.41 | -15.63 | -50.78 | -481.45 | -684.57 | -856.45 |
| PRESSURE | | | | | | |
| Left leg: 37 | 4,052.70 | 5,927.70 | 6,450.20 | 4,023.40 | 5,576.20 | 5,991.20 |
| Right leg: 38 | 4,028.30 | 5,249.00 | 5,478.50 | 3,955.10 | 4,638.70 | 5,263.70 |

| Component and gage | Test configuration 5,3 | | | Test configuration 5,4 | | |
|---|---|---|---|---|---|---|
| | Initial condition | After displacement | | Initial condition | After displacement | |
| | | Vertical | Horizontal | | Vertical | Horizontal |
| STRAIN | | | | | | |
| Canopy: | | | | | | |
| 68 | 14.65 | 43.95 | -1.95 | 23.44 | 64.45 | 2.93 |
| 69 | 4.88 | 25.39 | -3.91 | 13.67 | 42.97 | .98 |
| Left base: | | | | | | |
| 40 | 213.87 | 276.37 | 320.31 | NR | NR | NR |
| 41 | 404.30 | 526.37 | 427.73 | NR | NR | NR |
| 42 | 198.24 | 230.47 | 177.73 | NR | NR | NR |
| 43 | -69.34 | -95.70 | -66.41 | 8.79 | 12.70 | 10.74 |
| 44 | -37.11 | -47.85 | -62.50 | -3.91 | -3.91 | .98 |
| Right base: | | | | | | |
| 63 | 236.33 | 313.48 | 299.80 | NR | NR | NR |
| 64 | 512.70 | 672.85 | 637.70 | NR | NR | NR |
| 65 | 314.45 | 390.63 | 379.88 | NR | NR | NR |
| 66 | -124.02 | -161.13 | -157.23 | 32.23 | 47.85 | 41.02 |
| 67 | -56.64 | -69.34 | -66.41 | -14.65 | -17.58 | -18.56 |
| Caving shield: | | | | | | |
| 49 | -67.38 | -98.63 | -41.99 | -36.13 | -72.27 | -45.90 |
| 51 | 55.66 | 73.24 | -84.96 | 47.85 | 71.29 | 40.04 |
| 52 | -7.81 | -13.67 | -180.66 | 40.04 | 59.57 | 23.44 |
| 53 | 63.48 | 78.13 | 105.47 | 28.32 | 40.04 | 29.30 |
| 57 | 76.17 | 79.10 | 111.33 | 61.52 | 71.29 | 95.70 |
| 54 | 91.80 | 119.14 | 61.52 | 28.32 | 35.16 | -27.34 |
| 55 | 154.30 | 200.20 | 163.09 | 43.95 | 59.57 | -6.84 |
| 56 | 4.88 | 7.81 | 4.88 | 1.95 | -4.88 | -7.81 |
| Left front link: | | | | | | |
| 45 | 5.86 | 10.74 | 144.53 | -14.65 | -31.25 | -16.60 |
| 46 | 16.60 | 21.48 | 179.69 | -32.23 | -36.13 | -9.77 |
| Right front link: | | | | | | |
| 61 | -108.40 | -137.70 | -163.09 | -37.11 | -52.73 | -34.18 |
| 62 | -201.17 | -244.14 | -253.91 | -83.98 | -118.16 | -92.77 |
| Left rear link: | | | | | | |
| 47 | 112.30 | 154.30 | 253.91 | .00 | -5.86 | 22.46 |
| 48 | -506.84 | -686.52 | -1,097.70 | 20.51 | 44.92 | -88.87 |
| Right rear link: | | | | | | |
| 59 | -173.83 | -221.68 | -220.70 | -3.91 | -12.70 | 8.79 |
| 60 | 641.60 | 855.47 | 836.91 | -146.48 | -138.67 | -175.78 |
| PRESSURE | | | | | | |
| Left leg: 37 | 4,033.20 | 5,595.70 | 6,010.70 | 4,033.20 | 6,250.00 | 6,538.10 |
| Right leg: 38 | 3,999.00 | 4,970.70 | 4,917.00 | 4,013.70 | 5,454.10 | 5,581.10 |

NR No reading.

| Component and gage | Test configuration 6,1 | | | Test configuration 6,2 | | |
|---|---|---|---|---|---|---|
| | Initial condition | After displacement | | Initial condition | After displacement | |
| | | Vertical | Horizontal | | Vertical | Horizontal |
| STRAIN | | | | | | |
| Canopy: | | | | | | |
| 68 | 6.84 | 40.0 | 44.88 | 1.95 | 43.95 | 12.70 |
| 69 | 5.86 | 35.1 | 68.79 | 10.74 | 50.78 | 27.34 |
| Left base: | | | | | | |
| 40 | 157.23 | 188.48 | 199.22 | 149.41 | 221.68 | 225.59 |
| 41 | 360.35 | 496.09 | 471.68 | 470.70 | 612.30 | 604.49 |
| 42 | 115.23 | 138.67 | 157.23 | 193.36 | 257.81 | 263.67 |
| 43 | -62.50 | -89.84 | -98.63 | -56.64 | -82.03 | -85.94 |
| 44 | -30.27 | -41.02 | -47.85 | -39.06 | -50.78 | -49.80 |
| Right base: | | | | | | |
| 63 | 218.75 | 256.84 | 279.30 | -7.81 | -6.84 | -6.84 |
| 64 | 327.15 | 500.98 | 443.36 | -49.80 | -62.50 | -75.20 |
| 65 | 214.84 | 267.58 | 274.41 | -89.84 | -134.77 | -186.52 |
| 66 | -95.70 | -133.79 | -138.67 | 12.70 | 14.65 | 16.60 |
| 67 | -58.59 | -79.10 | -85.94 | -38.09 | -46.88 | -58.59 |
| Caving shield: | | | | | | |
| 49 | 31.25 | 19.53 | 23.44 | 94.73 | 100.59 | 117.19 |
| 51 | 11.72 | 4.88 | -.98 | -70.31 | -90.82 | -104.49 |
| 52 | 15.63 | 8.79 | -.98 | -41.99 | -52.73 | -67.38 |
| 53 | -2.93 | -4.88 | -4.88 | -13.67 | -15.63 | -17.58 |
| 57 | -4.88 | -7.81 | 7.81 | 81.06 | 86.91 | 106.45 |
| 54 | 24.41 | 19.53 | 2.93 | -252.93 | -332.03 | -387.70 |
| 55 | 20.51 | 18.56 | .98 | -273.44 | -351.56 | -413.09 |
| 56 | 4.88 | 4.88 | 6.84 | 271.48 | 330.08 | 375.00 |
| Left front link: | | | | | | |
| 45 | -5.86 | -.98 | 2.93 | -24.41 | -33.20 | -23.44 |
| 46 | -2.93 | 2.93 | 7.81 | -23.44 | -28.32 | -15.63 |
| Right front link: | | | | | | |
| 61 | -18.56 | -24.41 | 6.84 | 261.72 | 306.64 | 338.87 |
| 62 | -28.32 | -18.56 | 7.81 | 291.02 | 376.95 | 426.76 |
| Left rear link: | | | | | | |
| 47 | -18.56 | -12.70 | .00 | 24.41 | 24.41 | 33.20 |
| 48 | 73.24 | 45.90 | .00 | -142.58 | -142.58 | -185.55 |
| Right rear link: | | | | | | |
| 59 | 7.81 | 8.79 | 11.72 | 213.87 | 274.41 | 320.31 |
| 60 | -68.36 | -67.38 | -77.15 | -803.71 | -1,041.00 | -1,202.10 |
| PRESSURE | | | | | | |
| Left leg: 37 | 4,038.10 | 5,835.00 | 6,298.80 | 3,974.60 | 5,405.30 | 5,610.40 |
| Right leg: 38 | 4,023.40 | 5,825.20 | 6,406.30 | 3,974.60 | 4,975.60 | 5,752.00 |

| Component and gage | Test configuration 6,3 | | | Test configuration 6,4 | | |
|---|---|---|---|---|---|---|
| | Initial condition | After displacement | | Initial condition | After displacement | |
| | | Vertical | Horizontal | | Vertical | Horizontal |
| STRAIN | | | | | | |
| Canopy: | | | | | | |
| 68 | 23.44 | 32.23 | 7.81 | 2.93 | 8.79 | -26.37 |
| 69 | 12.70 | 19.53 | 5.86 | 4.88 | 11.72 | -11.72 |
| Left base: | | | | | | |
| 40 | 141.60 | 166.02 | 213.87 | 45.90 | 44.92 | 41.99 |
| 41 | 347.66 | 421.88 | 360.35 | | | |
| 42 | 162.11 | 178.71 | 159.18 | -10.74 | -37.11 | NR |
| 43 | -49.80 | -63.48 | -51.76 | 8.79 | 11.72 | 7.81 |
| 44 | -37.11 | -44.92 | -53.71 | .00 | .98 | 5.86 |
| Right base: | | | | | | |
| 63 | 135.74 | 192.38 | 208.98 | 9.77 | 9.77 | 9.77 |
| 64 | 489.26 | 623.05 | 597.66 | NR | NR | NR |
| 65 | 283.20 | 348.63 | 337.89 | NR | NR | NR |
| 66 | -123.05 | -150.39 | -147.46 | 28.32 | 41.02 | 38.09 |
| 67 | -52.73 | -63.48 | -60.55 | -14.65 | -18.56 | -21.48 |
| Caving shield: | | | | | | |
| 49 | 2.93 | -7.81 | 21.48 | 4.88 | 2.93 | 13.67 |
| 51 | 16.60 | 19.53 | -67.38 | 12.70 | 16.60 | -17.58 |
| 52 | -39.06 | -51.76 | -148.44 | 14.65 | 19.53 | -14.65 |
| 53 | -17.58 | -11.72 | -22.46 | 5.86 | 7.81 | .98 |
| 57 | 1.95 | -3.91 | 21.48 | 2.93 | .00 | 8.79 |
| 54 | 127.93 | 156.25 | 113.28 | 20.51 | 21.48 | .00 |
| 55 | 195.31 | 236.33 | 201.17 | 29.30 | 31.25 | 7.81 |
| 56 | -1.95 | 1.95 | -3.91 | 18.56 | 20.51 | 25.39 |
| Left front link: | | | | | | |
| 45 | 3.91 | .98 | 43.95 | -14.65 | -18.56 | 3.91 |
| 46 | 4.88 | 12.70 | 68.36 | -7.81 | -11.72 | 15.63 |
| Right front link: | | | | | | |
| 61 | -52.73 | -47.85 | -73.24 | -14.65 | -26.37 | 14.65 |
| 62 | -143.55 | -168.95 | -177.73 | -49.80 | -41.99 | .00 |
| Left rear link: | | | | | | |
| 47 | 130.86 | 180.66 | 251.95 | .00 | -4.88 | 20.51 |
| 48 | -641.60 | -860.35 | -1,201.20 | 5.86 | 9.77 | -96.68 |
| Right rear link: | | | | | | |
| 59 | -221.68 | -261.72 | -255.86 | 17.58 | 12.70 | 24.41 |
| 60 | 916.99 | 1,112.30 | 1,070.30 | -147.46 | -147.46 | -162.11 |
| PRESSURE | | | | | | |
| Left leg: 37 | 4,038.10 | 4,975.60 | 5,263.70 | 4,038.10 | 6,108.40 | 6,513.70 |
| Right leg: 38 | 4,013.70 | 4,814.50 | 4,799.80 | 4,038.10 | 6,123.00 | 6,655.30 |

NR No reading.

# APPENDIX C.–LOAD DISTRIBUTION AND SHIELD MECHANICS FOR SYMMETRIC-UNSYMMETRIC CONTACT CONFIGURATIONS

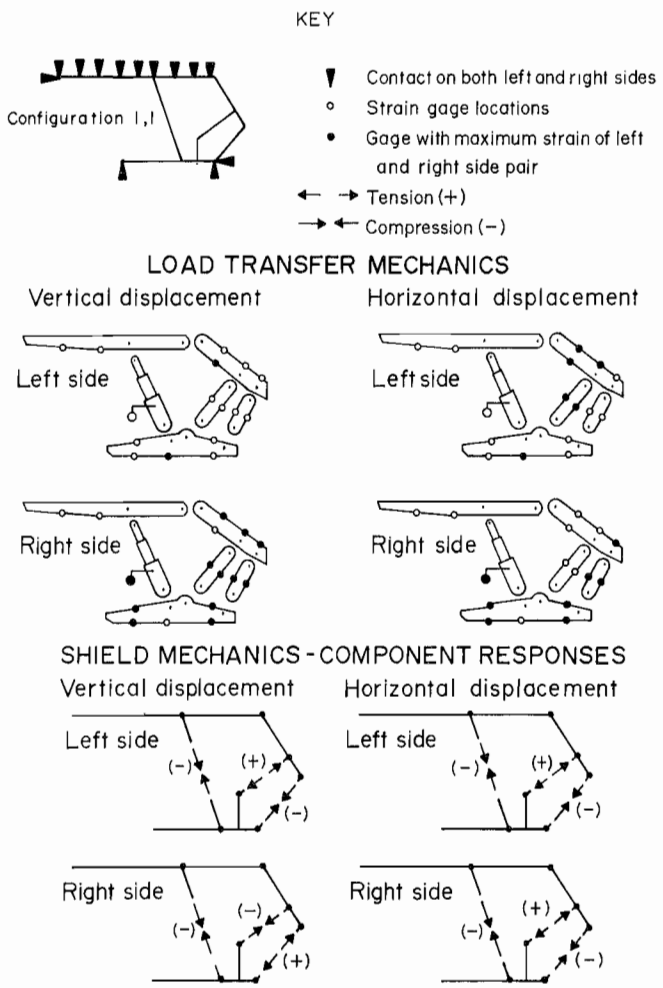


**Figure C-1.–Load distribution and component responses for symmetric two-point base contact with full canopy contact.**

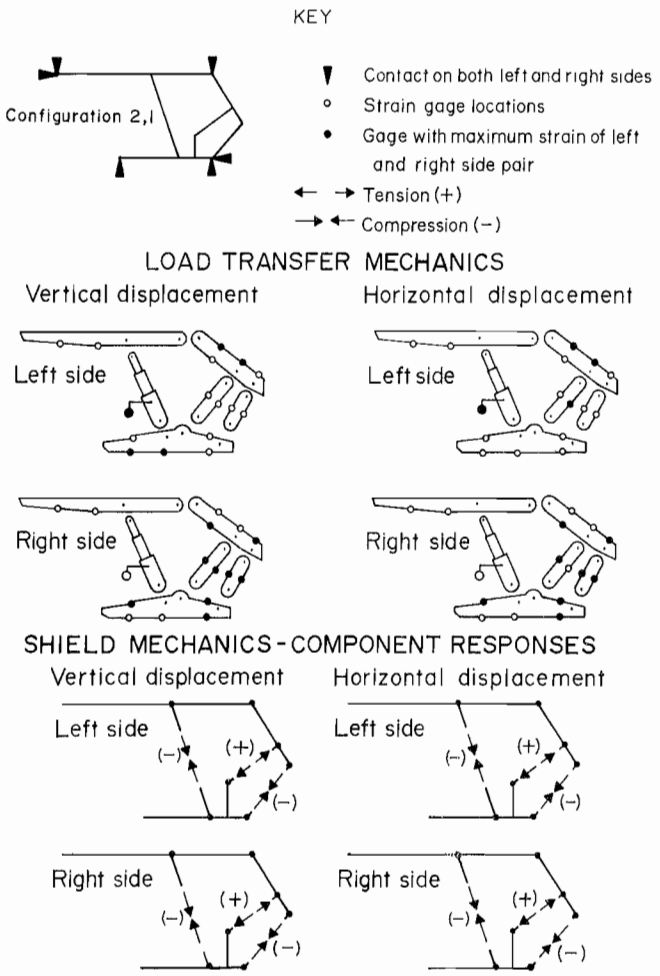


**Figure C-2.–Load distribution and component responses for symmetric two-point canopy and base contact.**

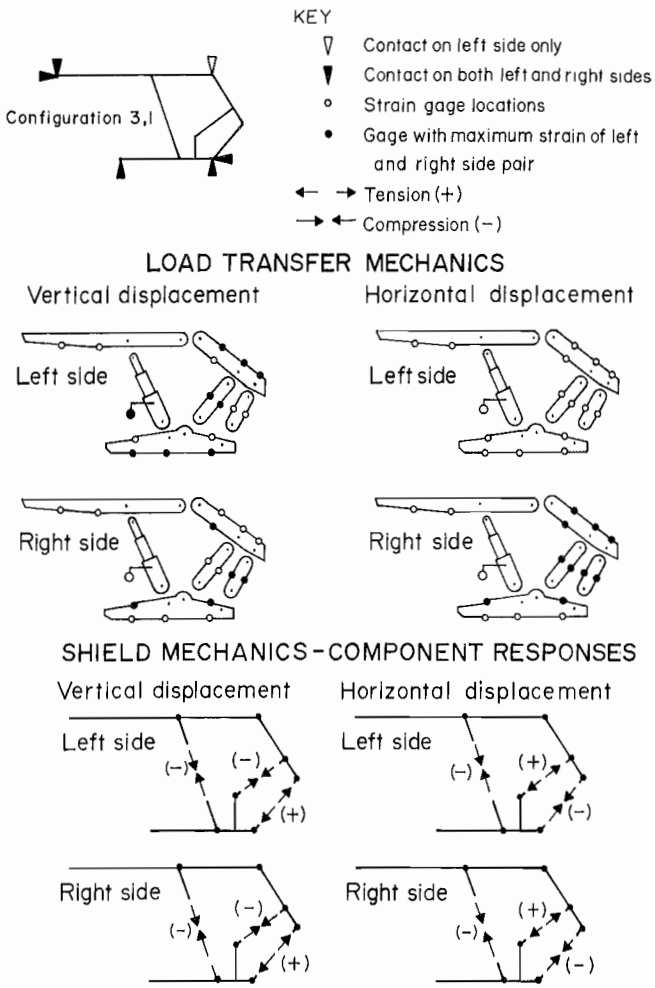


**Figure C-3.–Load distribution and component responses for unsymmetric canopy rear contact with symmetric two-point base contact.**

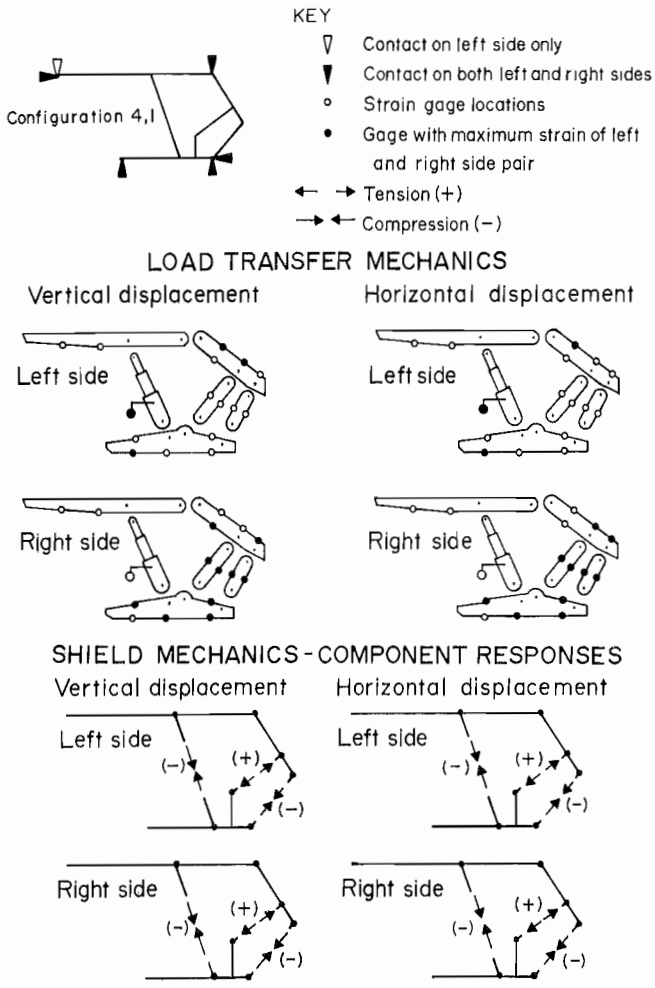


**Figure C-4.–Load distribution and component responses for unsymmetric canopy tip contact with symmetric two-point base contact.**

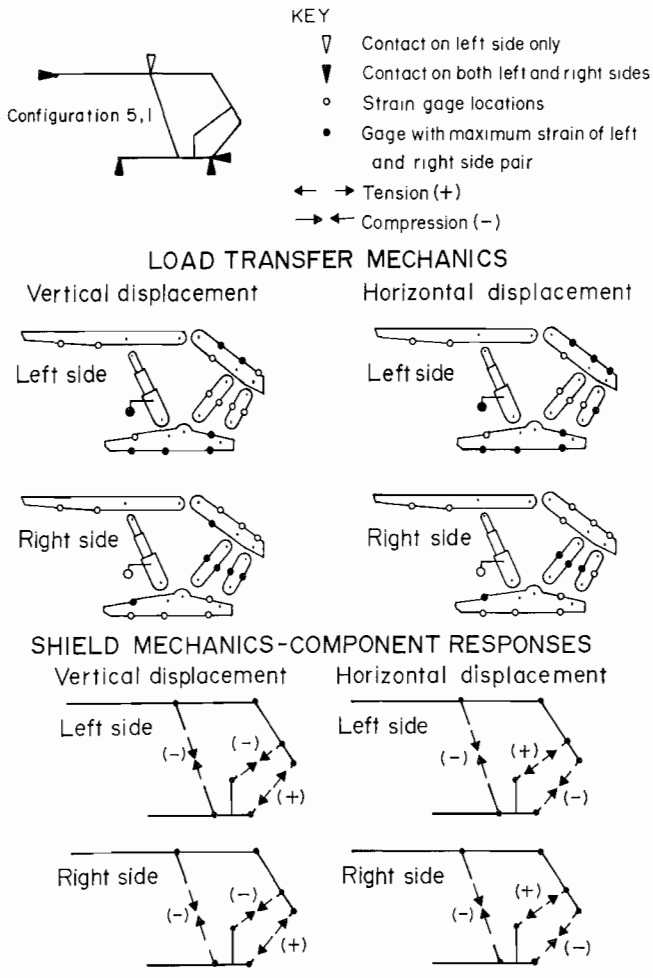


**Figure C-5.–Load distribution and component responses for unsymmetric canopy leg contact with symmetric two-point base contact.**

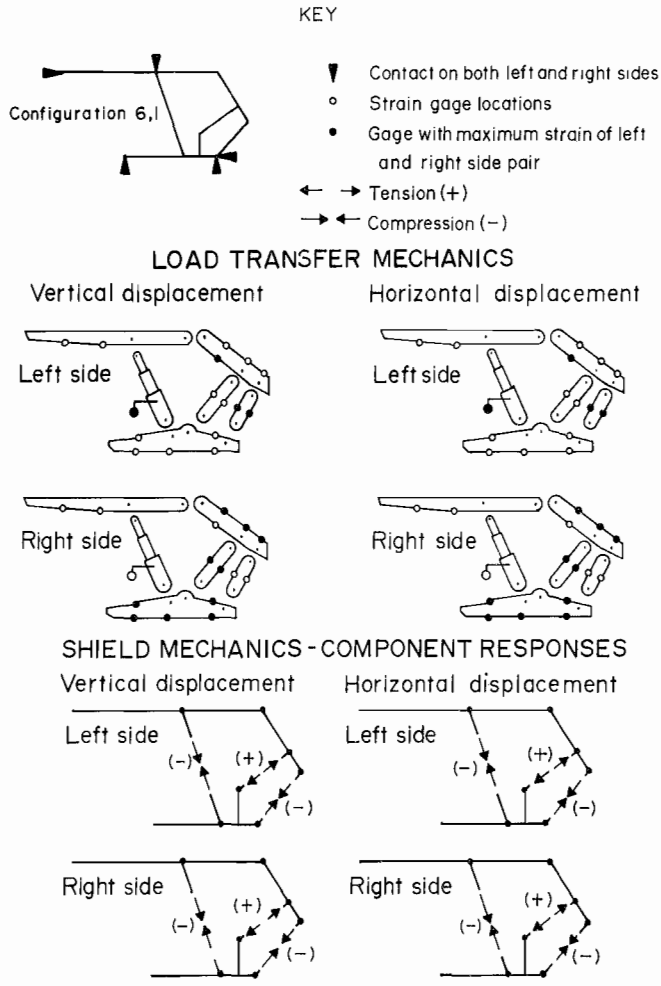


**Figure C-6.–Load distribution and component responses for symmetric canopy leg contact and symmetric two-point base contact.**

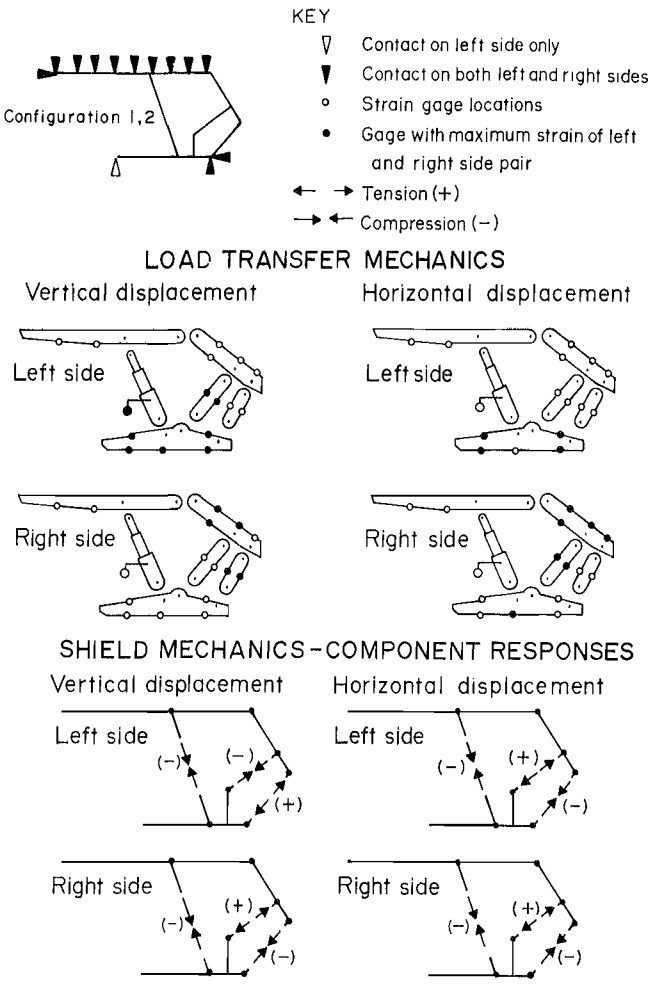


**Figure C-7.–Load distribution and component responses for unsymmetric base-on-rear contact with full canopy contact.**

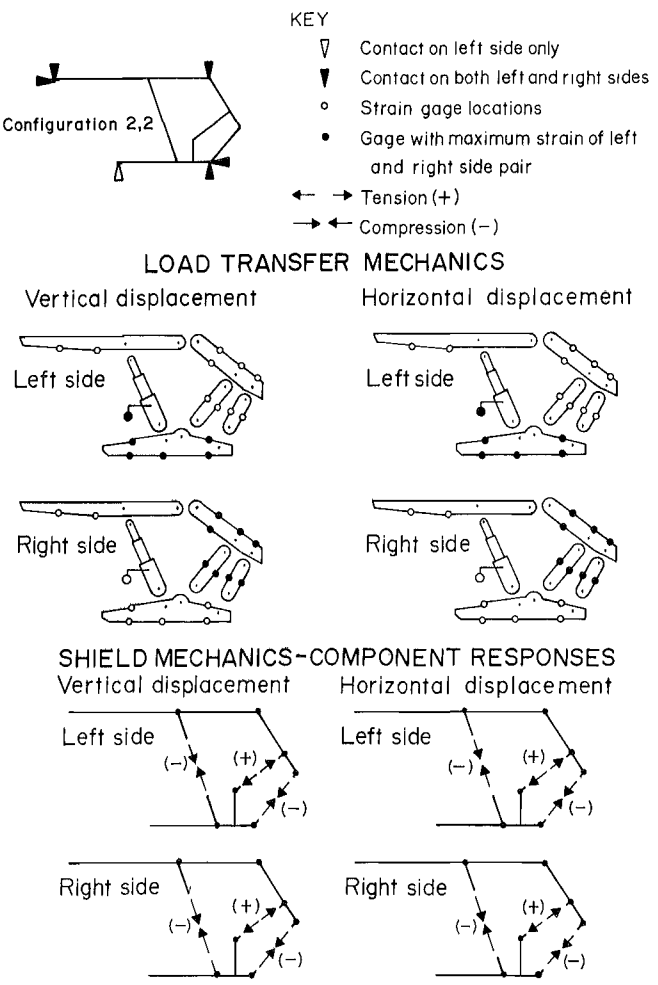


**Figure C-8.–Load distribution and component responses for unsymmetric base-on-rear contact with symmetric two-point canopy contact.**

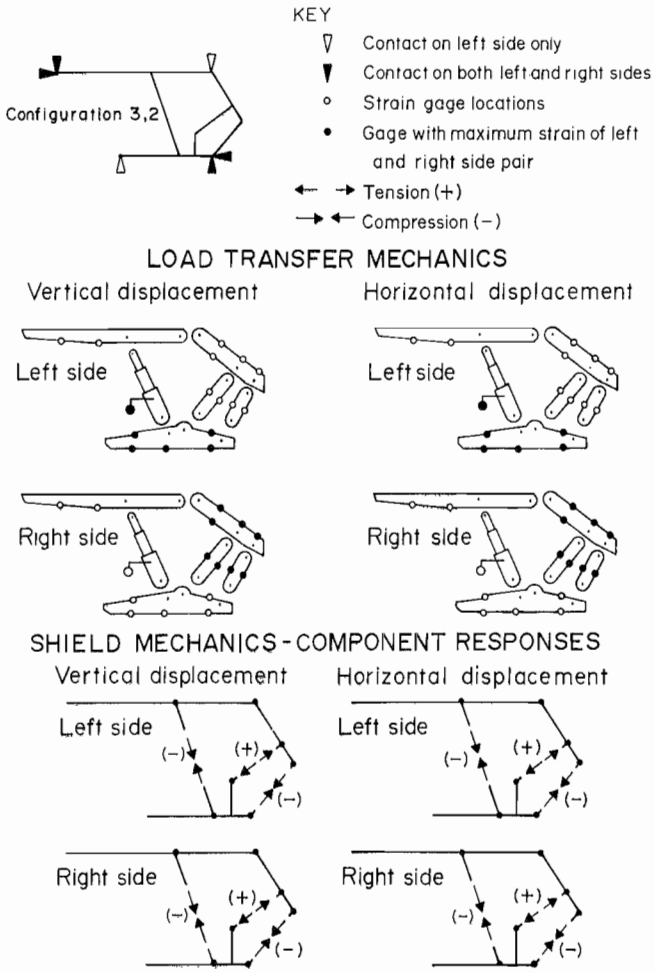


**Figure C-9.–Load distribution and component responses for unsymmetric base-on-rear contact with unsymmetric canopy rear contact.**

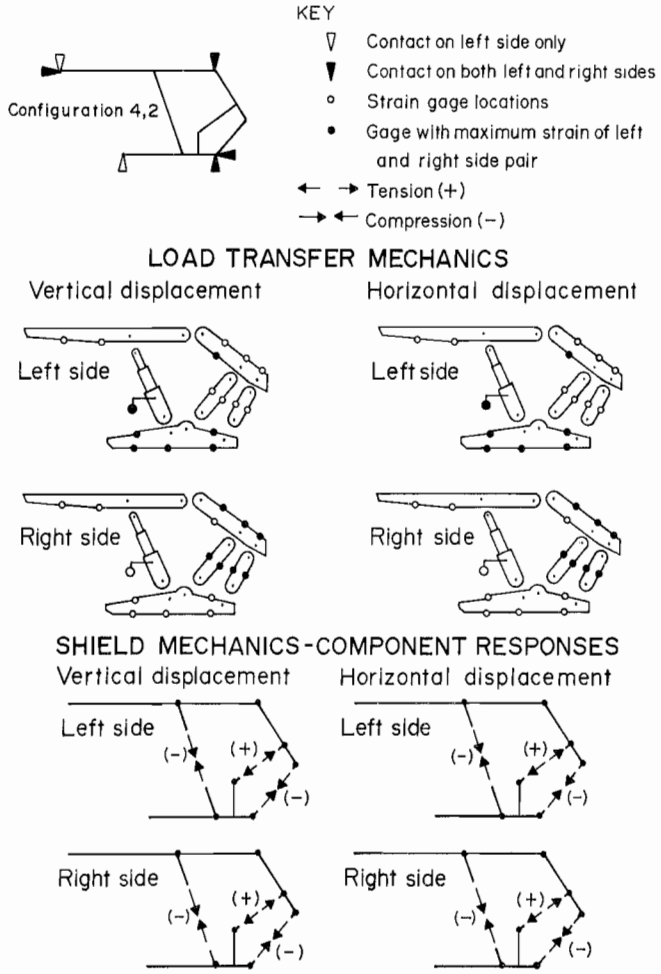


**Figure C-10.–Load distribution and component responses for unsymmetric base-on-rear contact with unsymmetric canopy tip contact.**

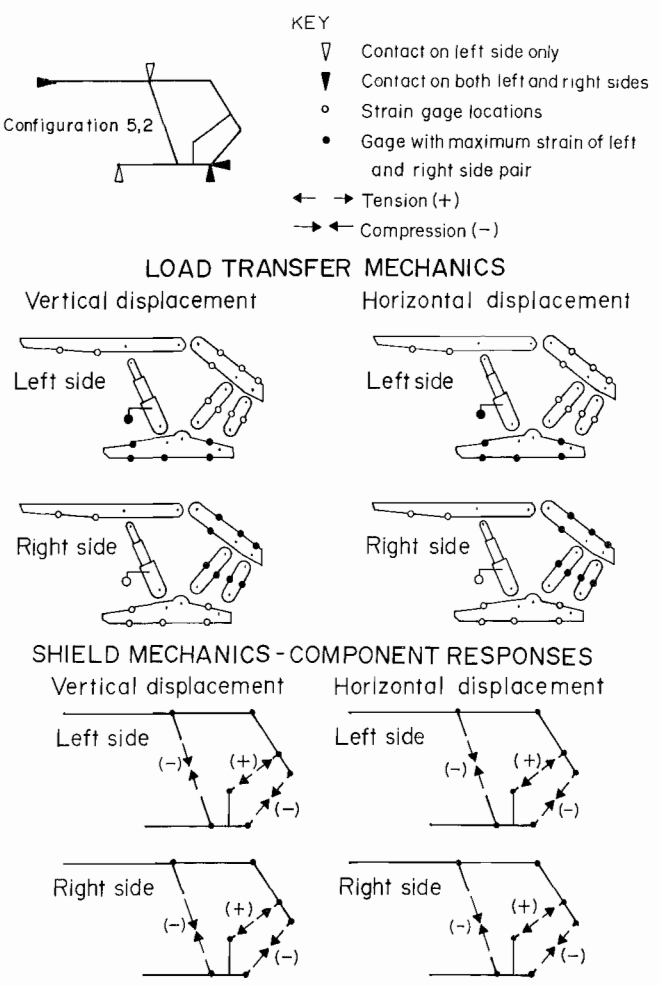


**Figure C-11.–Load distribution and component responses for unsymmetric base-on-rear contact with unsymmetric canopy leg contact.**

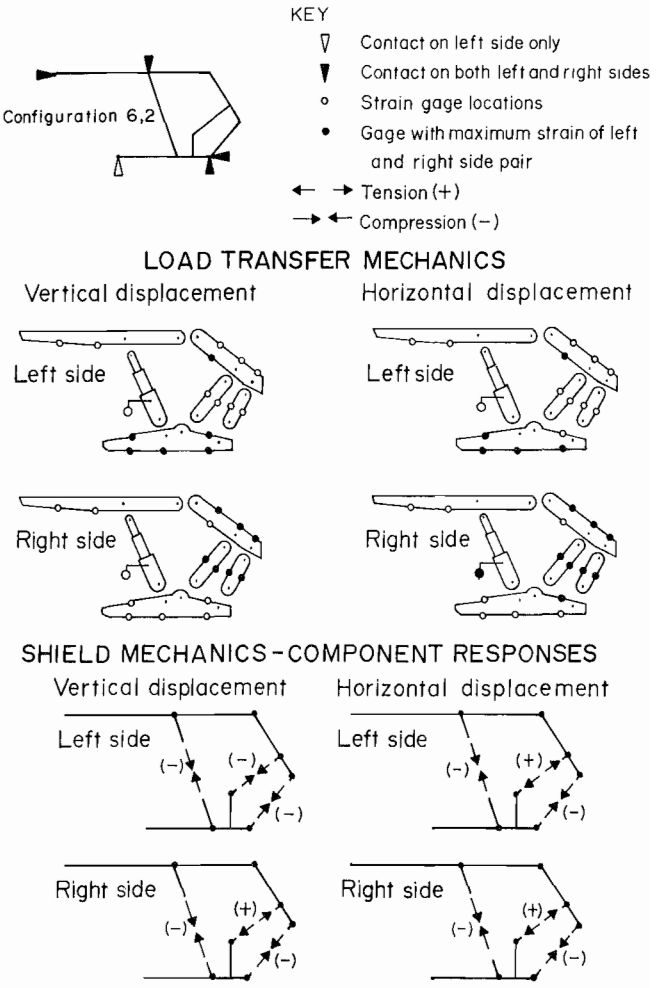


**Figure C-12.–Load distribution and component responses for unsymmetric base-on-rear contact with symmetric leg contact.**

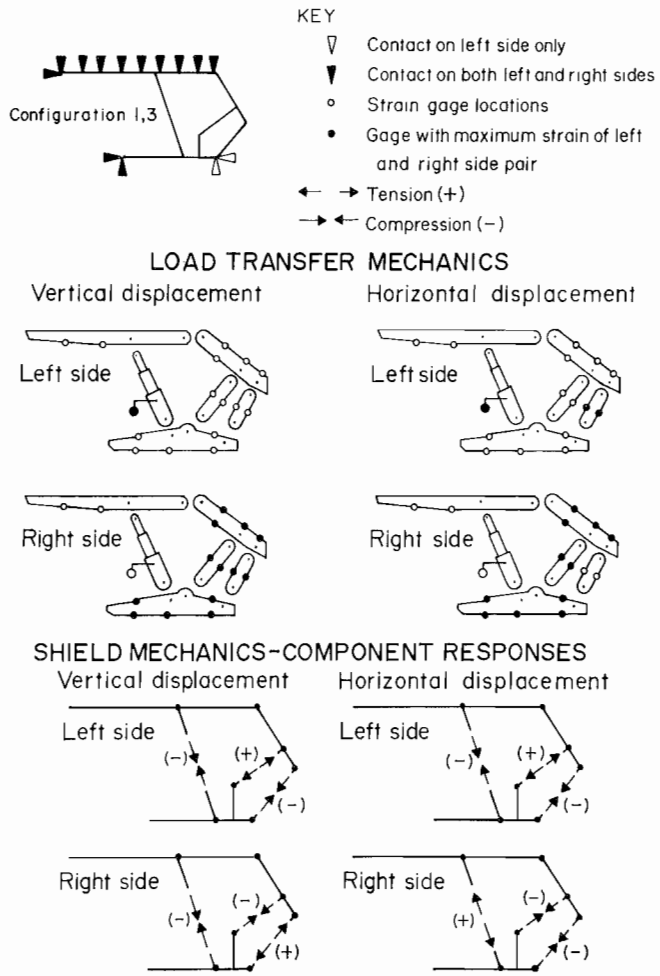


**Figure C-13.–Load distribution and component responses for unsymmetric base-on-toe contact with full canopy contact.**

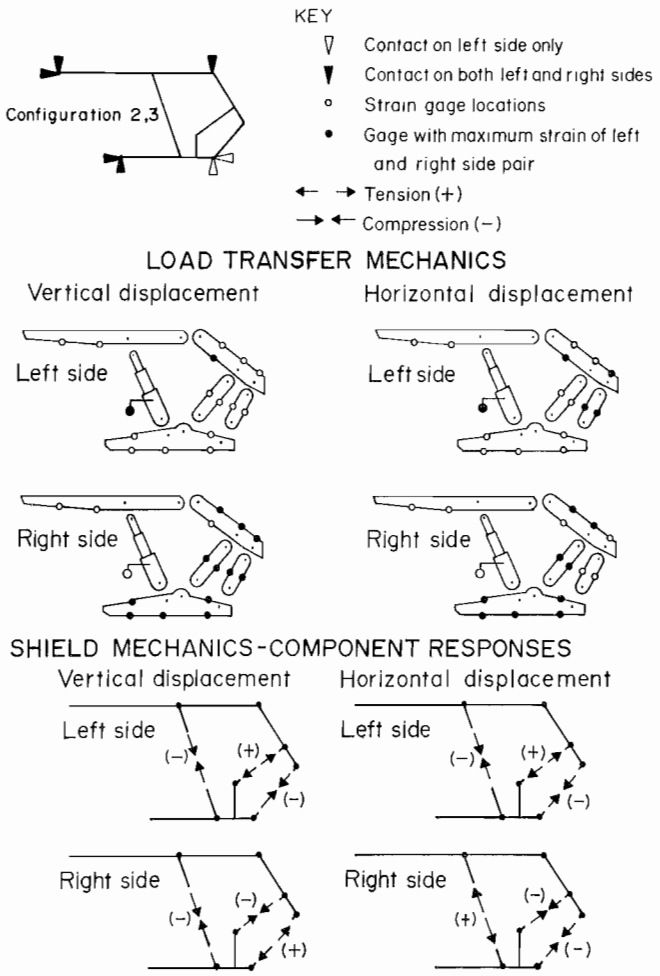


**Figure C-14.–Load distribution and component responses for unsymmetric base-on-toe contact with symmetric two-point canopy contact.**

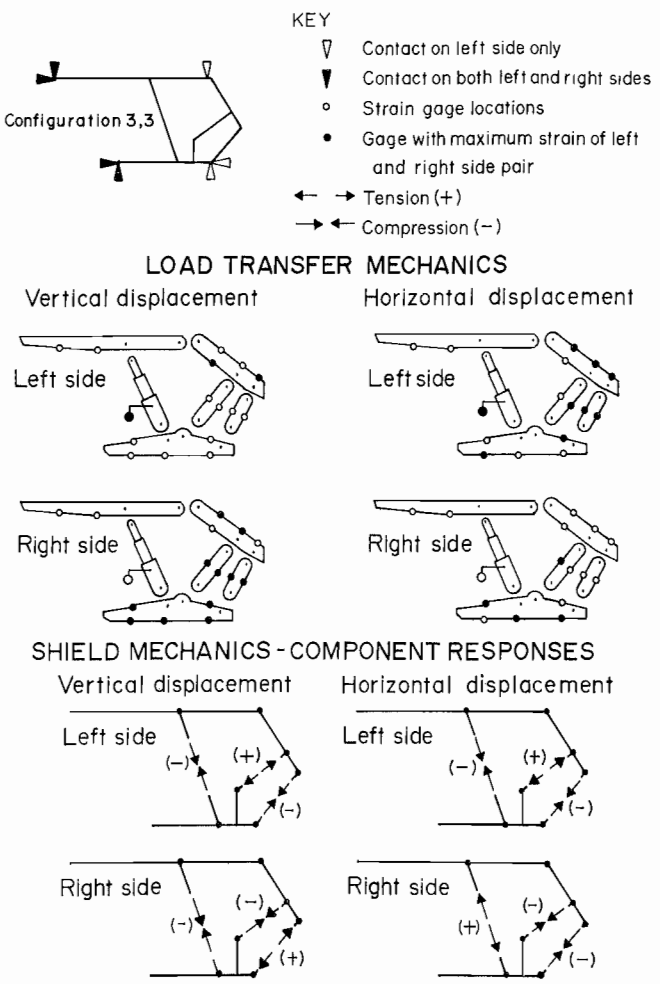


**Figure C-15.–Load distribution and component responses for unsymmetric base-on-toe contact with unsymmetric canopy rear contact.**

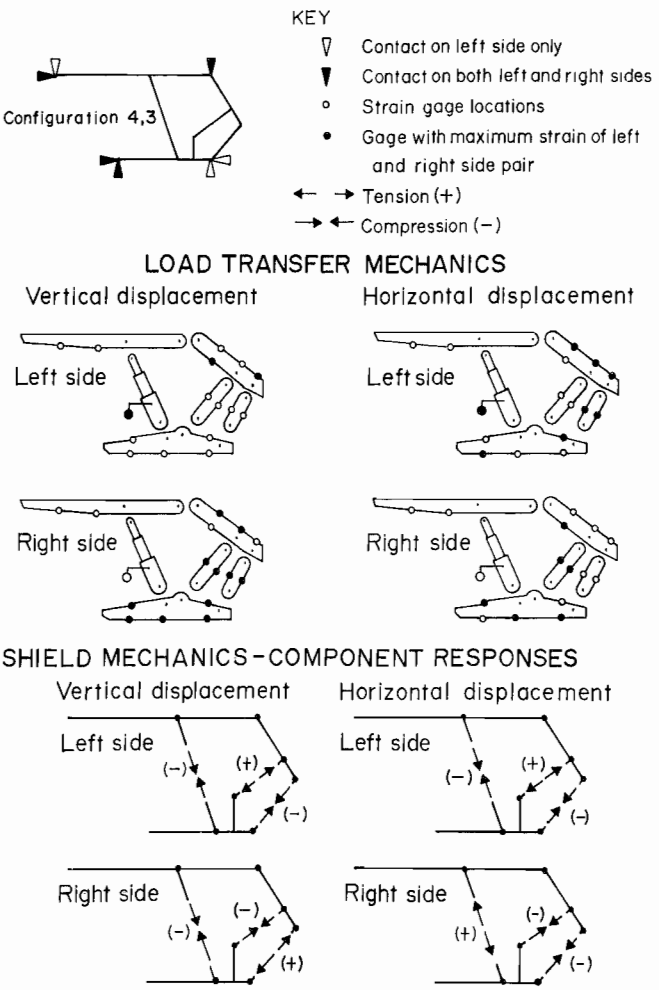


**Figure C-16.–Load distribution and component responses for unsymmetric base-on-toe contact with unsymmetric canopy tip contact.**

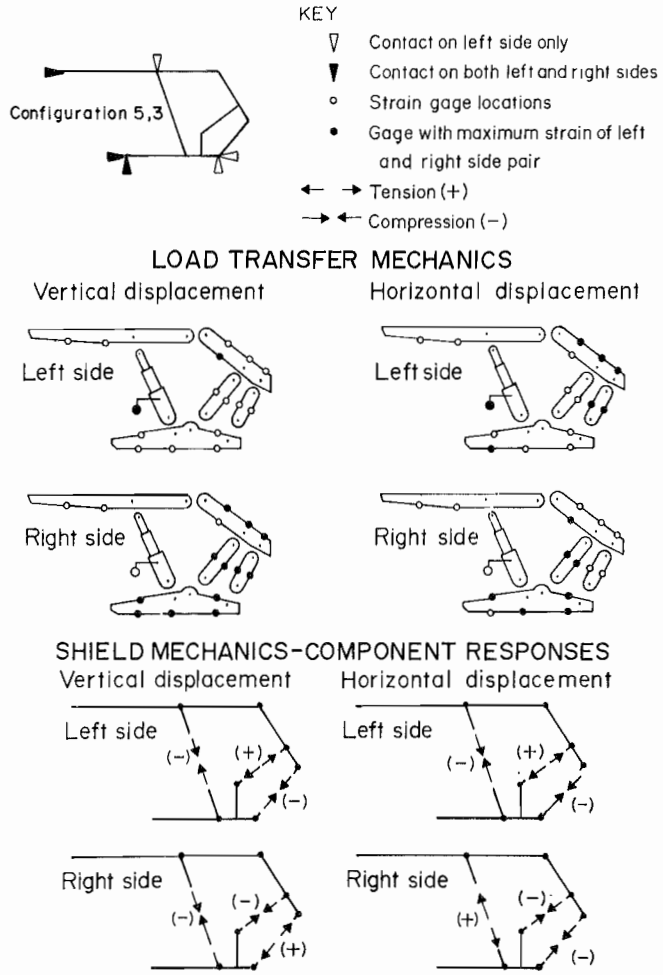


**Figure C-17.–Load distribution and component responses for unsymmetric base-on-toe contact with unsymmetric canopy leg contact.**

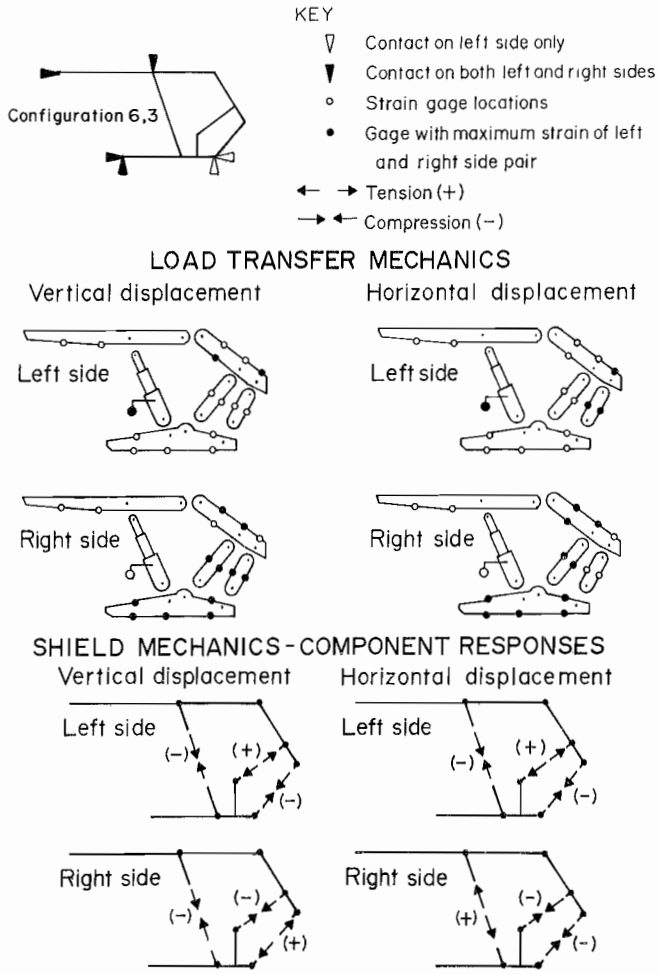


**Figure C-18.–Load distribution and component responses for unsymmetric base-on-toe contact with symmetric canopy leg contact.**

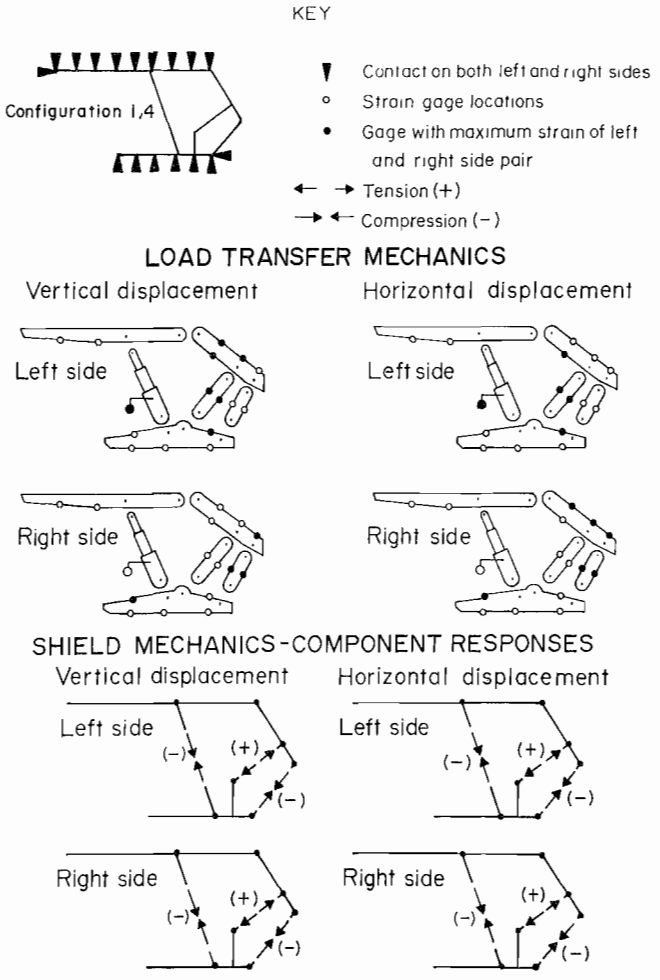


**Figure C-19.–Load distribution and component responses for full canopy and base contact.**

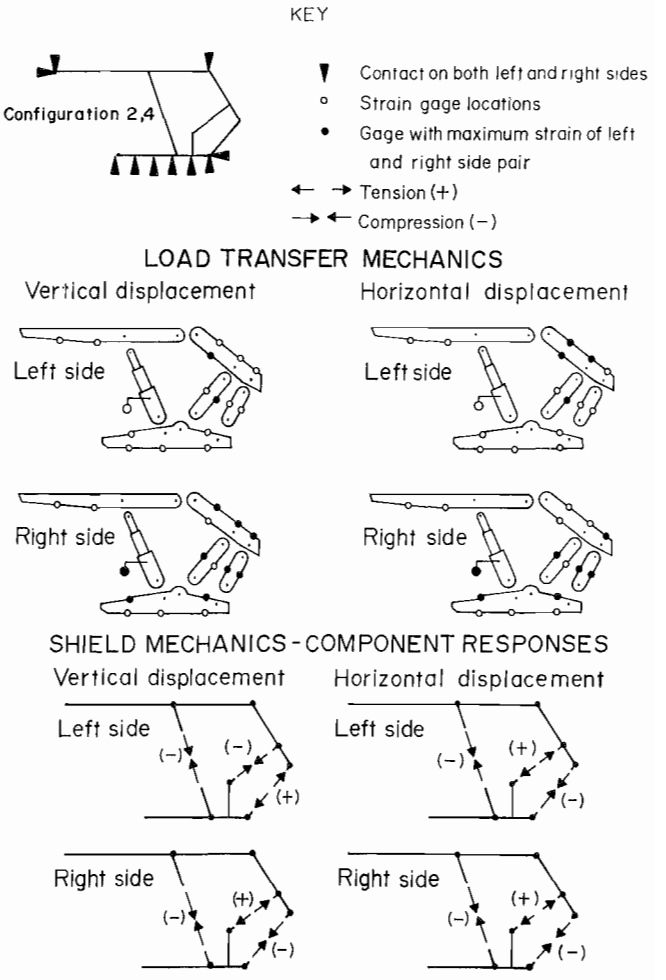


**Figure C-20.–Load distribution and component responses for two-point canopy contact with full base contact.**

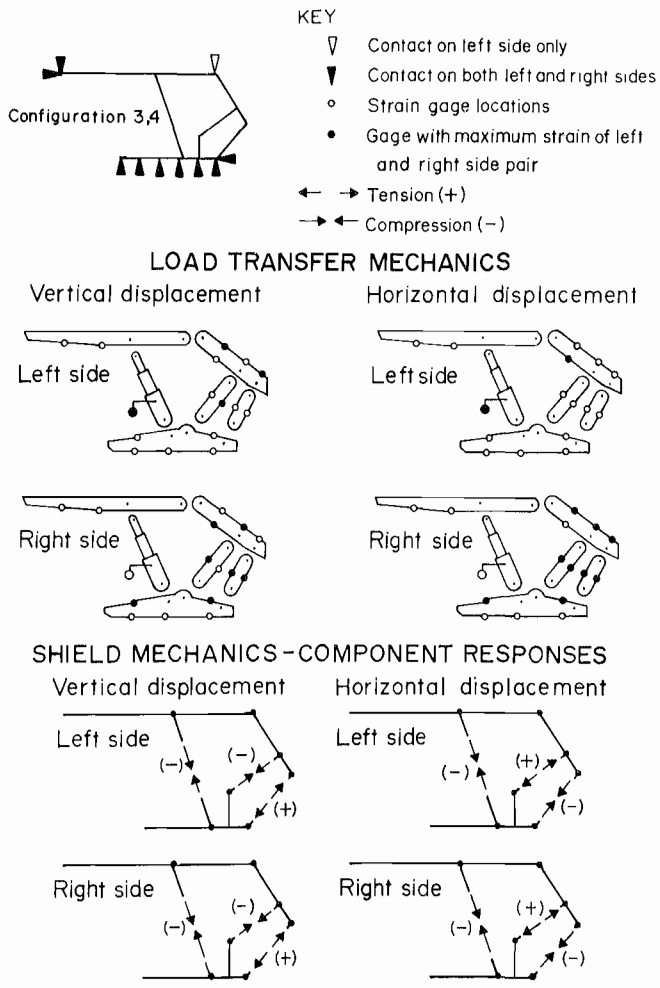


**Figure C-21.–Load distribution and component responses for unsymmetric canopy rear contact with full base contact.**

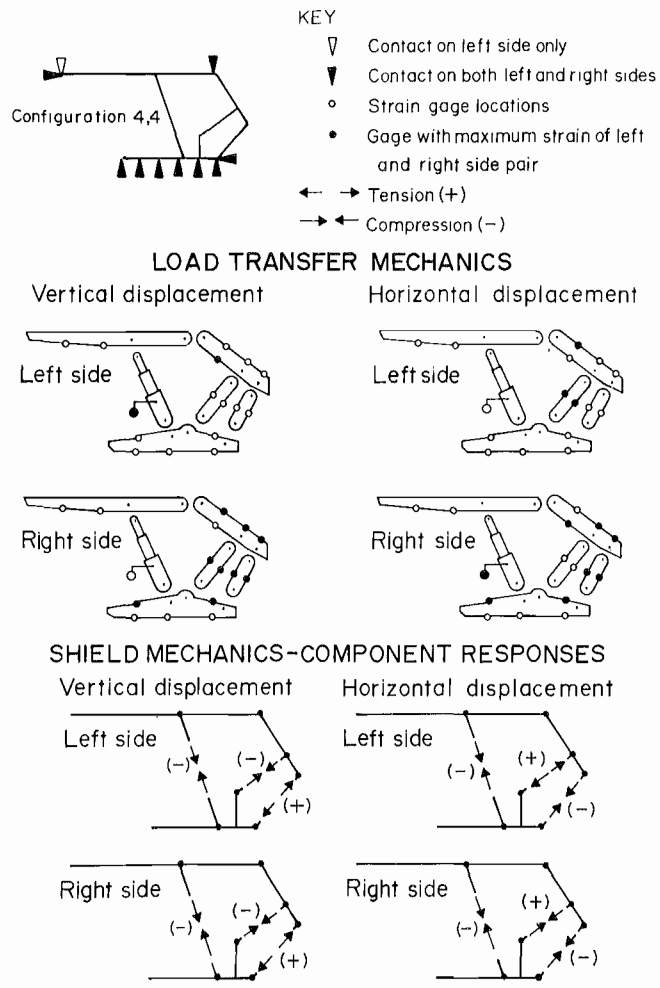


**Figure C-22.–Load distribution and component responses for unsymmetric canopy tip contact with full base contact.**

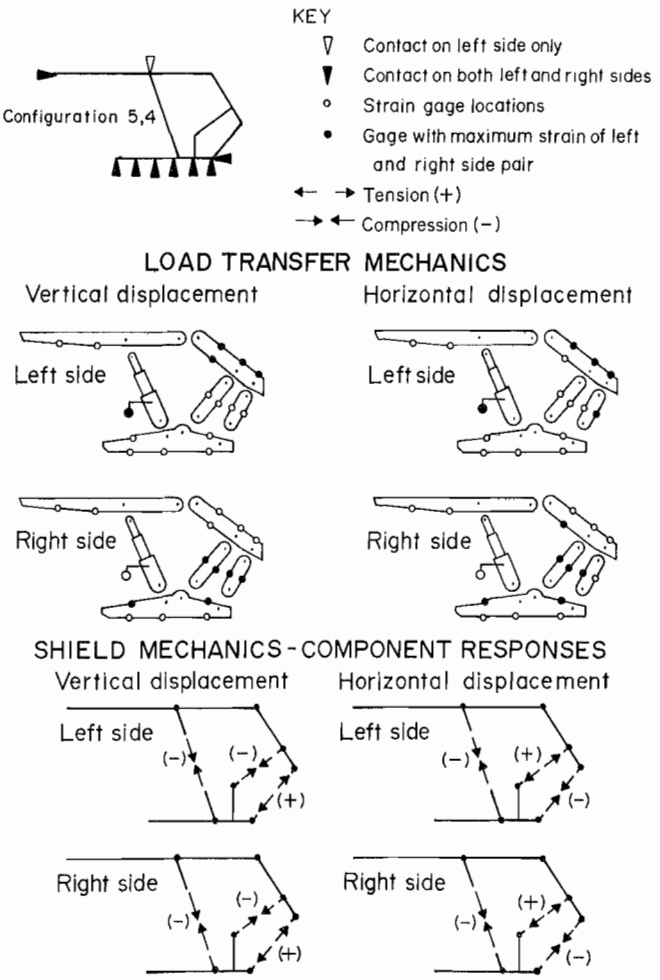


**Figure C-23.–Load distribution and component responses for unsymmetric canopy leg contact with full base contact.**

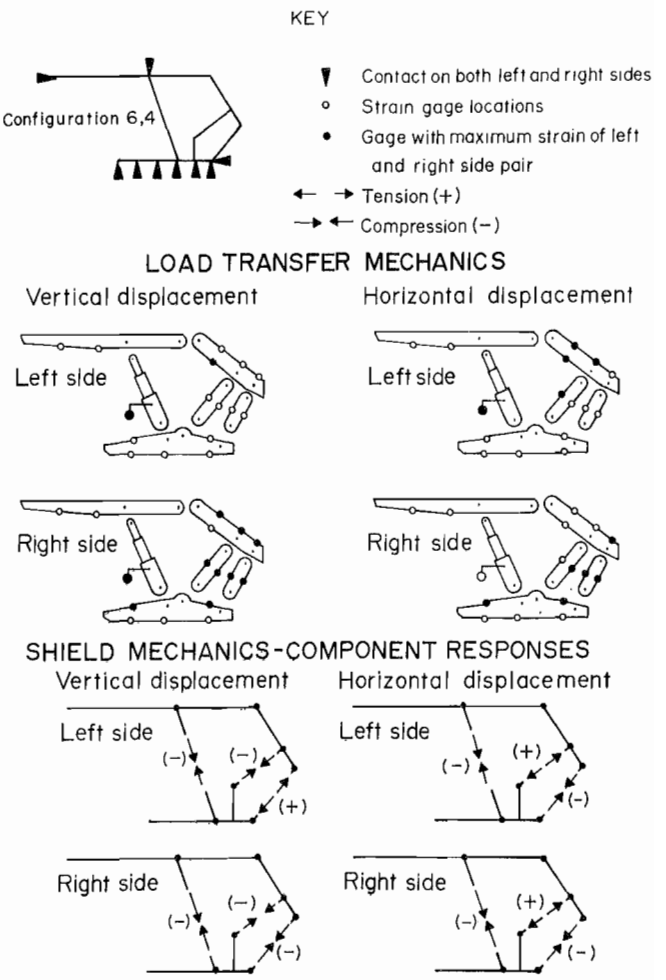


**Figure C-24.–Load distribution and component responses for symmetric canopy contact with full base contact.**

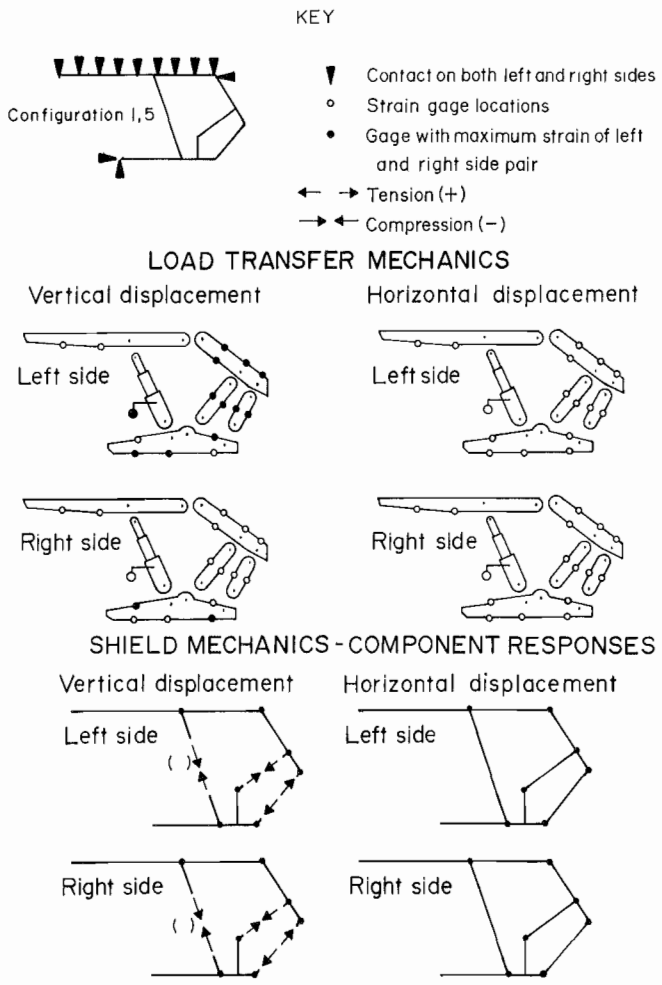


**Figure C-25.–Load distribution and component responses for symmetric base-on-toe contact with full canopy contact.**

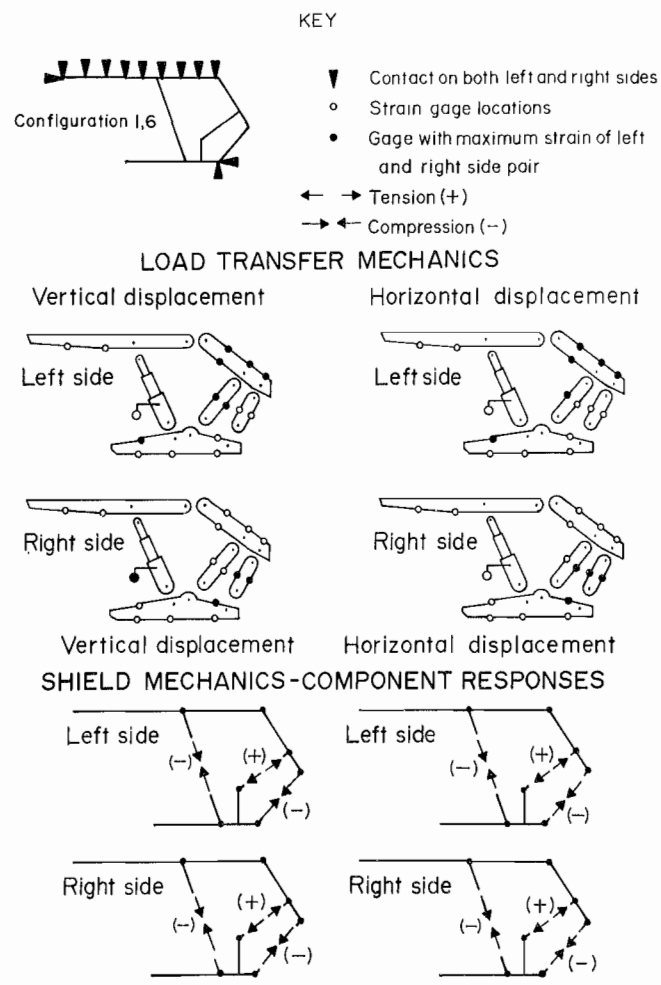


**Figure C-26.–Load distribution and component responses for symmetric base-on-rear contact with full canopy contact.**

# APPENDIX D.–STRAIN DEVELOPMENT FOR LIKE BASE CONTACTS

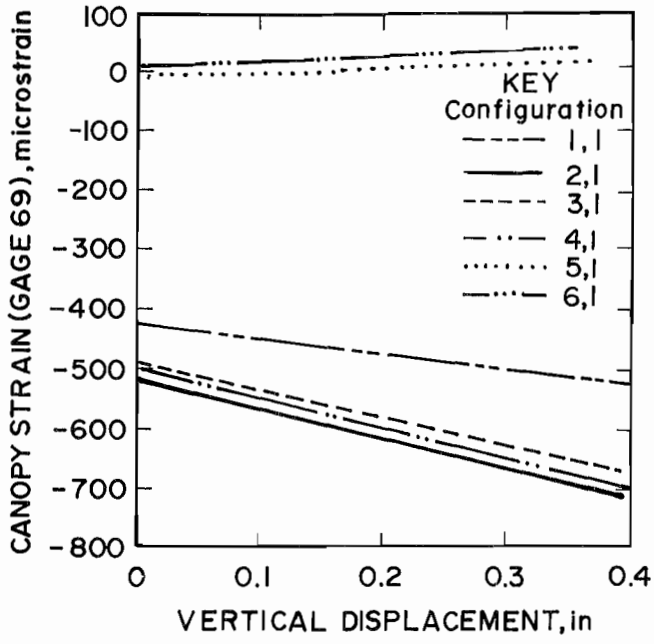


Figure D-1.–Canopy strain development for various canopy contact configurations with two-point base contacts.

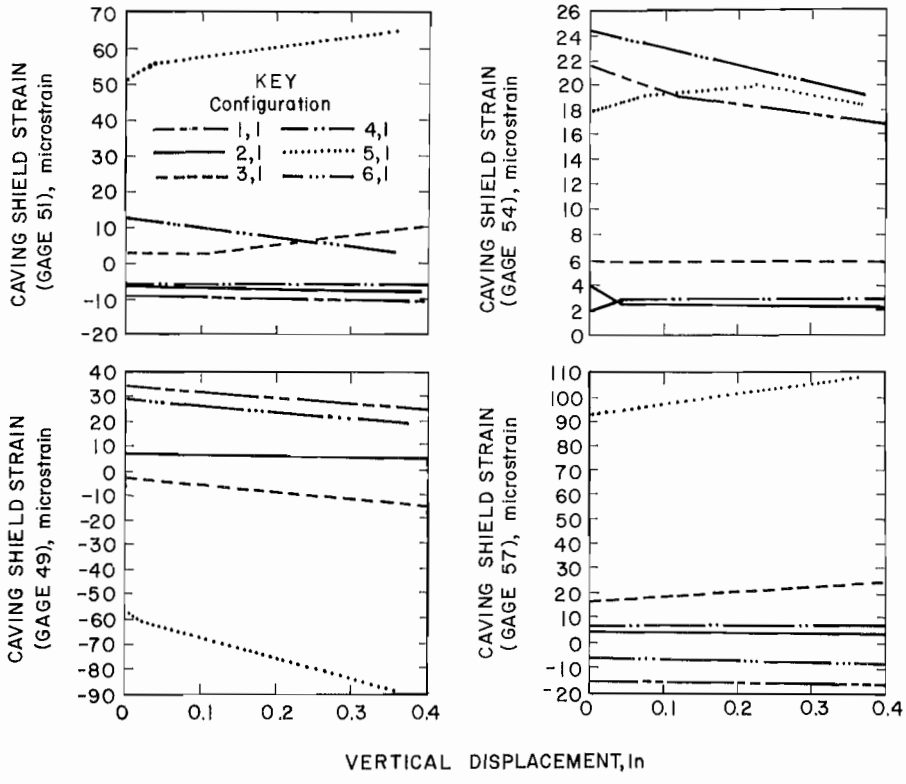


Figure D-2.–Caving shield strain development for various canopy contact configurations with two-point base contacts.

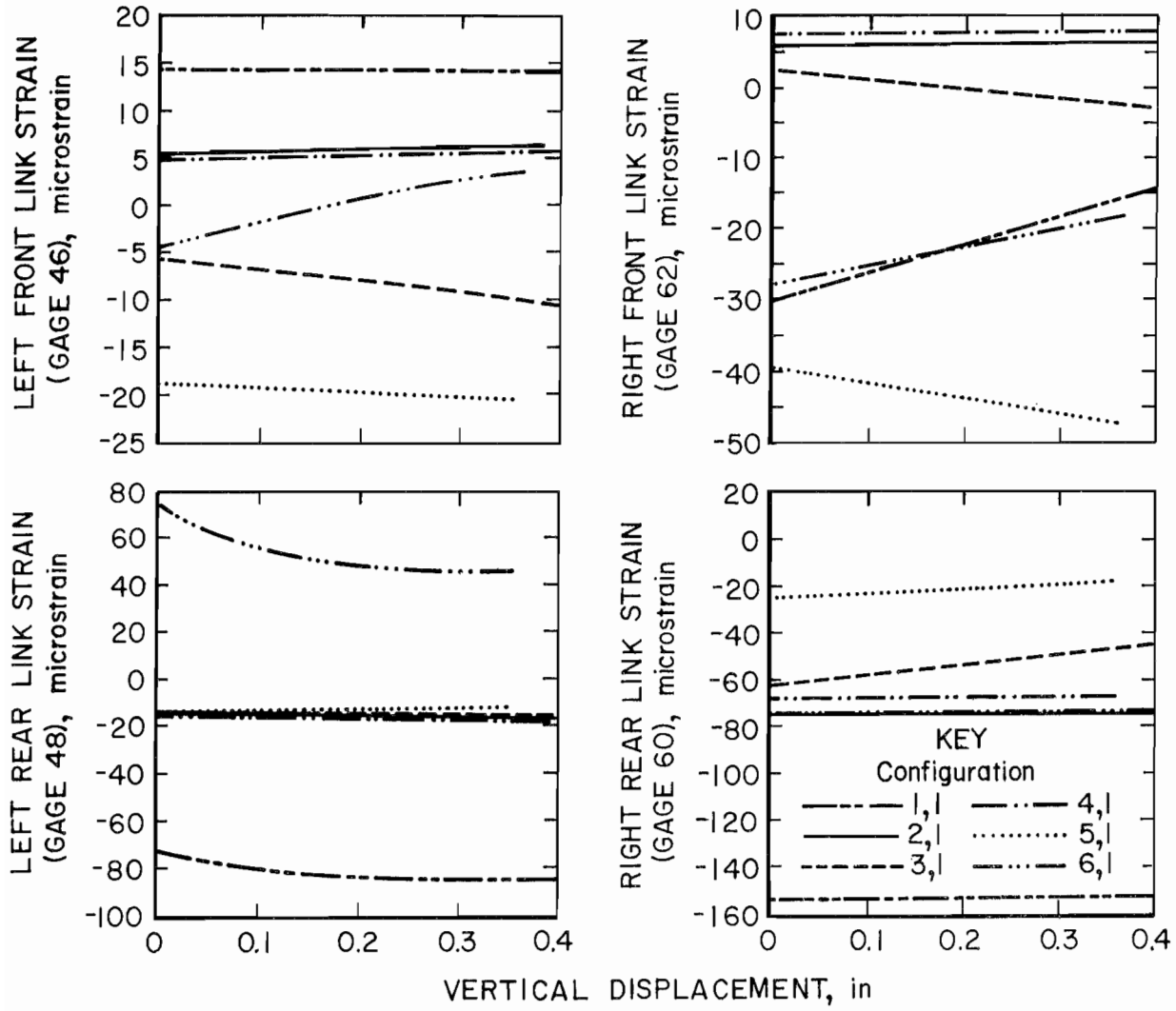


**Figure D-3.–Link strain development for various canopy contact configurations with two-point base contacts.**

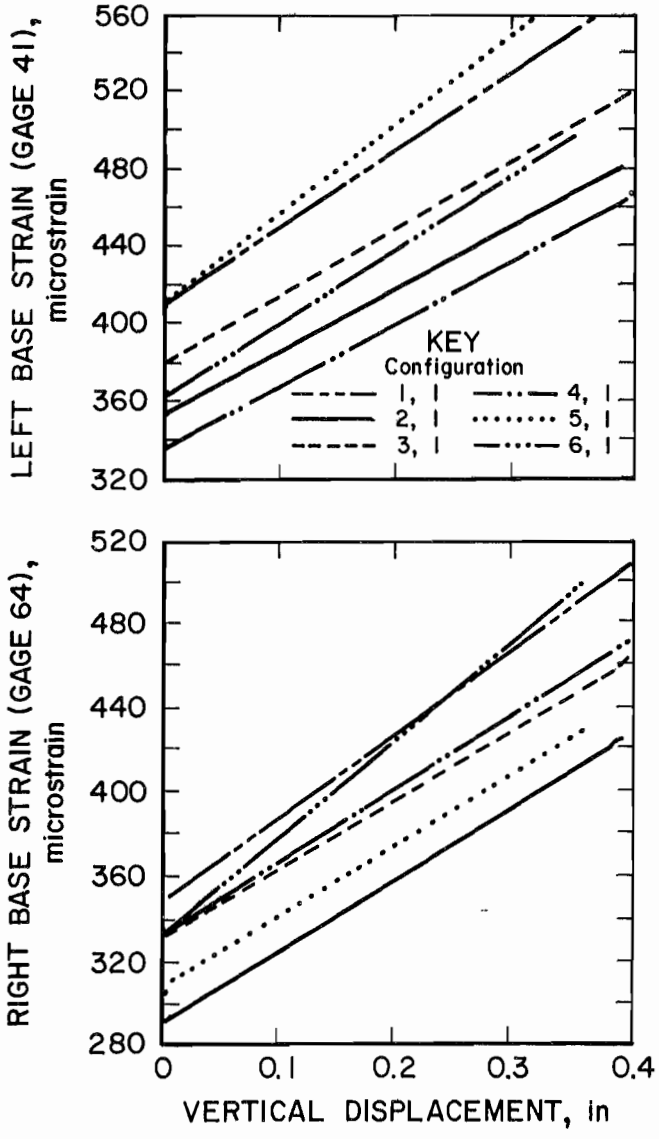


Figure D-4.–Base strain development for various canopy contact configurations with two-point base contacts.

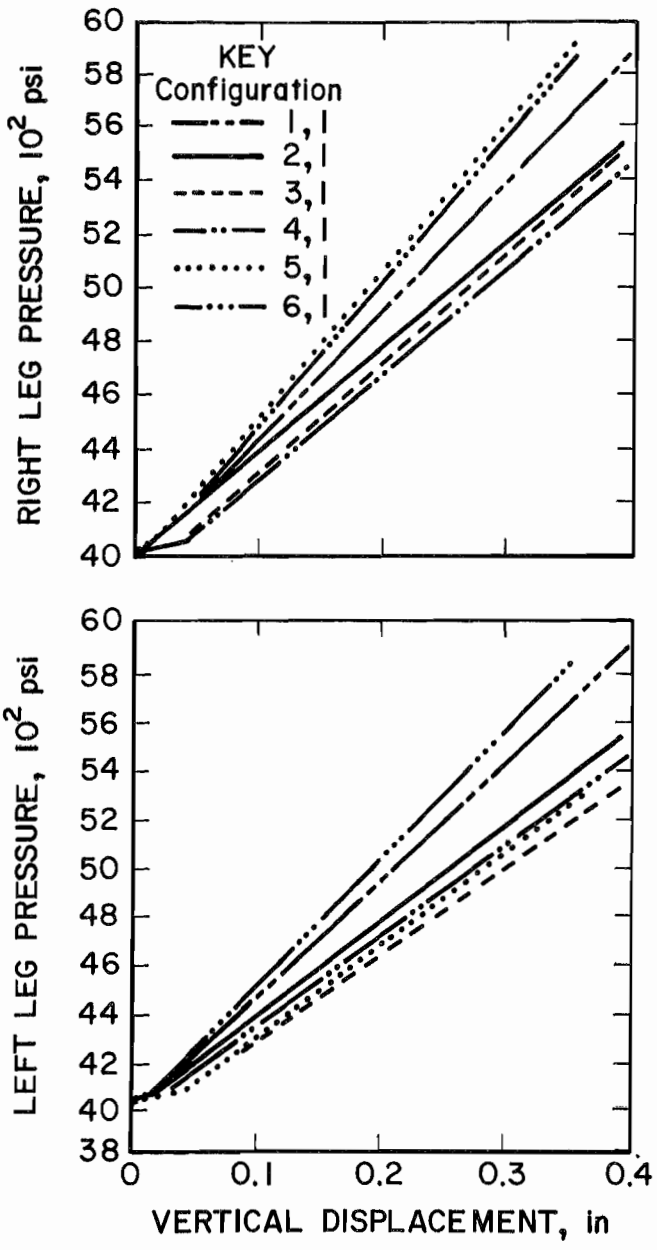


Figure D-5.–Leg pressure development for various canopy contact configurations with two-point base contacts.

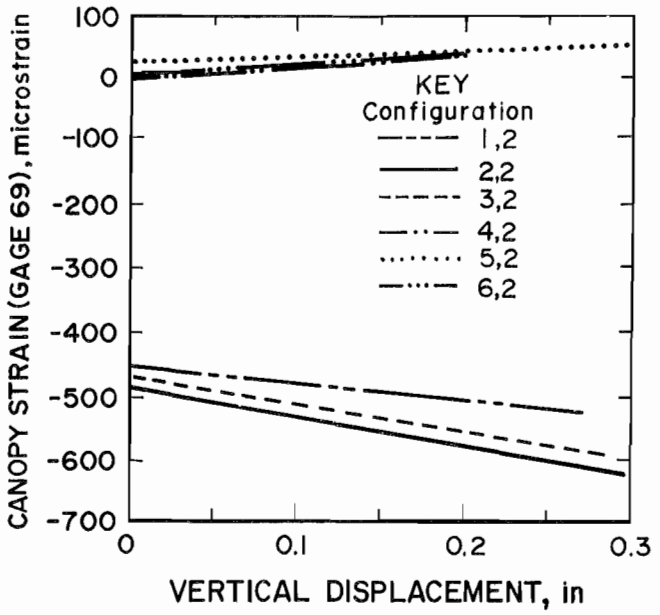


**Figure D-6.–Canopy strain development for various canopy contact configurations with unsymmetric base-on-rear contacts.**

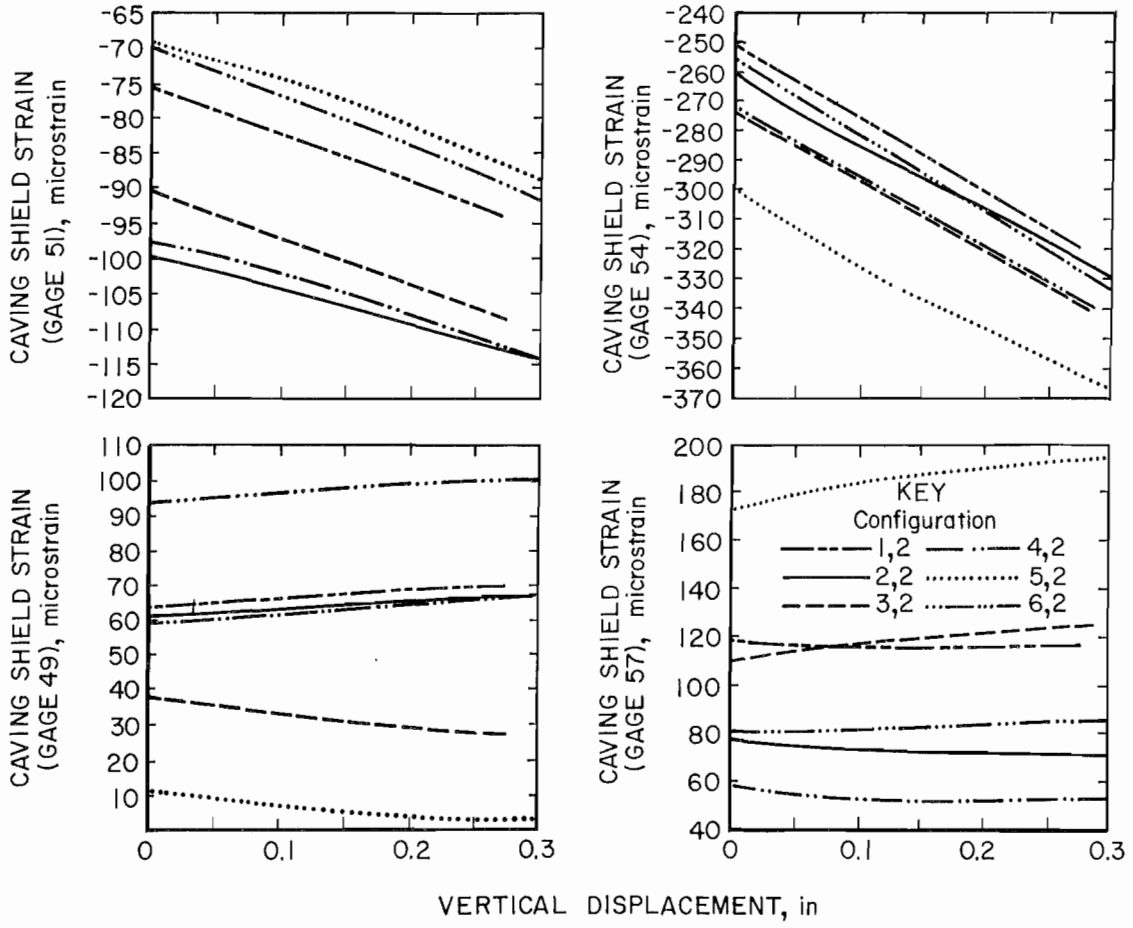


**Figure D-7.–Caving shield strain development for various canopy contact configurations with unsymmetric base-on-rear contacts.**

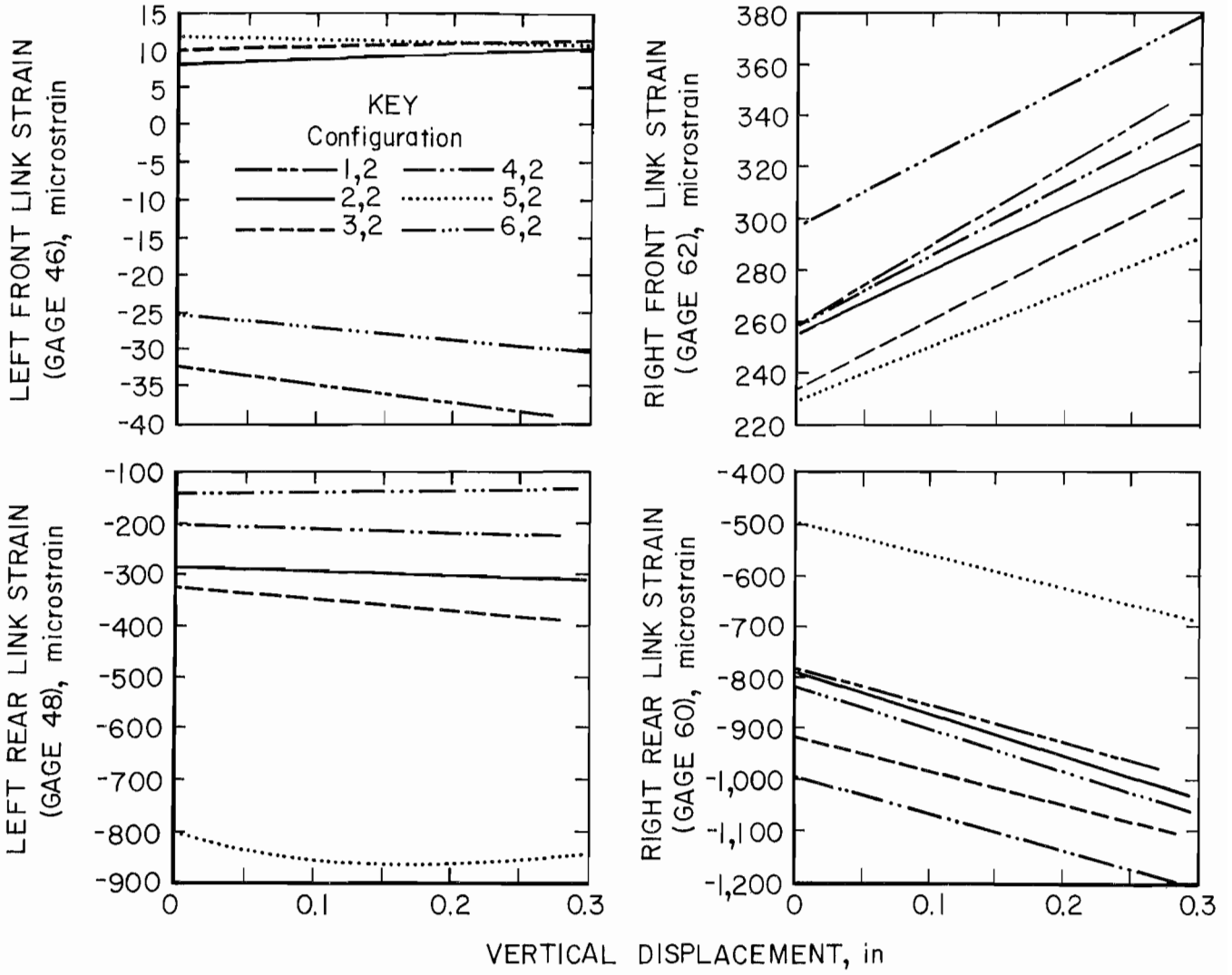


**Figure D-8.–Link strain development for various canopy contact configurations with unsymmetric base-on-rear contacts.**

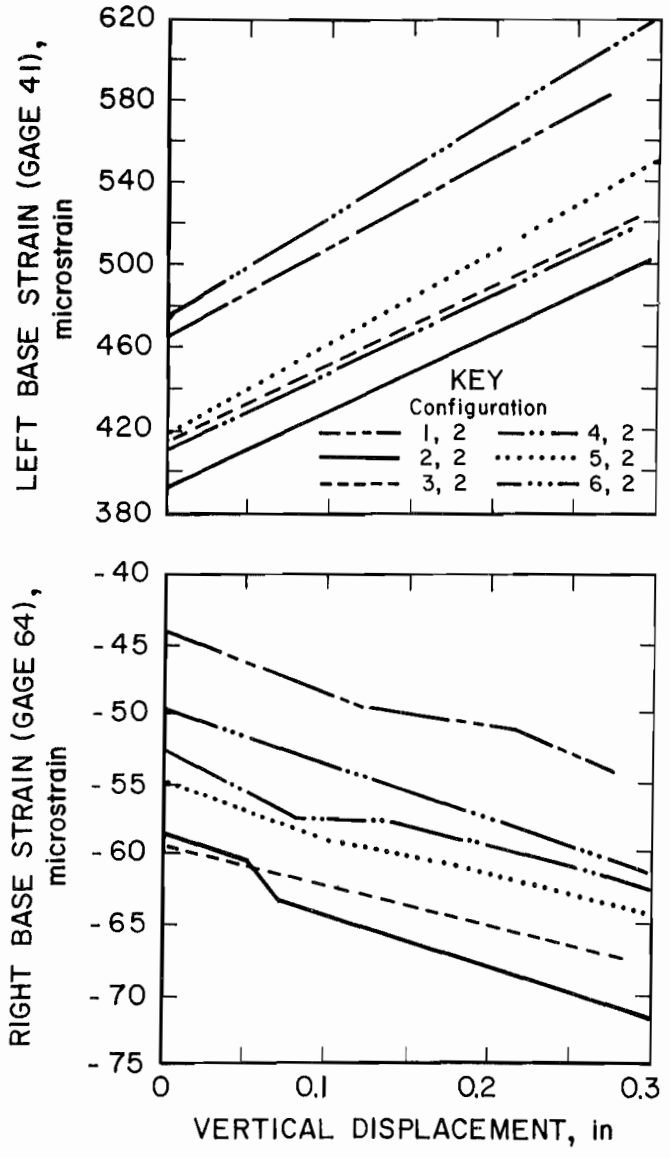


Figure D-9.–Base strain development for various canopy contact configurations with unsymmetric base-on-rear contacts.

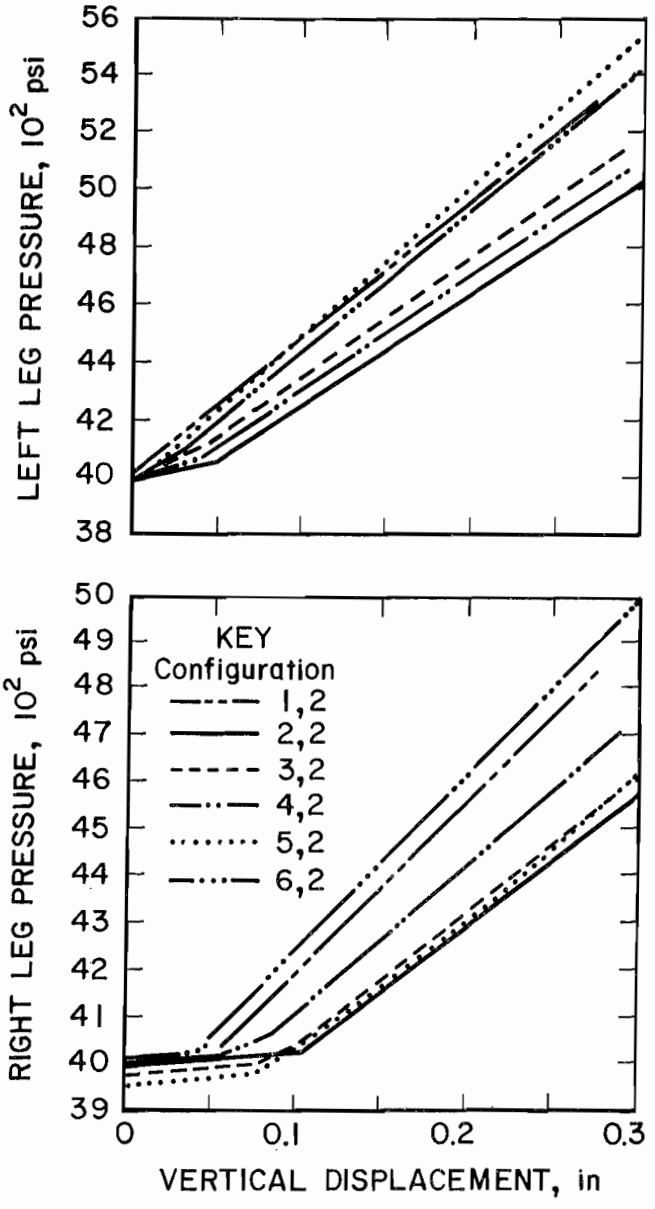


Figure D-10.–Leg pressure development for various canopy contact configurations with unsymmetric base-on-rear contacts.

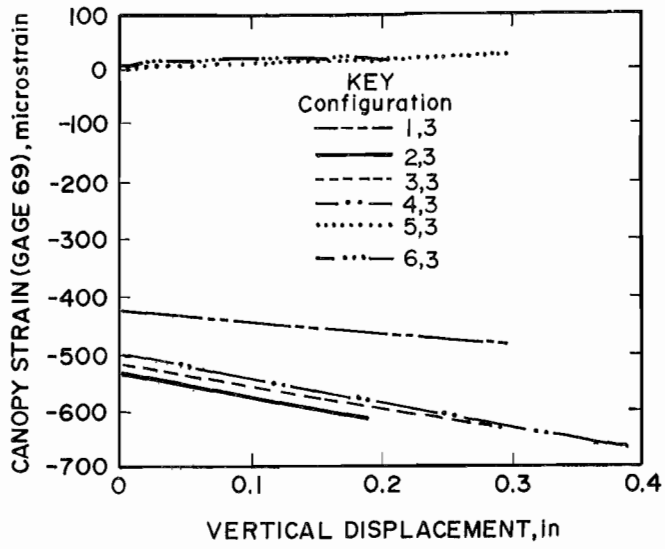


Figure D-11.–Canopy strain development for various canopy contact configurations with unsymmetric base-on-toe contacts.

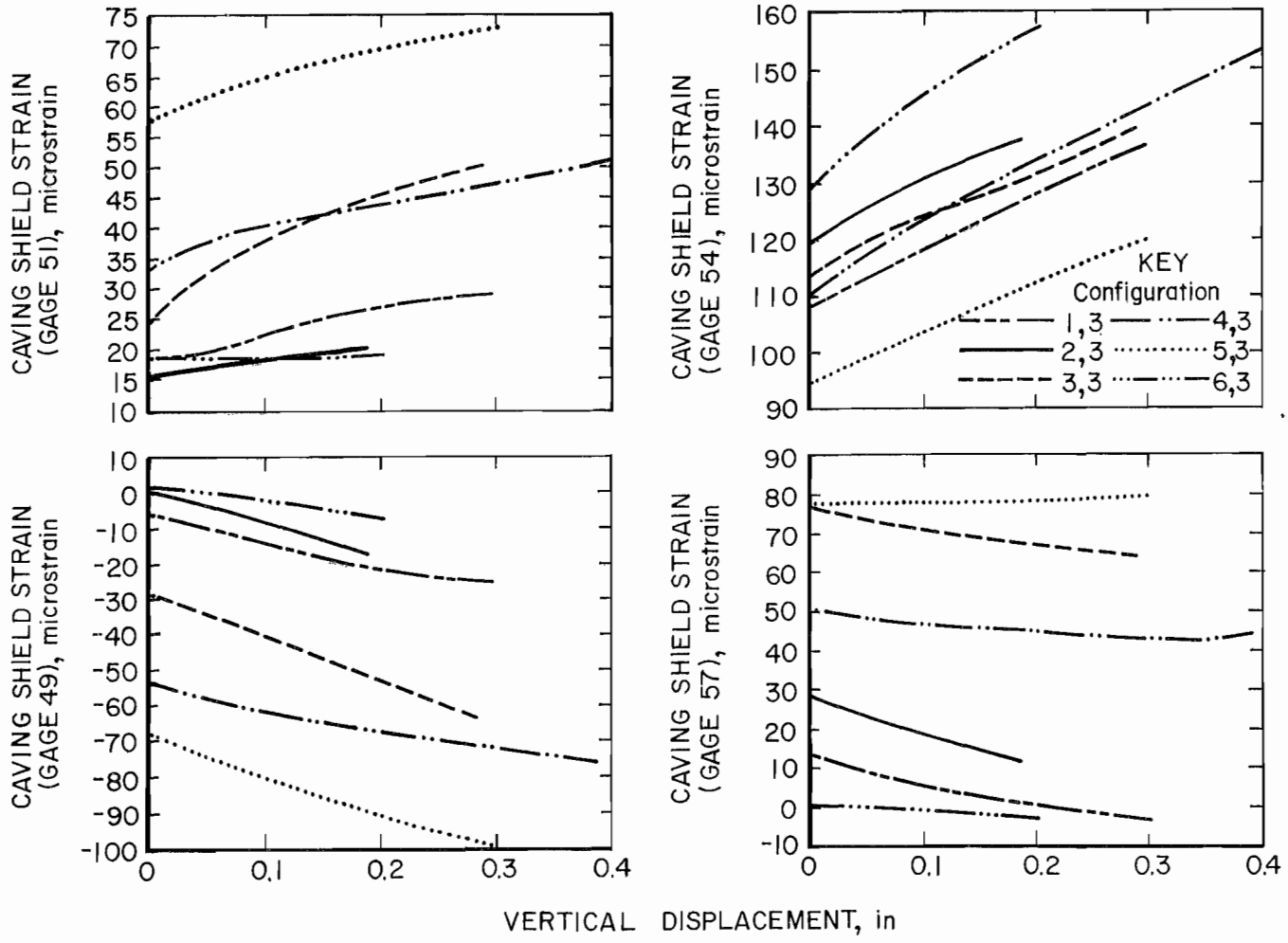


Figure D-12.–Caving shield strain development for various canopy contact configurations with unsymmetric base-on-toe contacts.

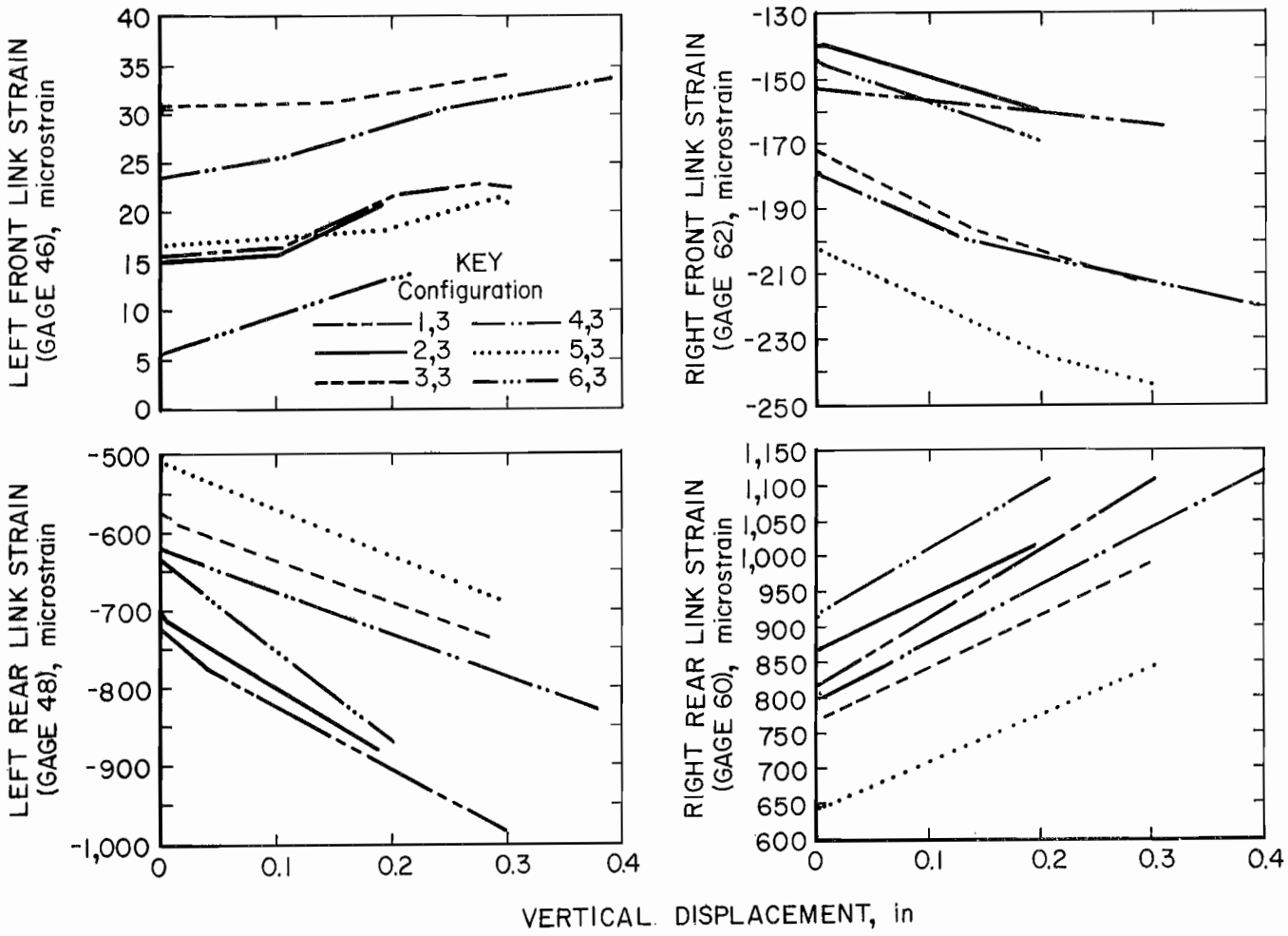


**Figure D-13.–Link strain development for various canopy contact configurations with unsymmetric base-on-toe contacts.**

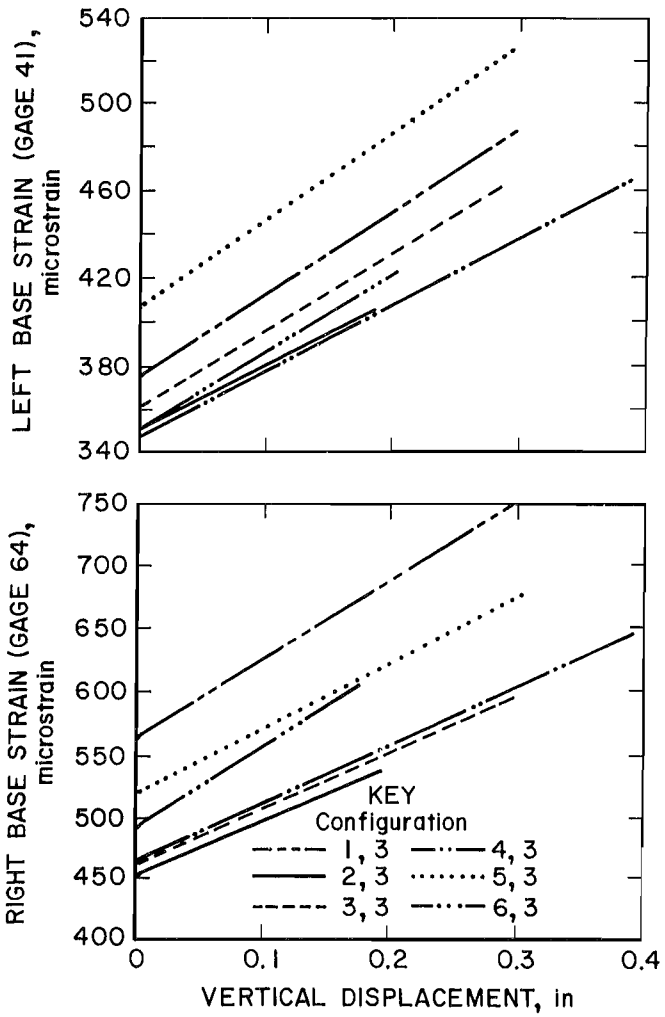


Figure D-14.–Base strain development for various canopy contact configurations with unsymmetric base-on-toe contacts.

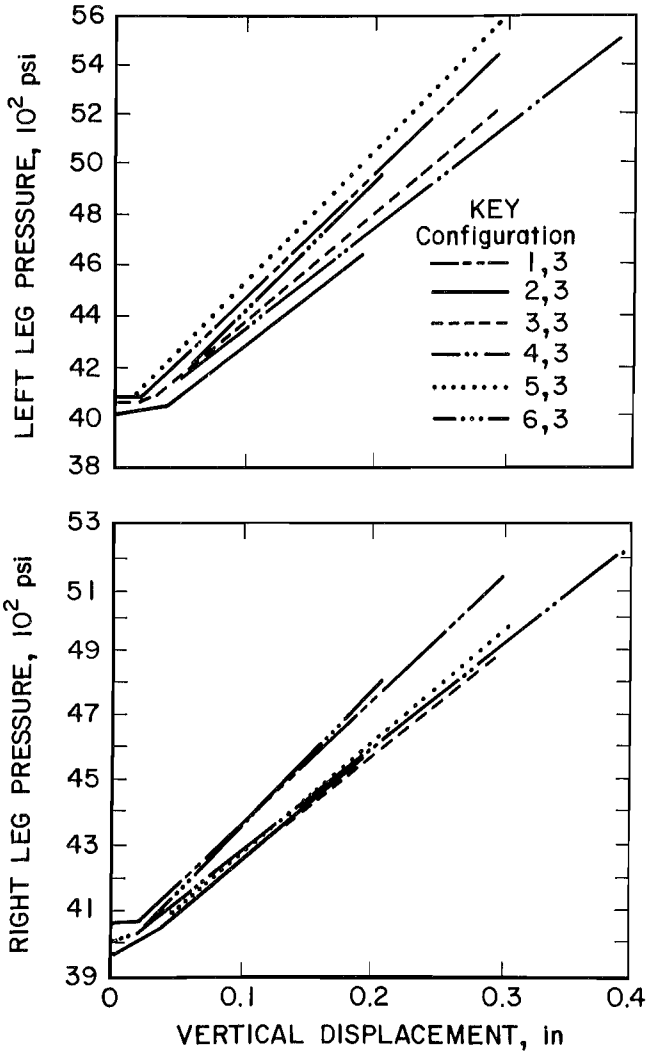


Figure D-15.–Leg pressure development for various canopy contact configurations with unsymmetric base-on-toe contacts.

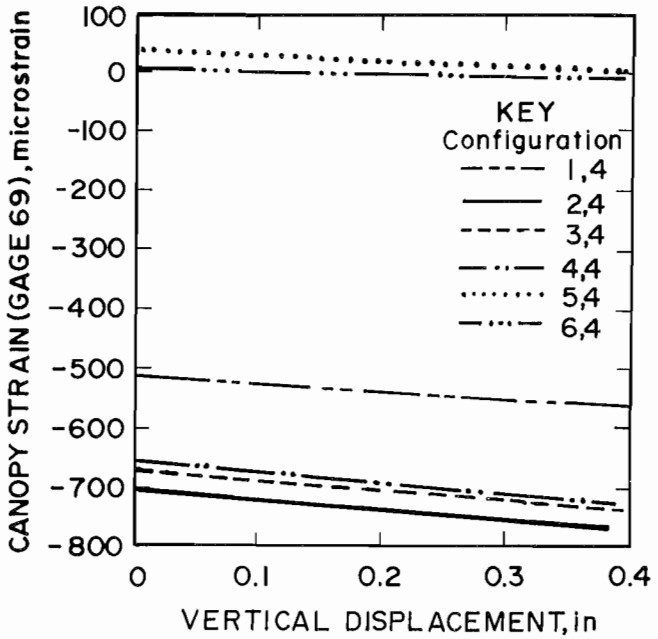


**Figure D-16.–Canopy strain development for various canopy contact configurations with full base contact.**

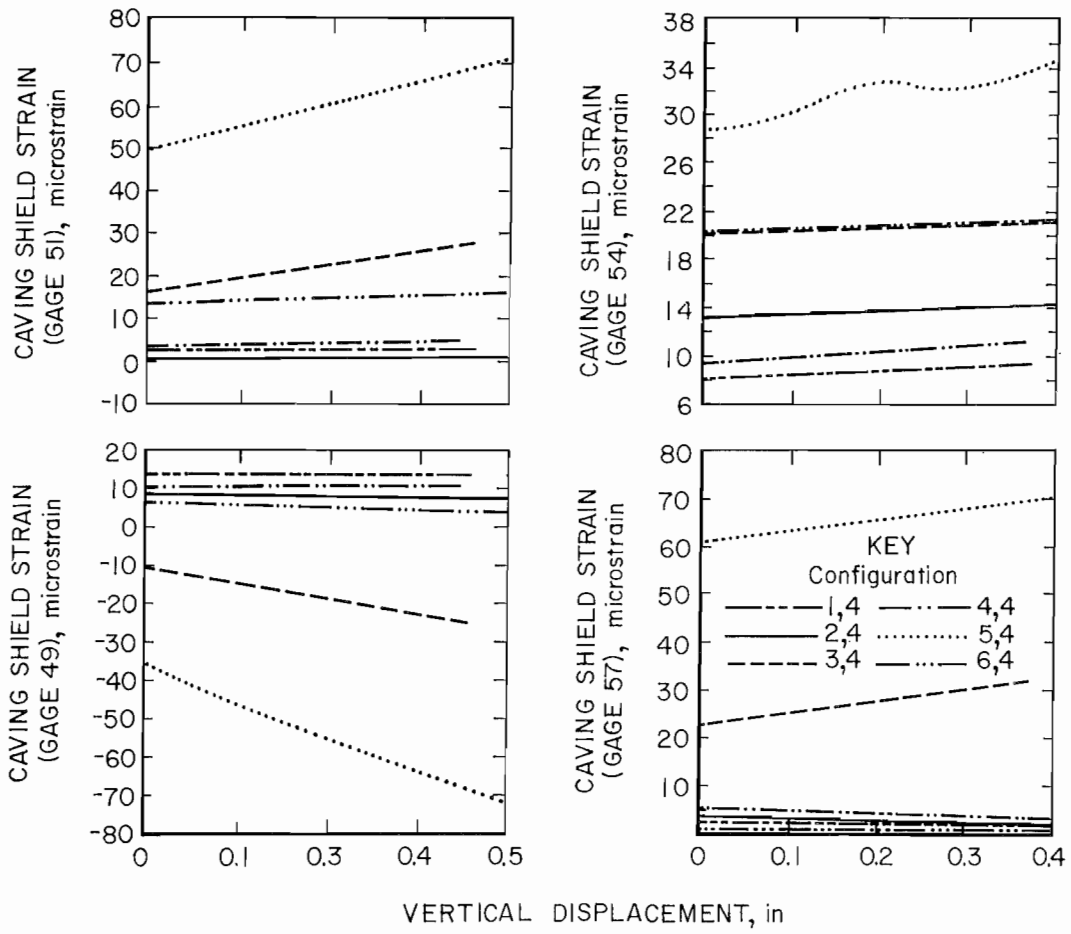


**Figure D-17.–Caving shield strain development for various canopy contact configurations with full base contact.**

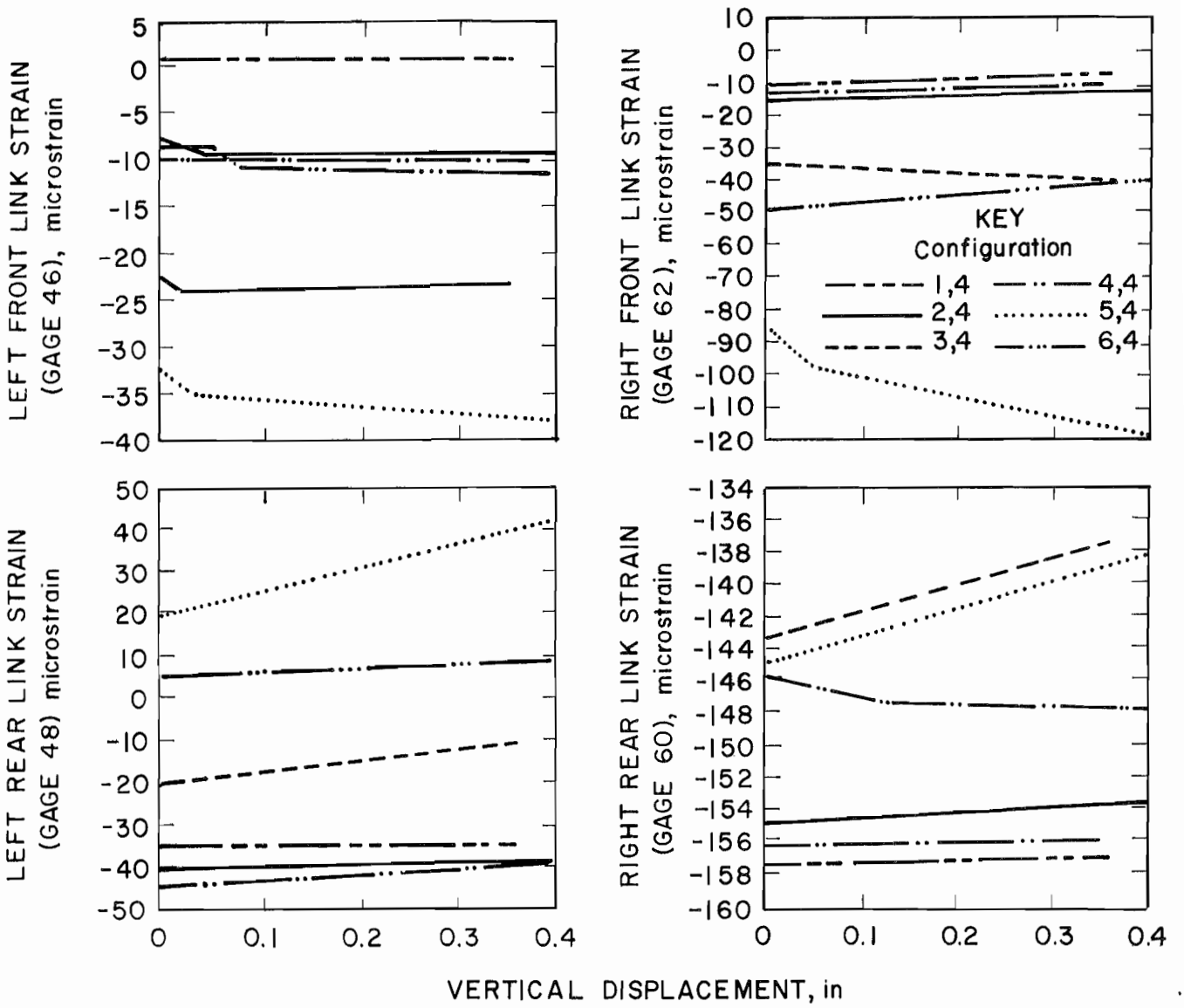


**Figure D-18.–Link strain development for various canopy contact configurations with full base contact.**

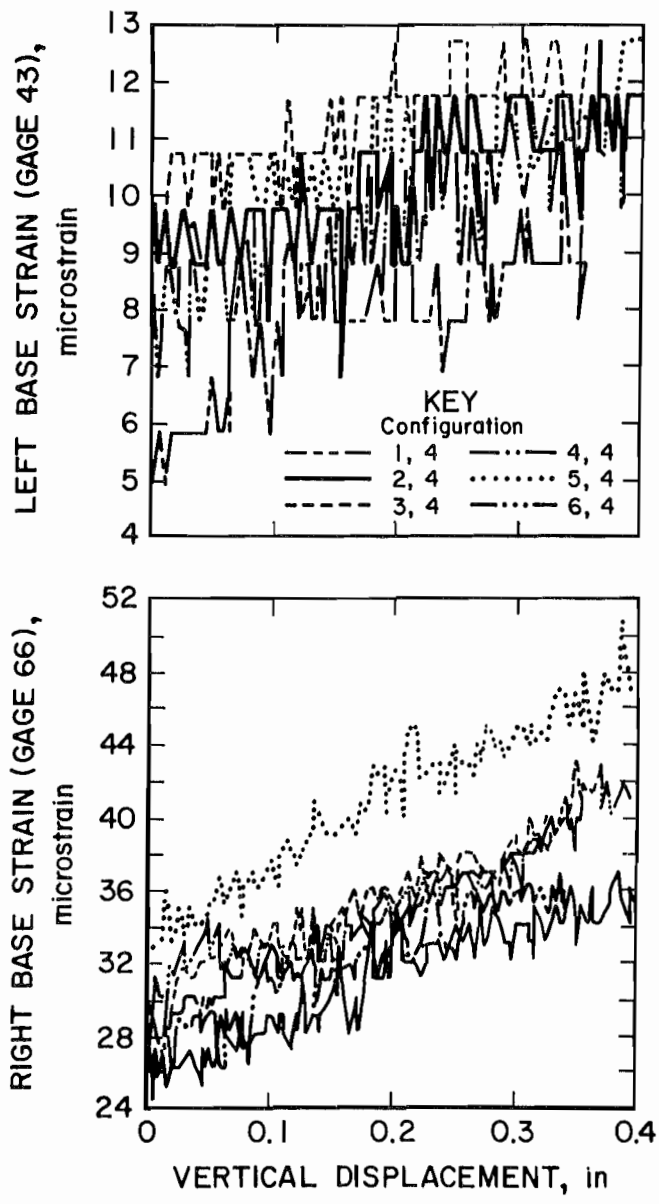


Figure D-19.–Base strain development for various canopy contact configurations with full base contact.

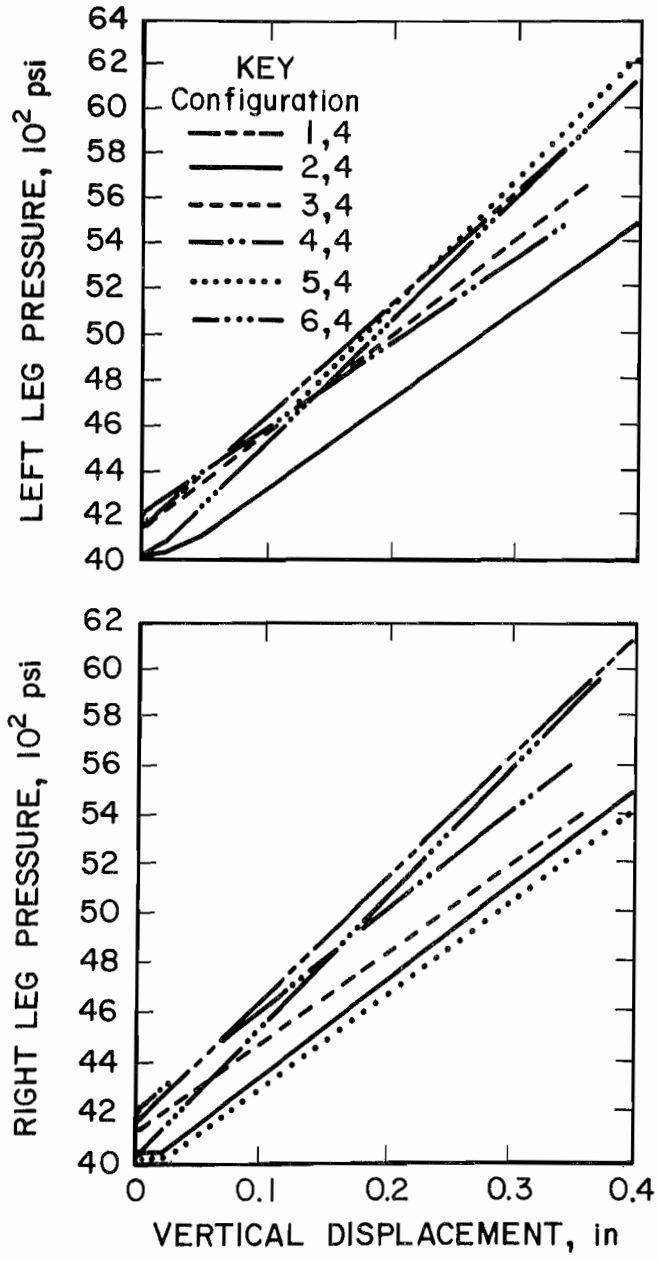


Figure D-20.–Leg pressure development for various canopy contact configurations with full base contact.

# APPENDIX E.–STRAIN DEVELOPMENT FOR LIKE CANOPY CONTACTS

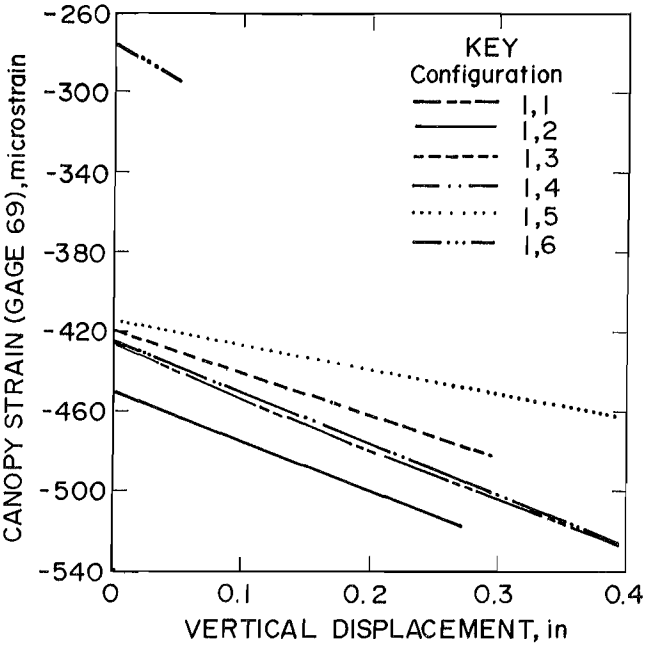


Figure E-1.–Canopy strain development for various base contact configurations with full canopy contact.

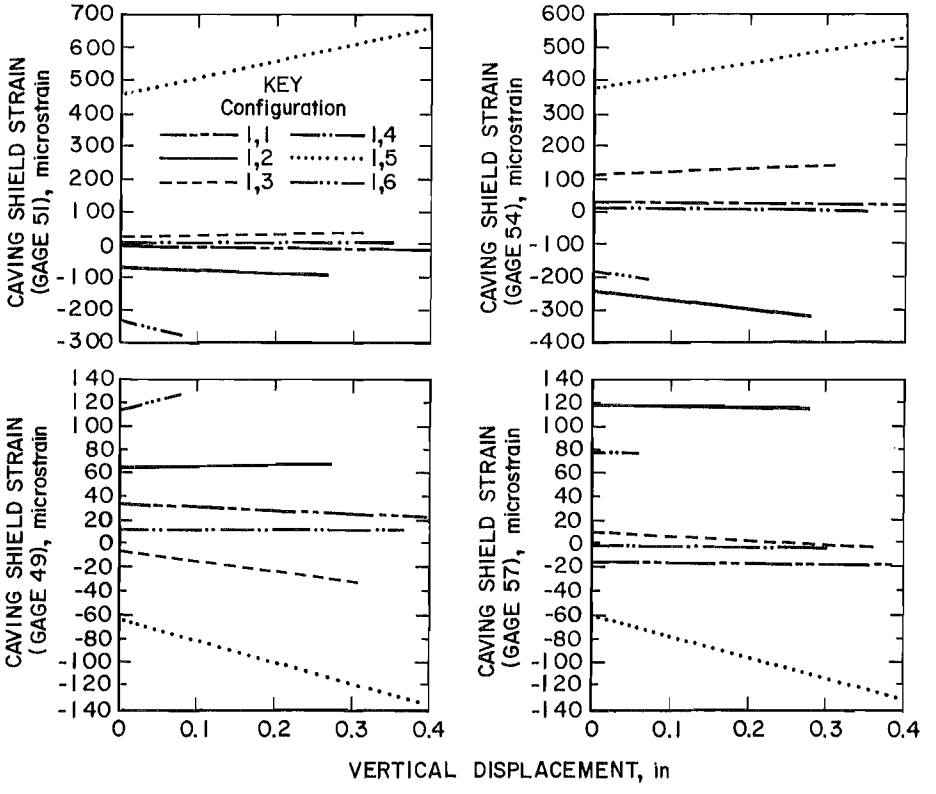


Figure E-2.–Caving shield strain development for various base contact configurations with full canopy contact.

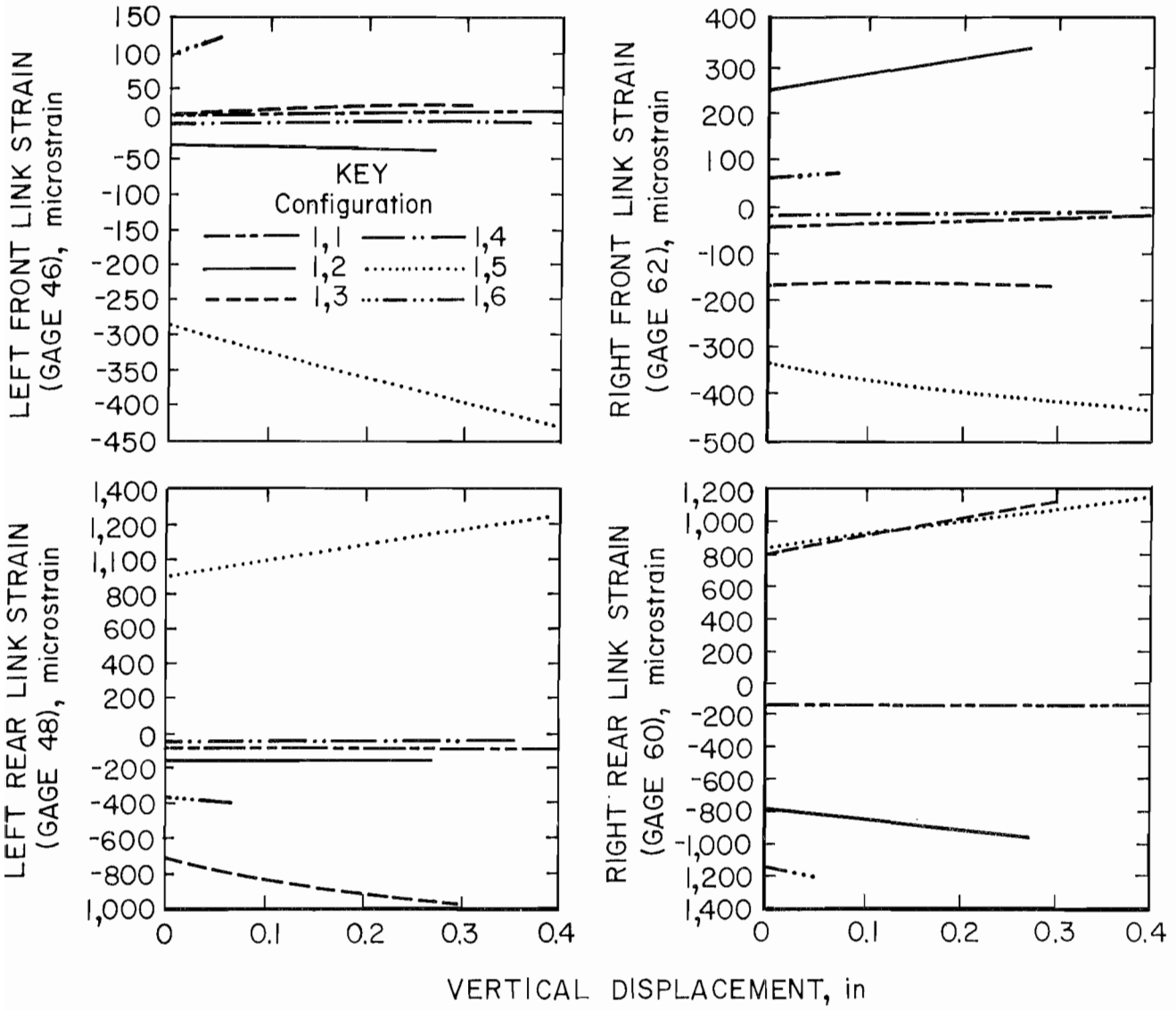


Figure E-3.–Link strain development for various base contact configurations with full canopy contact.

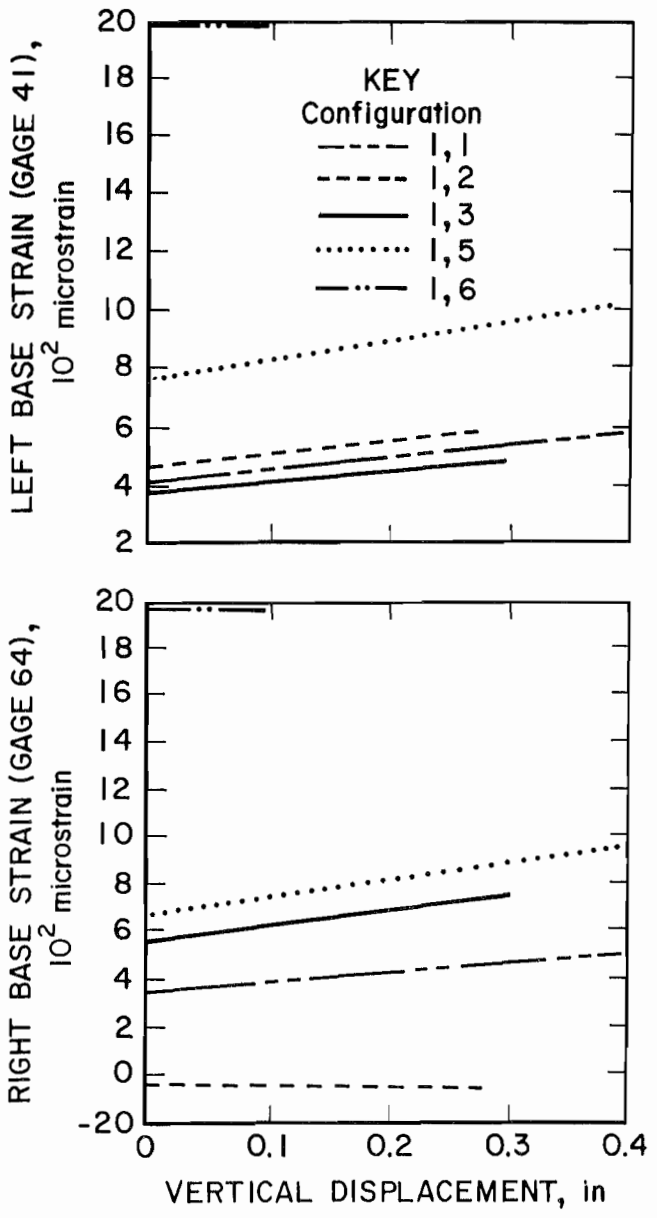


Figure E-4.–Base strain development for various base contact configurations with full canopy contact.

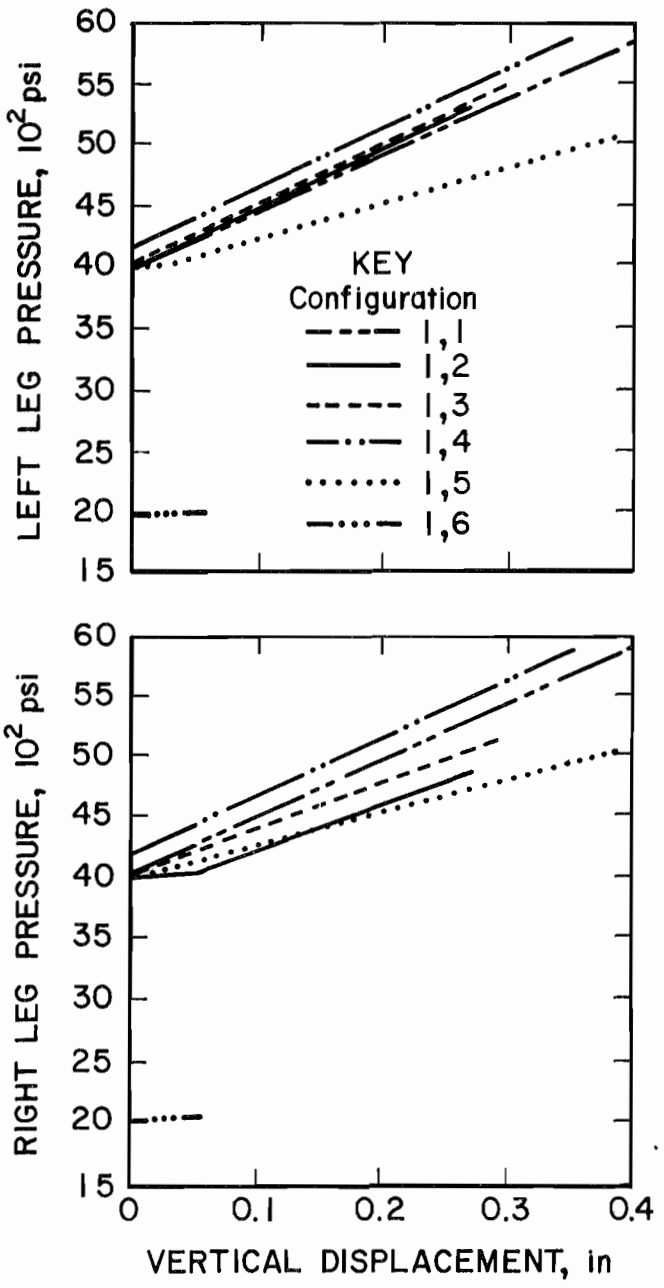


Figure E-5.–Leg pressure development for various base contact configurations with full canopy contact.

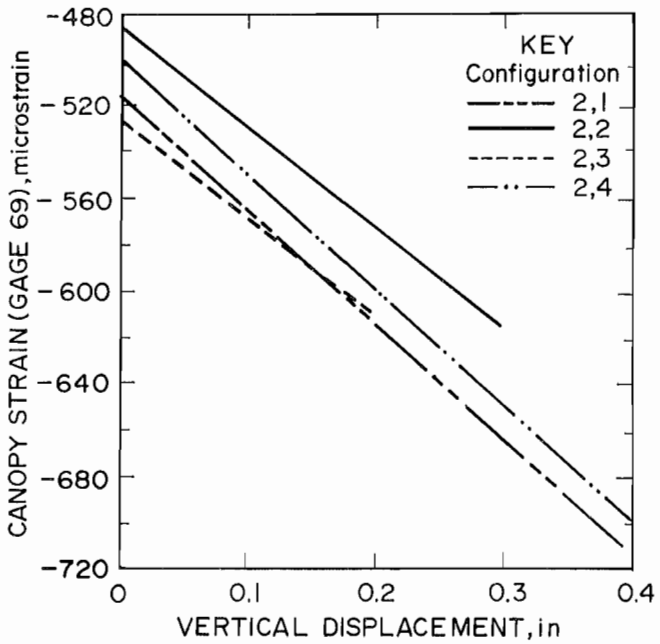


**Figure E-6.–Canopy strain development for various base contact configurations with symmetric two-point canopy contact.**

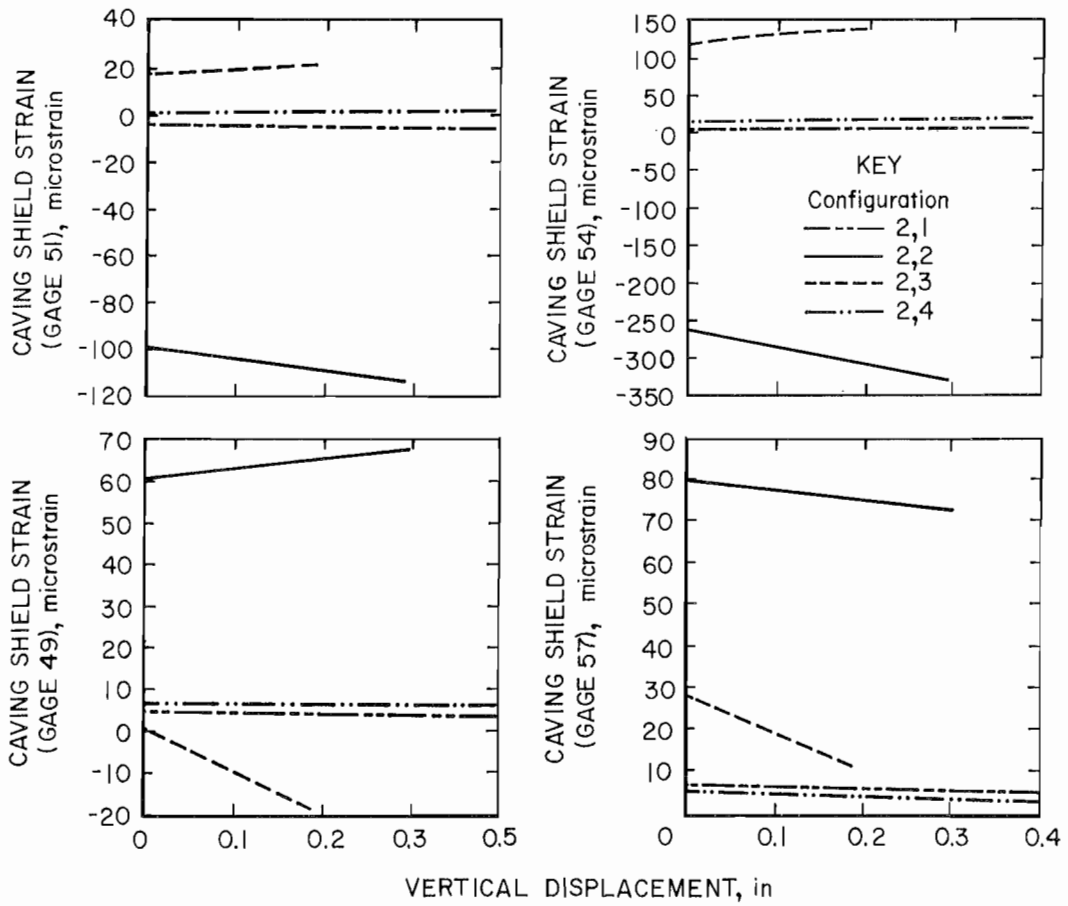


**Figure E-7.–Caving shield strain development for various base contact configurations with symmetric two-point canopy contact.**

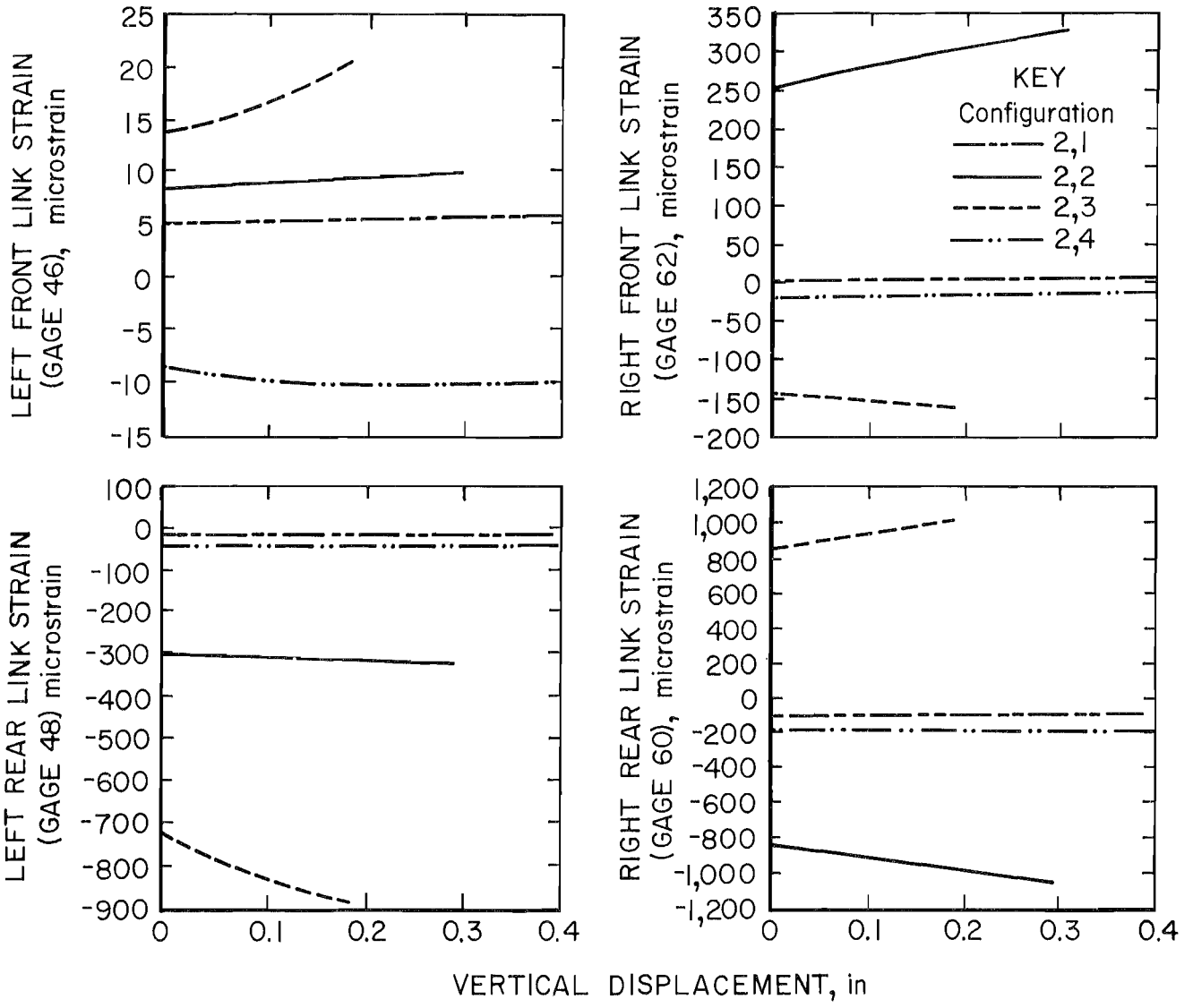


**Figure E-8.–Link strain development for various base contact configurations with symmetric two-point canopy contact.**

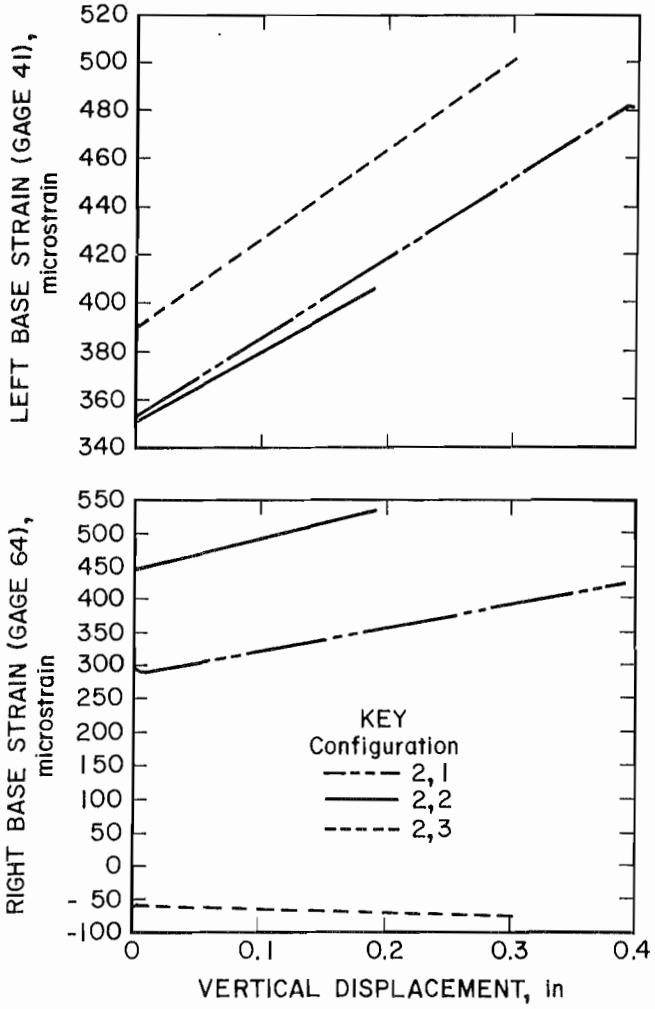


Figure E-9.–Base strain development for various base contact configurations with symmetric two-point canopy contact.

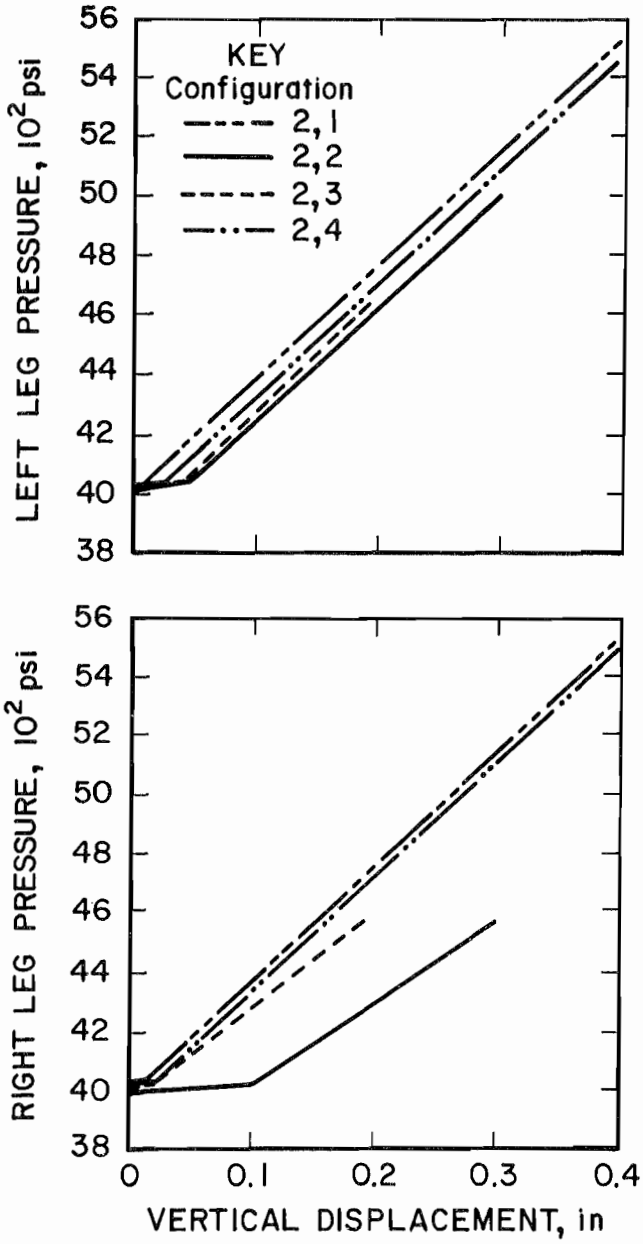


Figure E-10.–Leg pressure development for various base contact configurations with symmetric two-point canopy contact.

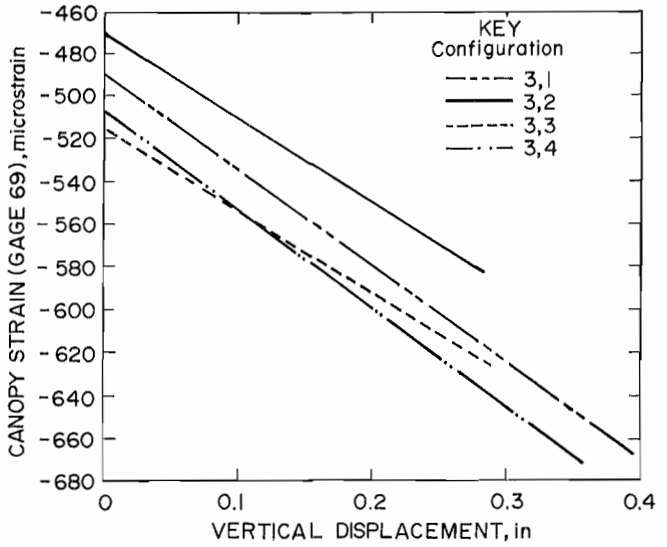


**Figure E-11.–Canopy strain development for various base contact configurations with unsymmetric canopy rear contact.**

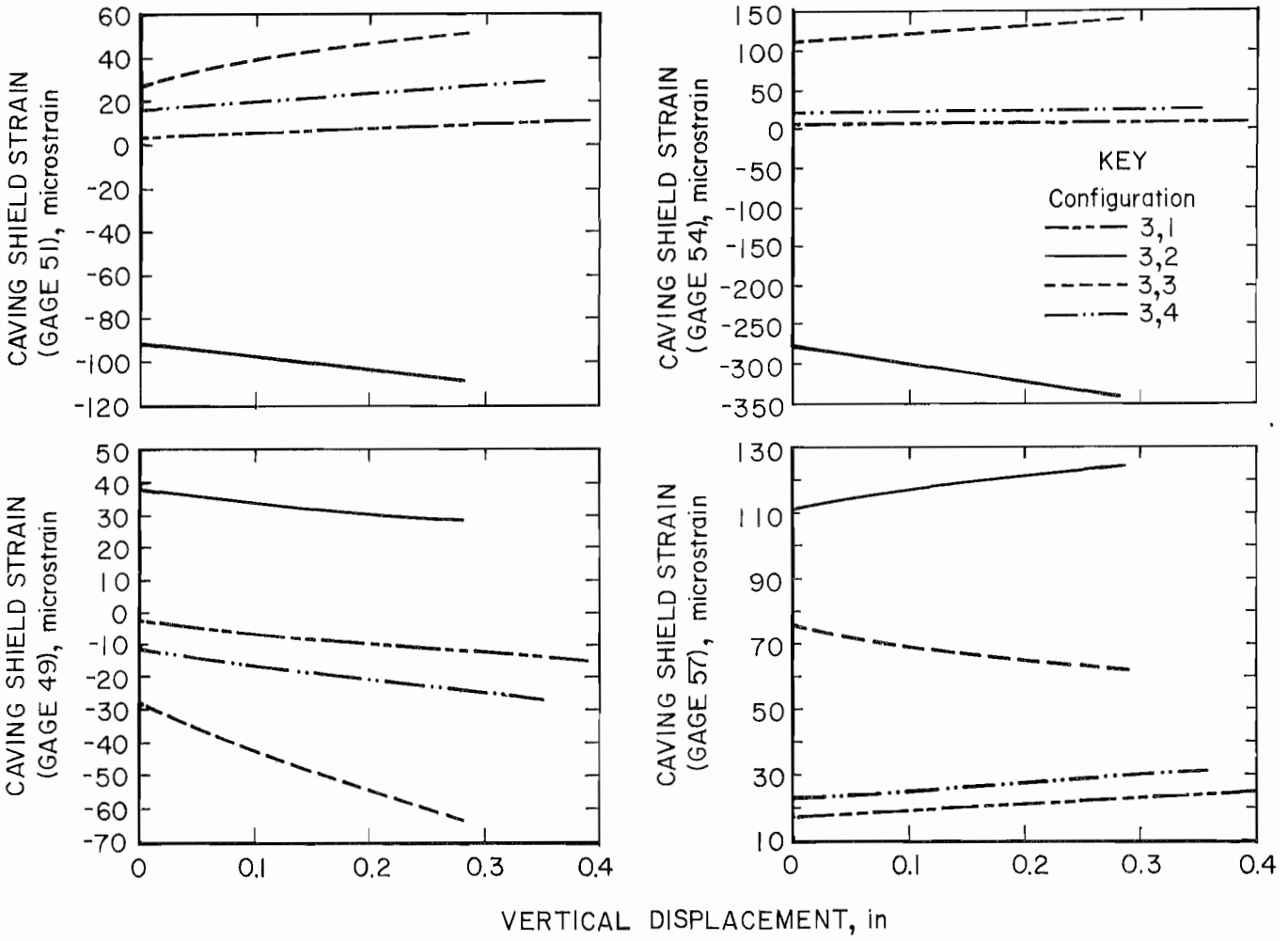


**Figure E-12.–Caving shield strain development for various base contact configurations with unsymmetric canopy rear contact.**

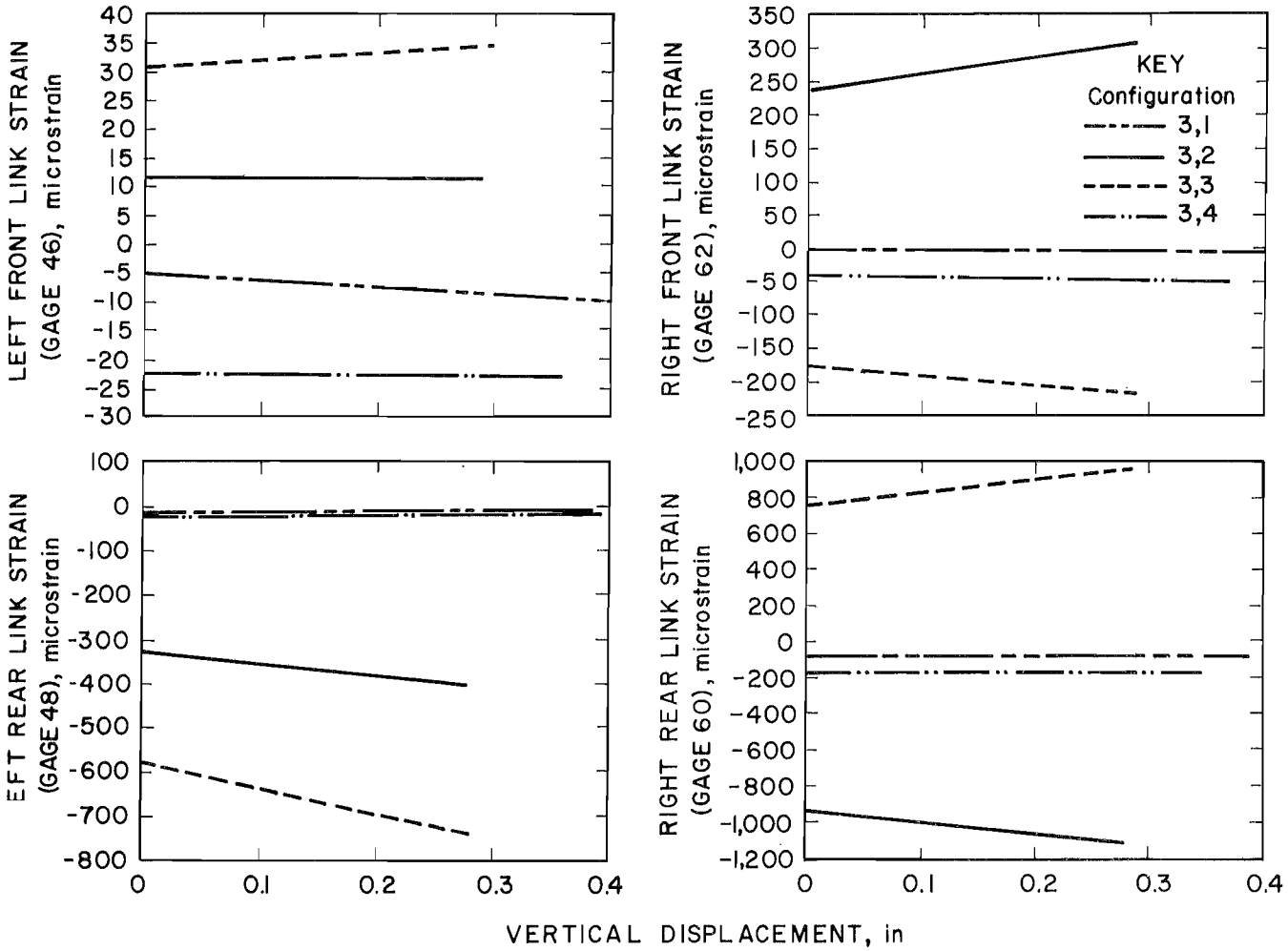


Figure E-13.–Link strain development for various base contact configurations with unsymmetric canopy rear contact.

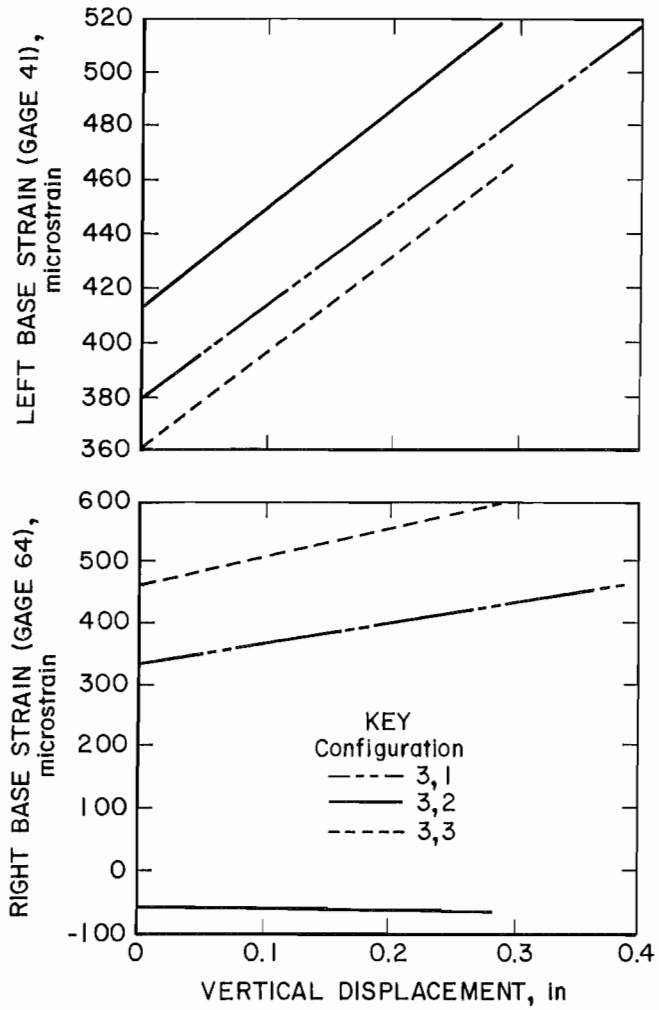


Figure E-14.–Base strain development for various base contact configurations with unsymmetric canopy rear contact.

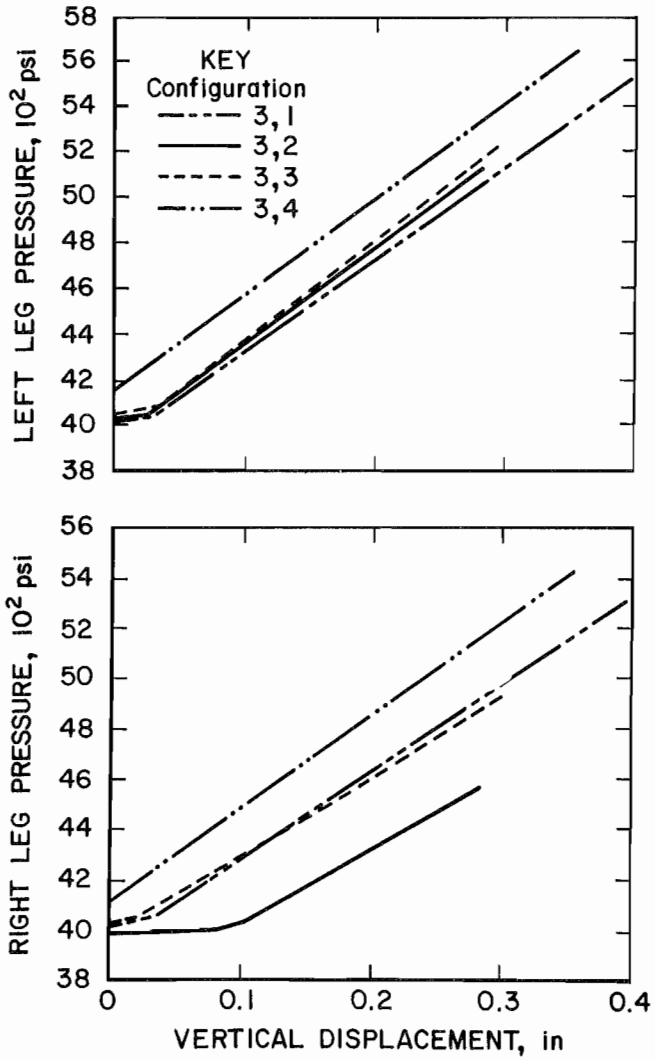


Figure E-15.–Leg pressure development for various base contact configurations with unsymmetric canopy rear contact.

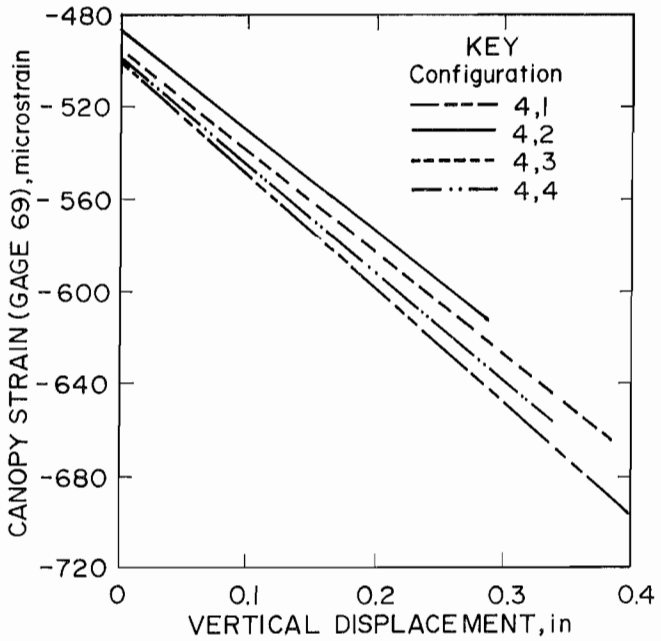


**Figure E-16.–Canopy strain development for various base contact configurations with unsymmetric canopy tip contact.**

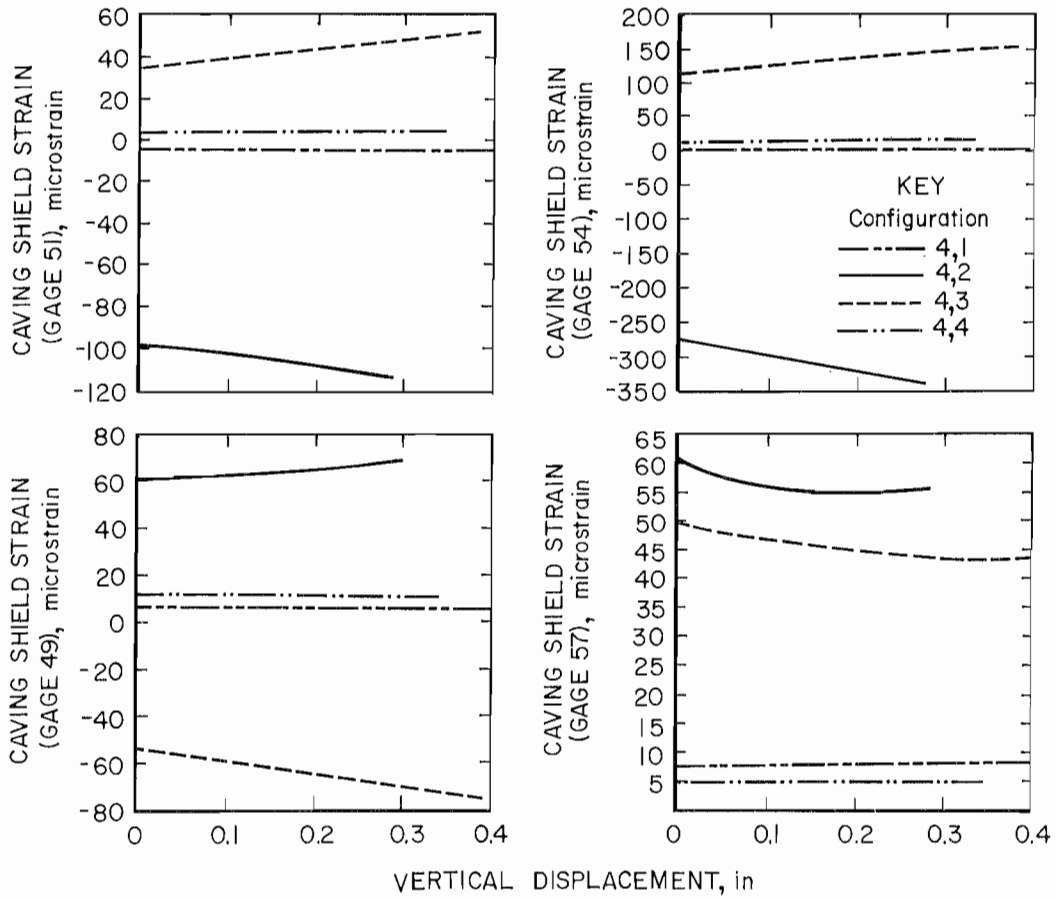


**Figure E-17.–Caving shield strain development for various base contact configurations with unsymmetric canopy tip contact.**

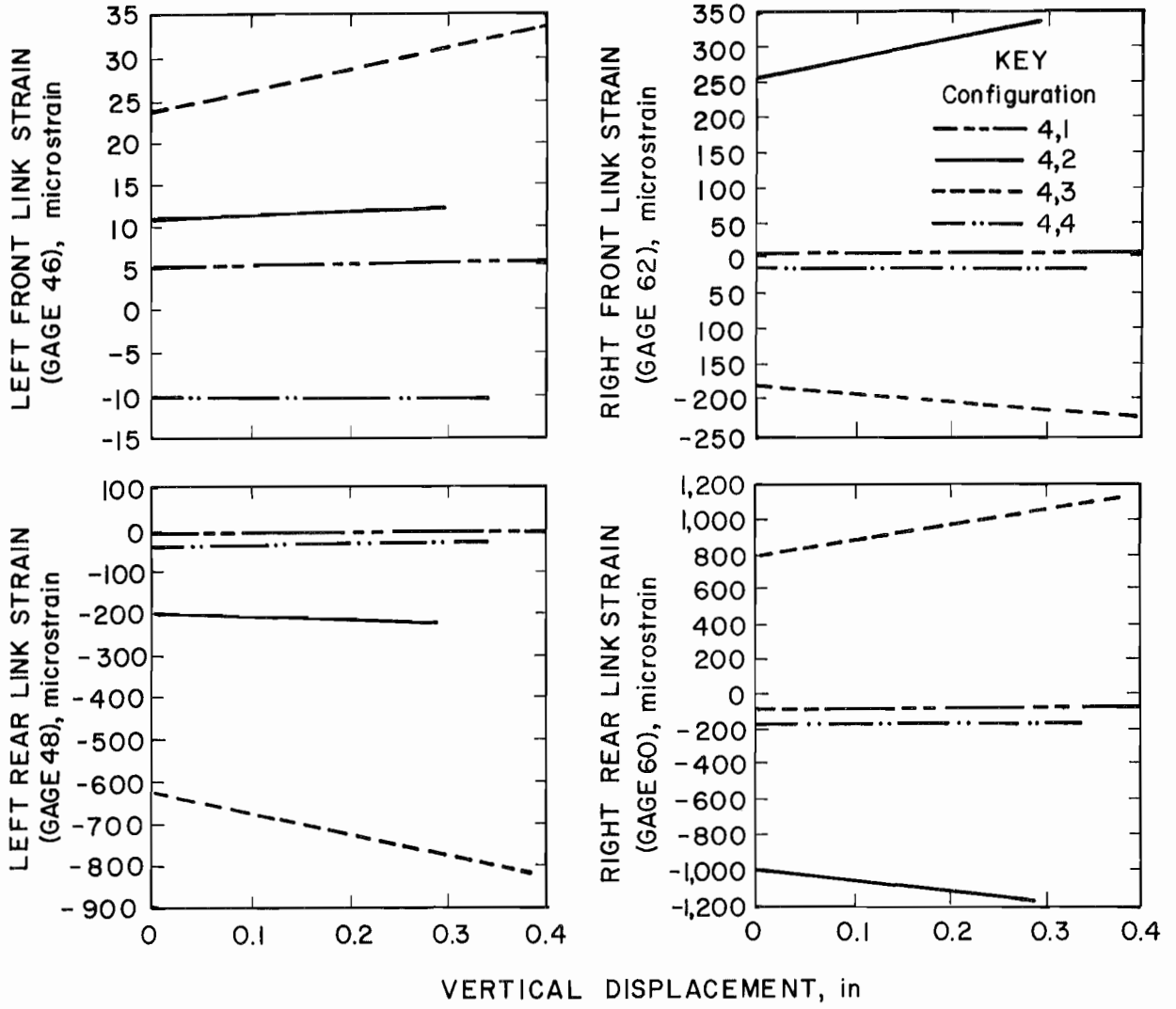


Figure E-18.–Link strain development for various base contact configurations with unsymmetric canopy tip contact.

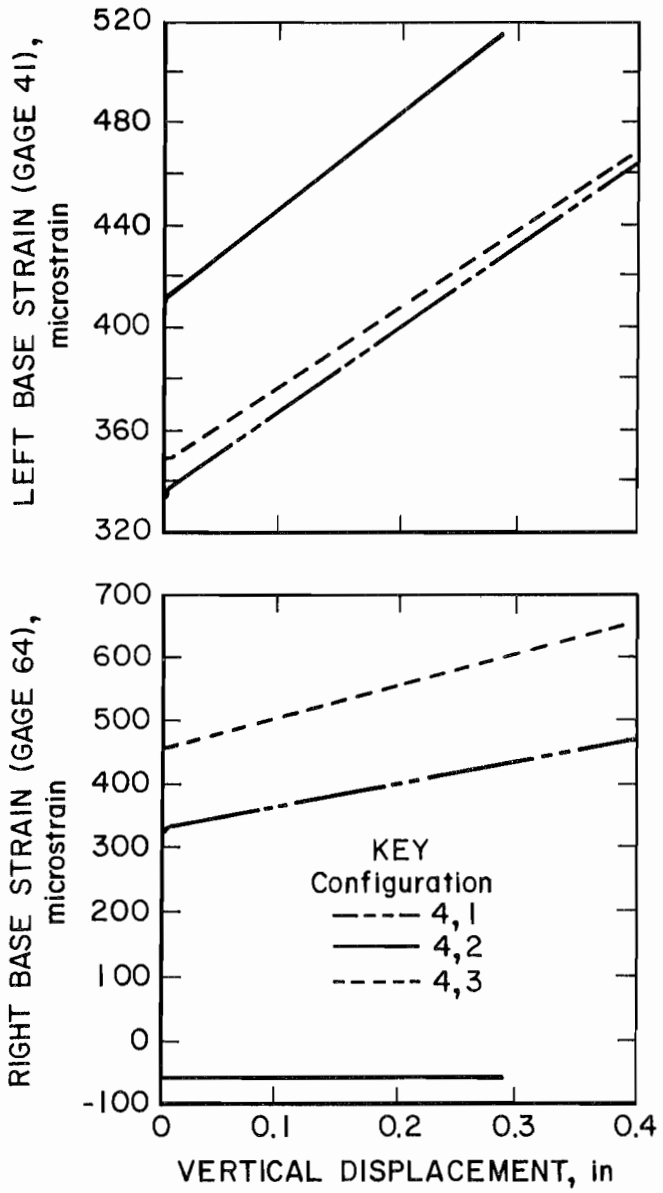


Figure E-19.–Base strain development for various base contact configurations with unsymmetric canopy tip contact.

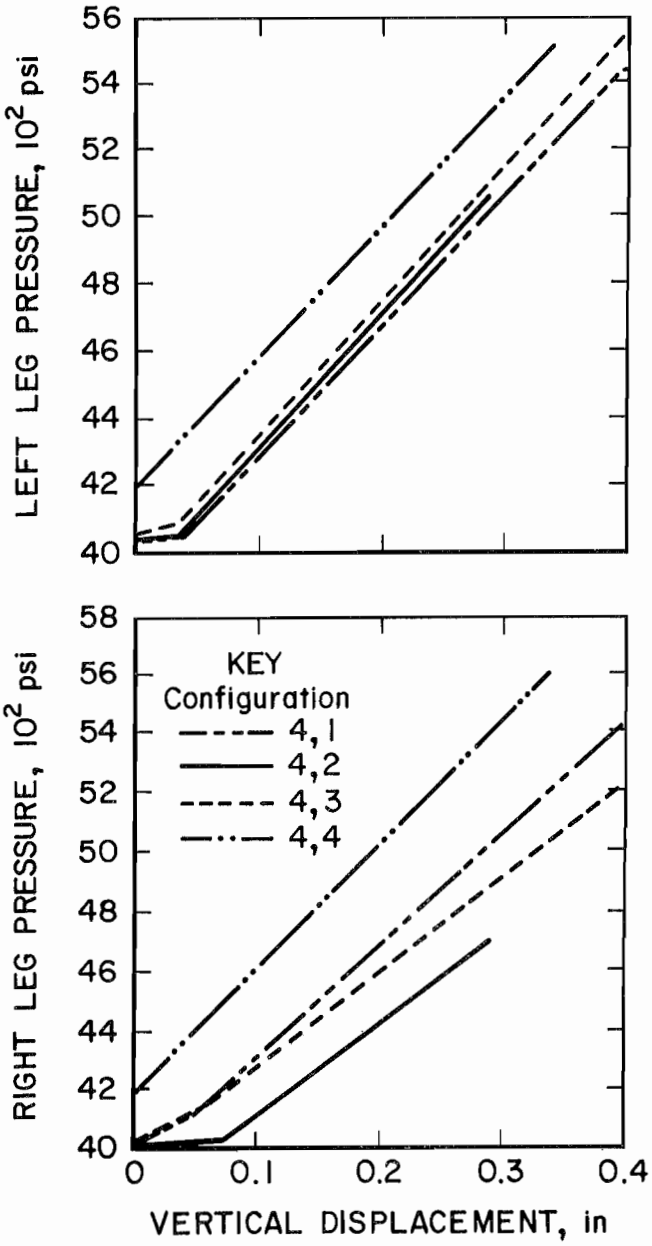


Figure E-20.–Leg pressure development for various base contact configurations with unsymmetric canopy tip contact.

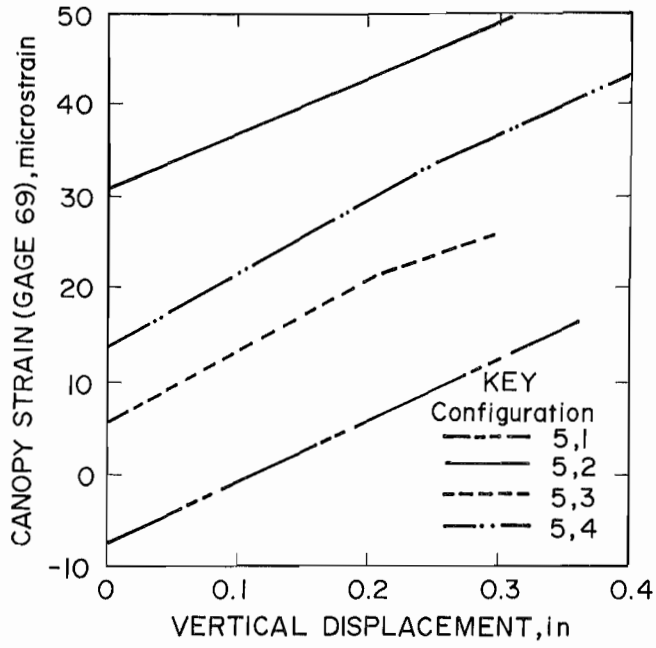


**Figure E-21.–Canopy strain development for various base contact configurations with unsymmetric canopy leg contact.**

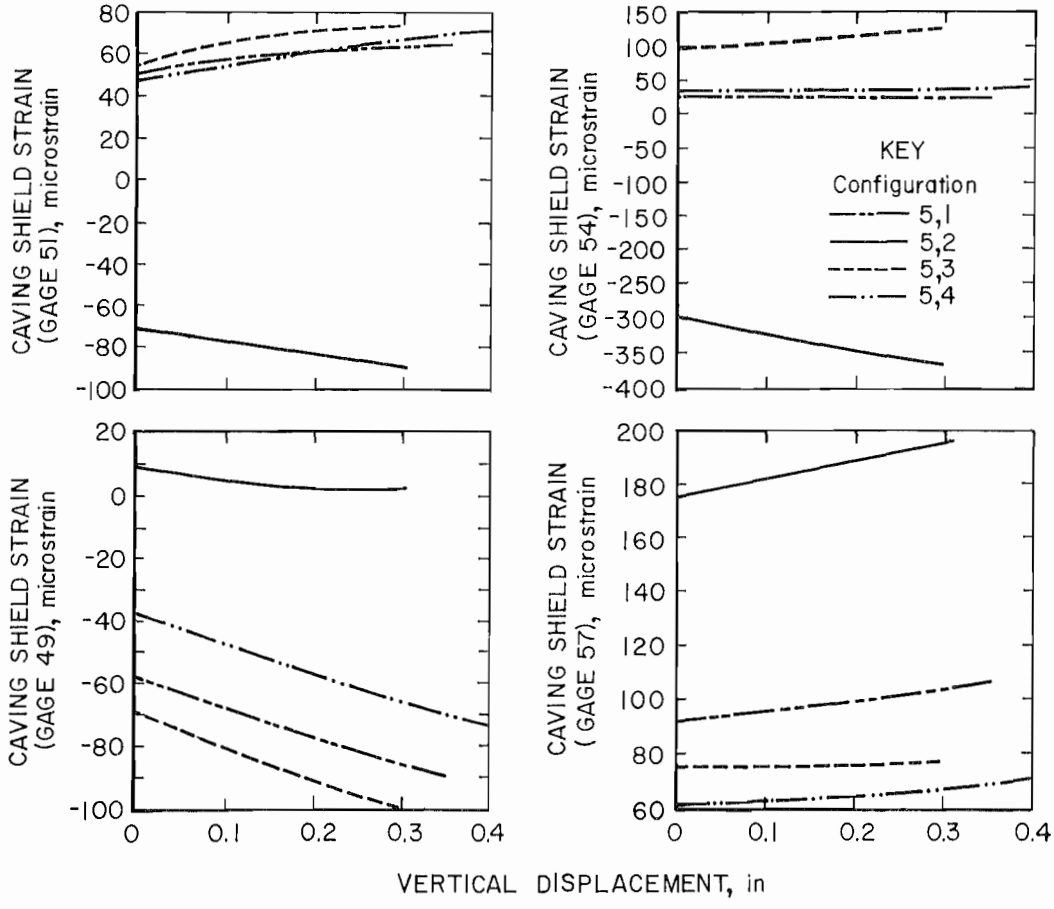


**Figure E-22.–Caving shield strain development for various base contact configurations with unsymmetric canopy leg contact.**

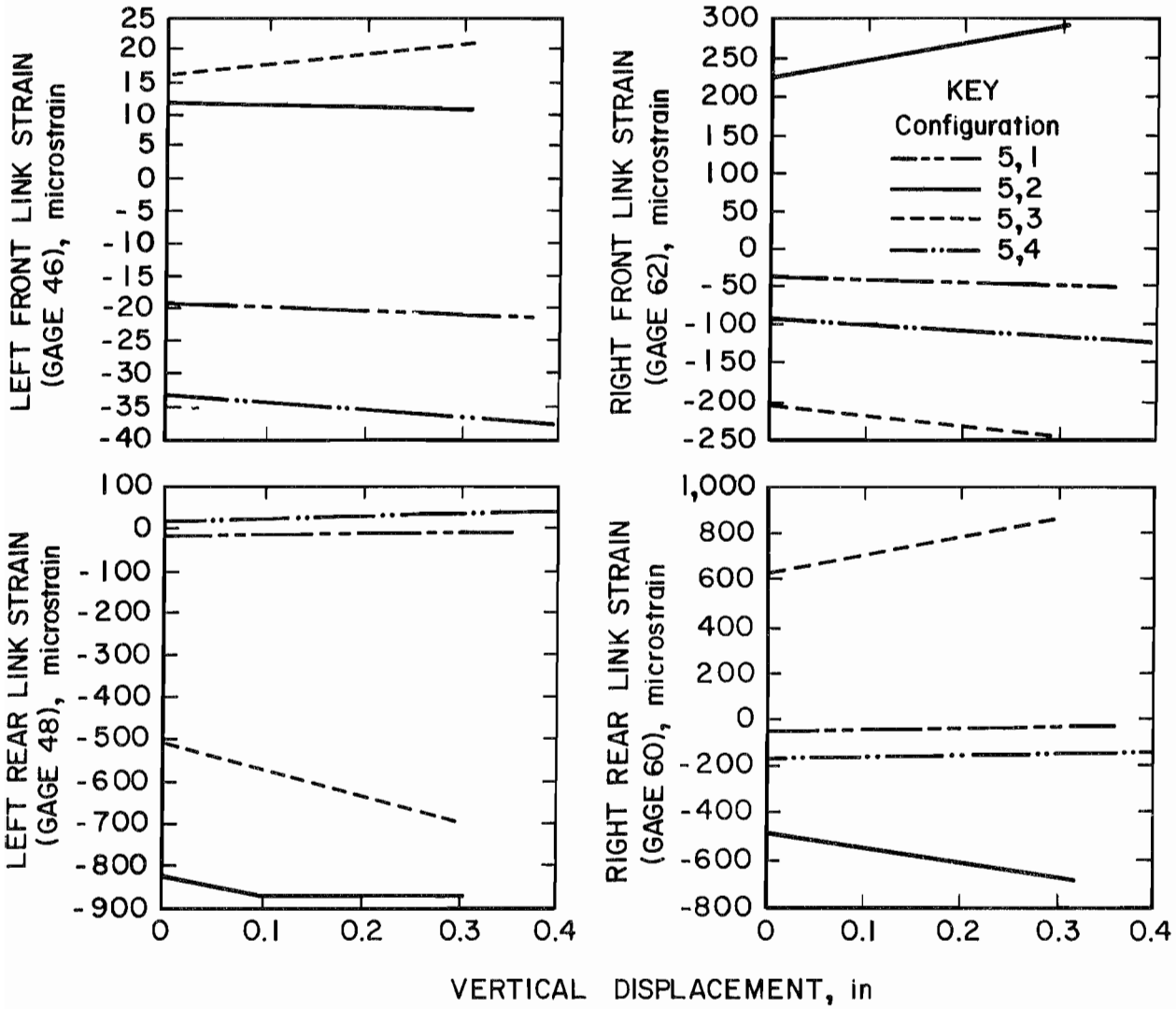


Figure E-23.–Link strain development for various base contact configurations with unsymmetric canopy leg contact.

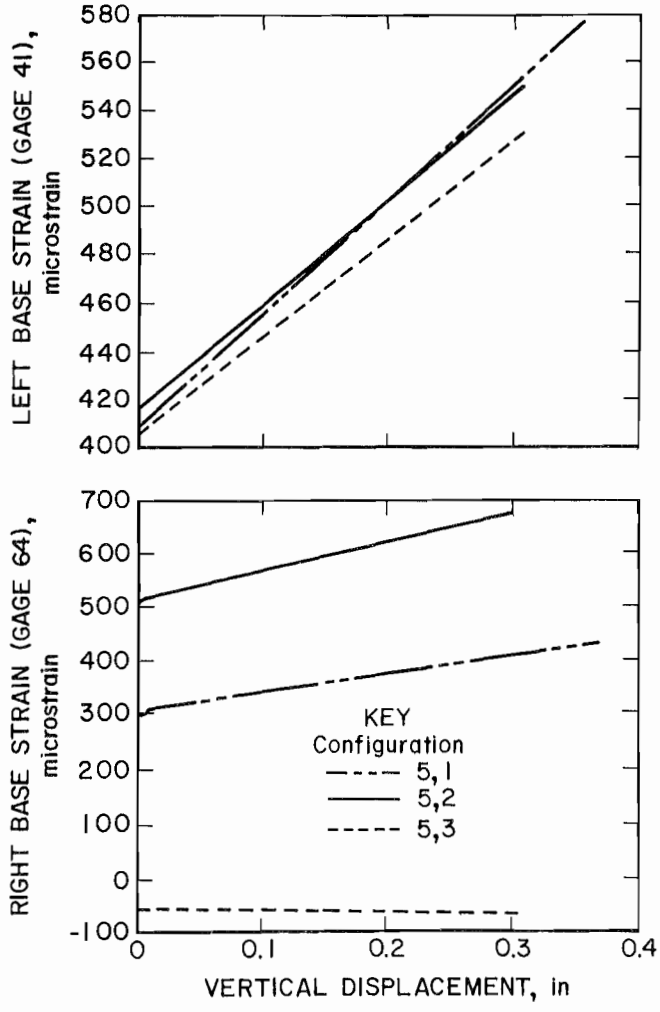


Figure E-24.–Base strain development for various base contact configurations with unsymmetric canopy leg contact.

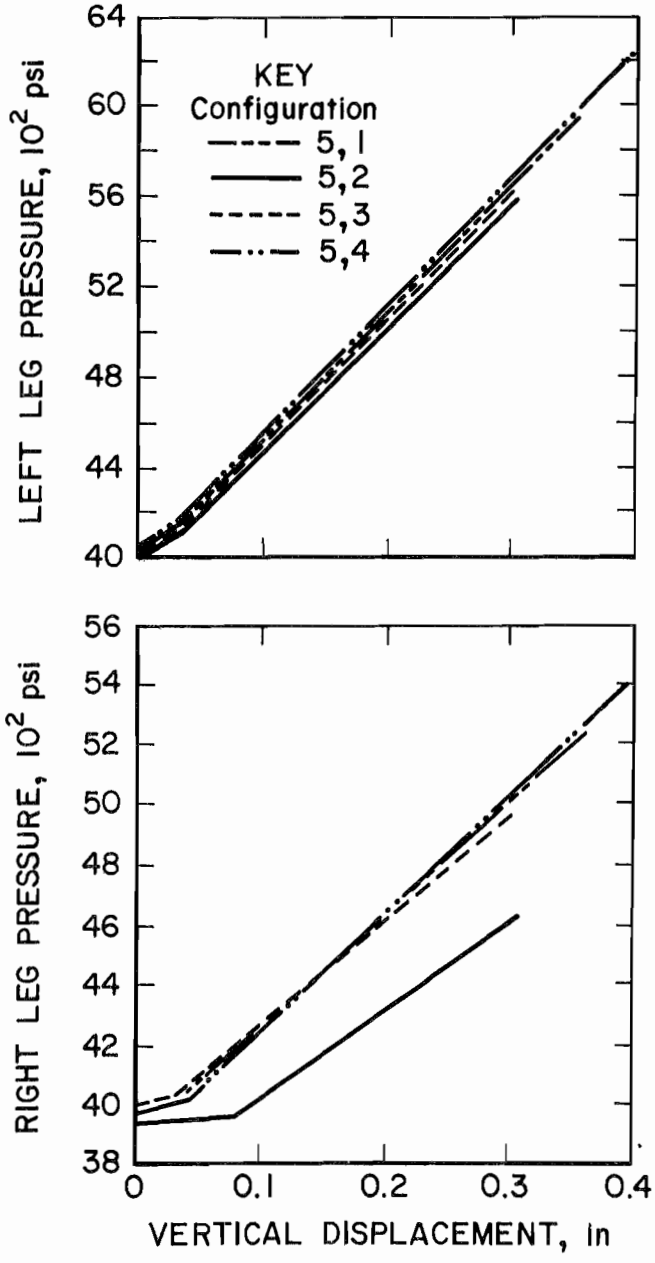


Figure E-25.–Leg pressure development for various base contact configurations with unsymmetric canopy leg contact.

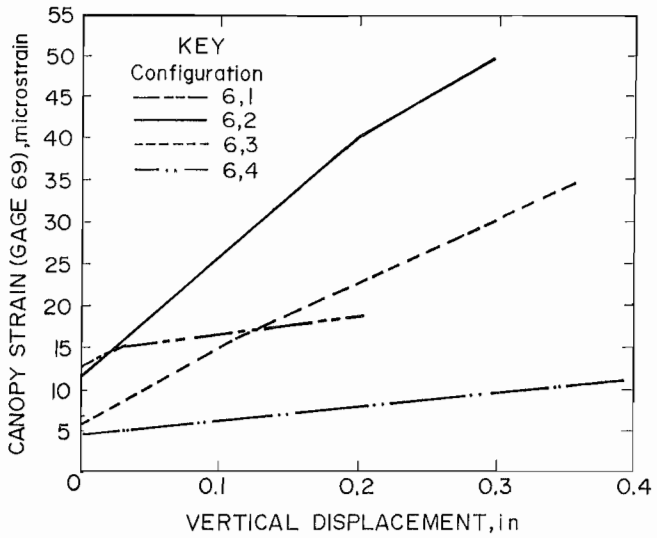


Figure E-26.–Canopy strain development for various base contact configurations with symmetric canopy leg contact.

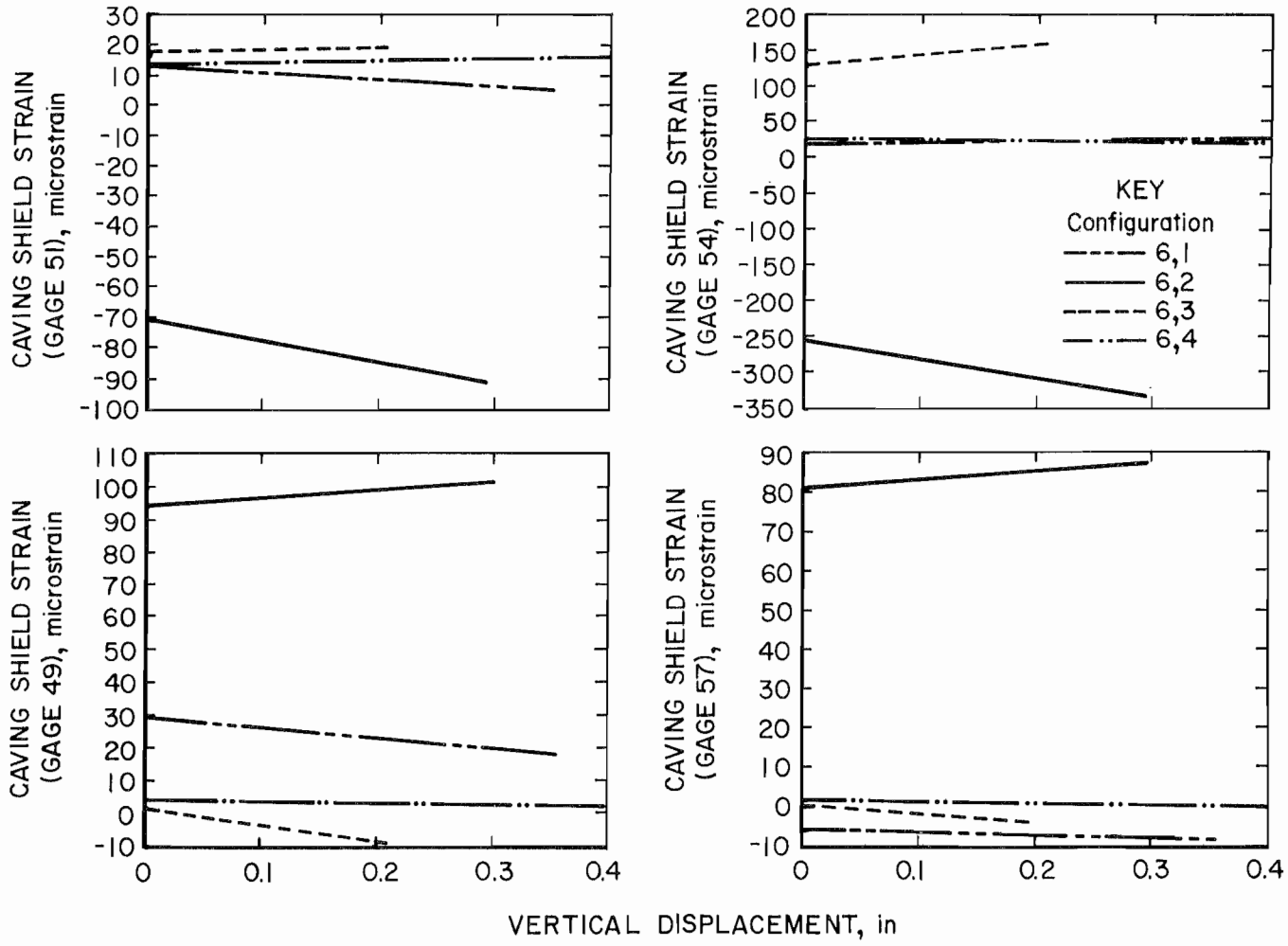


Figure E-27.–Caving shield strain development for various base contact configurations with symmetric canopy leg contact.

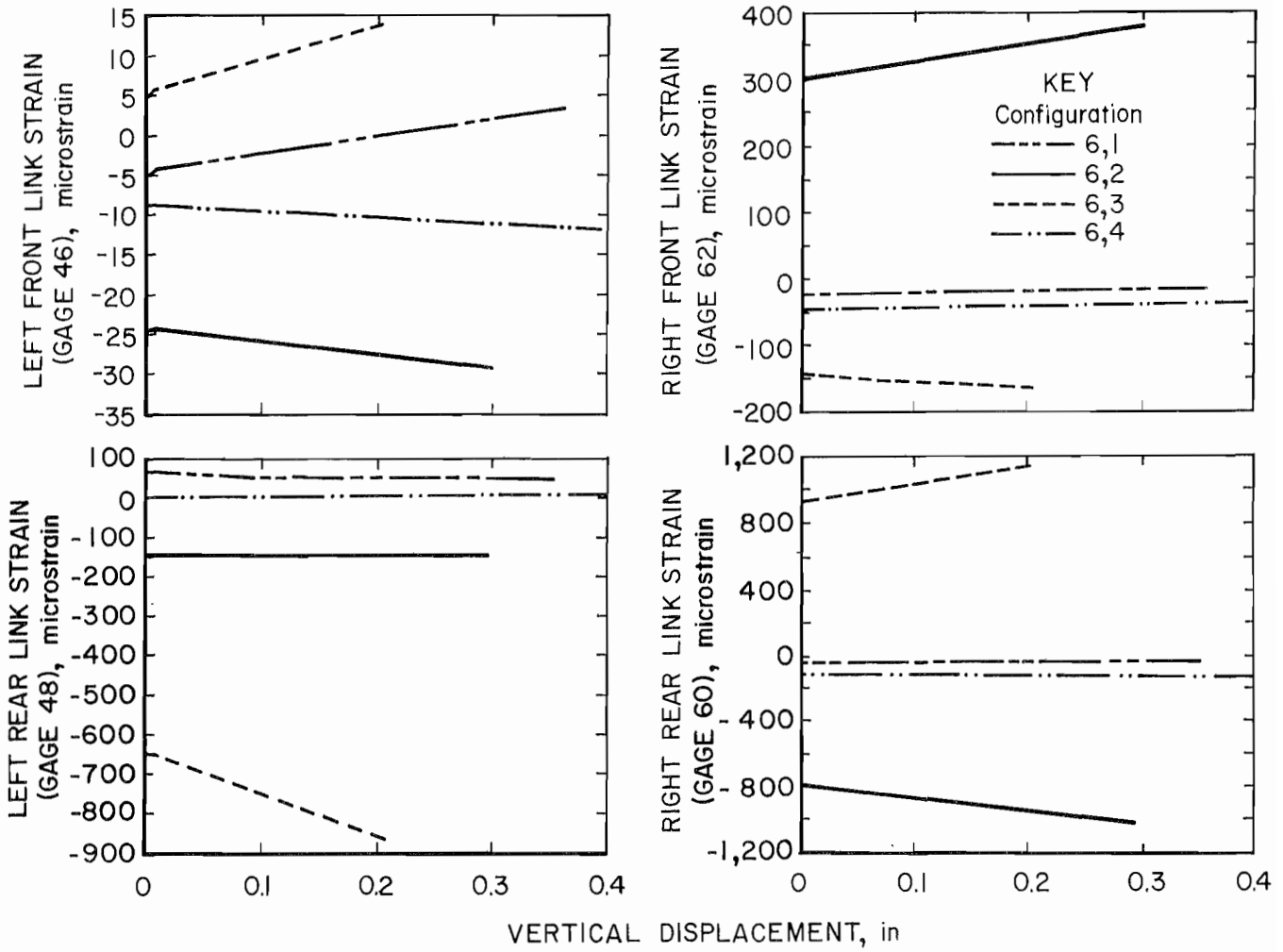


**Figure E-28.–Link strain development for various base contact configurations with symmetric canopy leg contact.**

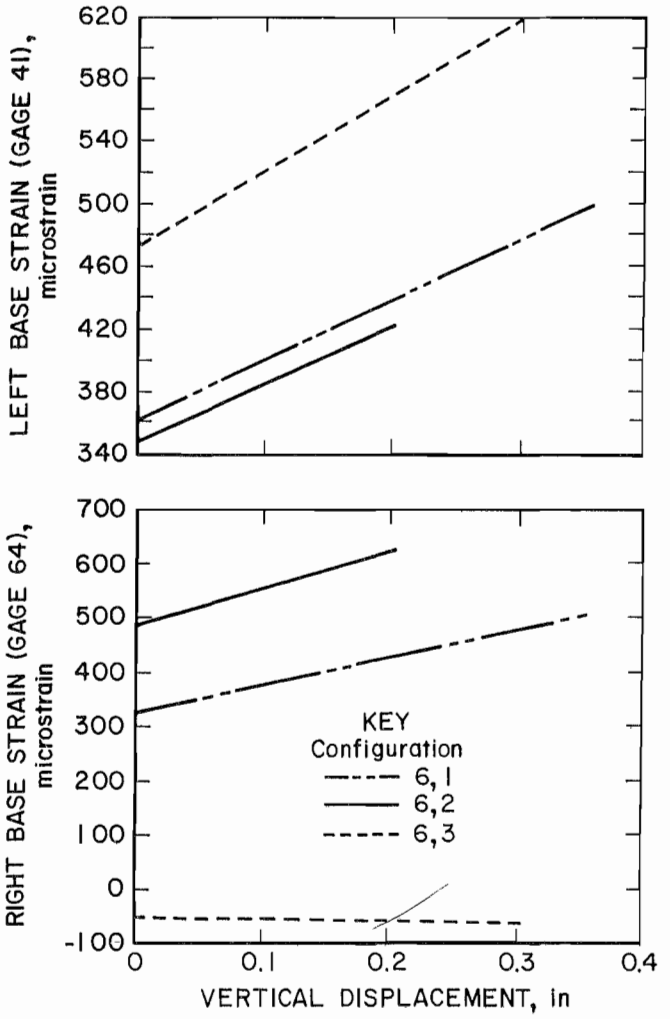


Figure E-29.–Base strain development for various base contact configurations with symmetric canopy leg contact.

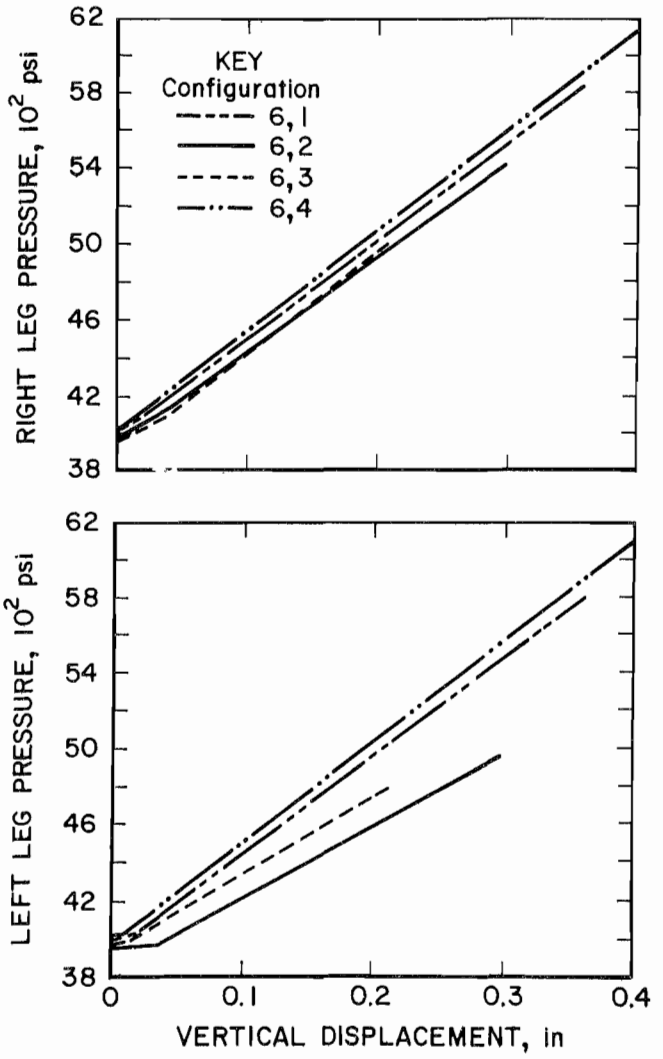


Figure E-30.–Leg pressure development for various base contact configurations with symmetric canopy leg contact.